The effects of mixing on arsenic mobilization and transport in a shallow lake

Samantha Fung

A dissertation
submitted in partial fulfillment of the
requirements for the degree of

Doctor of Philosophy

University of Washington

2023

Reading Committee:
Rebecca Neumann, Co-chair
Alexander Horner-Devine, Co-chair
James Gawel

Program Authorized to Offer Degree:

Civil and Environmental Engineering

University of Washington

Abstract

The effects of mixing on arsenic mobilization and transport in a shallow lake

Samantha Fung

Chairs of the Supervisory Committee:
Rebecca Neumann, Alexander Horner-Devine
Department of Civil and Environmental Engineering

Arsenic, a heavy metal, is a neurotoxin and carcinogen that has been released into the environment at accelerated rates due to human activities. Arsenic has accumulated in the sediments of many lakes around the world and continues to have negative impacts on lake ecosystems and lake users. The negative effects of arsenic are magnified in shallow lakes, where spatial proximity between high arsenic concentrations and biota allow for the uptake of elevated levels of the arsenic into the aquatic food web. In this dissertation, I examine the basis of this phenomenon by examining how physical factors affect biogeochemical conditions and processes in a shallow, urban lake.

In Chapter 2, I investigate lake mixing and arsenic distribution in Lake Killarney on a seasonal timescale during 2018 and 2019. We found that stratification and mixing exhibited seasonal patterns and greatly affected the fate of arsenic within the lake. Arsenic built up in lake bottom waters during the early and mid-summer when the water column remained stratified for week to multiweek periods. Warmer sediment temperatures during early summer, compared to the springtime, were shown to expediate the production of reducing conditions in the bottom water, a prerequisite for the buildup and maintenance of mobile arsenic in this region. Stratification was weaker and mixing occurred more frequently in the late summer. Frequent lake

mixing during the late summer led to a more homogenous distribution of arsenic throughout the lake water column, with elevated surface water concentrations and diminished bottom water concentrations compared to early summer conditions. Thermal convection, rather than wind, was the main mixing force during the summertime in Lake Killarney and was responsible for the vertical transport of arsenic through the lake water column. This work provides a mechanistic understanding for why contaminated, polymictic lakes have high ecosystem and human health risks and underscores the need to prioritize these systems in management efforts.

In Chapter 3, we present observations of repeated diel cycles in bottom water arsenic concentrations. Arsenic concentrations were highest in the early morning to midday and lowest in the evening. Bottom water manganese and iron concentrations exhibited diel signals that coincided with those in arsenic, demonstrating that the fluxes of these three metals were interconnected and likely caused by redox processes at the lakebed. Redox conditions were thus determined to control near-bed availability of arsenic. However, timescale analysis illustrated that redox processes occurring at the sediment water interface could not solely have led to the observed diel cycles in bottom water metals. Significantly, convective mixing was shown to occur nightly and create spikes in vertical turbulence that overlapped with periods when arsenic concentrations were increasing. Estimates of turbulent diffusivities were used to calculate an approximate transport time of arsenic from the lakebed to the bottom water and yielded results that could reasonably explain the observed diel arsenic cycles. Although short term oscillations in arsenic concentrations have been documented in rivers, there is a paucity of studies describing and investigating this phenomenon in lentic systems. Consequently, this study provides an important example of diel cycling in lakes and presents an explanation of the mechanisms behind these cycles. Our findings illustrate the need for lake sampling to include methods that integrate

metal concentrations over multi-day periods in order to attain accurate representations of contaminant levels in lake water and the potential effects on biota and lake users.

Finally, in Chapter 4, I expand on the findings in Chapter 2 by investigating the interannual variability in arsenic concentrations in the lake water and biota between the summers of 2018 and 2019. Mixing frequency varied between the two study years and was found to be a key control on aqueous and biological arsenic concentrations. Specifically, less frequent mixing caused a two-fold increase in arsenic concentrations in lake bottom water, phytoplankton, and zooplankton. Summertime meteorology did not differ significantly between the two years; although meteorology did have a prominent effect on surface thermal structure in both summers, surface stratification was transient and had minimal implications for the release of arsenic into lake bottom waters. Instead, bottom thermal structure, which was set by sediment temperature and the resulting sediment – water temperature difference, was the most important factor in lake mixing frequency and, thus, on the fate of arsenic diffusing upwards from sediment porewaters. Our findings demonstrate that lake mixing behavior and the fate of contaminants can change significantly from year-to-year, highlighting the necessity of understanding the ranges of these processes for effective lake management.

Table of Contents

Acknowledgements ..... ***i***

List of Figures ..... ***iii***

List of Tables ..... ***v***

List of Equations ..... ***vi***

1. Chapter 1: Introduction ***1***

1.1. Shallow lakes **1**

1.1.1. Global significance 1

1.1.2. Physical and biogeochemical characteristics 2

1.1.3. Shallow, urban lakes 4

1.2. Arsenic contamination of lentic systems **5**

1.3. Dissertation overview **7**

1.4. References **10**

2. Chapter 2: Seasonal patterns of mixing and arsenic distribution in a shallow, urban lake ***15***

2.1. Abstract **15**

2.2. Introduction **16**

2.3. Methods **20**

2.3.1. Study site 20

2.3.2. Chemical parameter data collection 20

2.3.3. Physical parameter data collection 22

2.3.4. Data processing 24

2.4. Results **27**

2.4.1. Meteorological forcing 27

2.4.2. Stratification and turbulence 29

2.4.3. As and DO concentrations 33

2.4.4. Summertime patterns of stratification, As, and DO 36

2.4.5. Effects of sediment temperature and stratification on DO and As concentrations 38

2.5. Discussion **41**

2.5.1. Summary 41

2.5.2. Dependence of arsenic mobilization on stratification, dissolved oxygen, and temperature 43

2.5.3. Vertical turbulent mixing of arsenic 45

2.5.4. Seasonal patterns 46

2.5.5. Study implications 48

2.6. References **50**

3. Chapter 3: Short term arsenic cycling in a shallow, polymictic lake ***56***

3.1. Abstract **56**

3.2. Introduction **56**

3.3. Methods **60**

3.3.1. Study Site 60

3.3.2. Data collection 61

3.3.3. Data processing 63

3.4. Results **65**
3.4.1. Meteorological conditions 65
3.4.2. Stratification and mixing 67
3.4.3. As, Mn, Fe, and DO 69
3.4.4. Physical control on As trends 71

3.5. Discussion **73**
3.5.1. Biogeochemical conditions 73
3.5.2. Physical processes 75
3.5.3. Hypotheses 76
3.5.3.1. pH control 76
3.5.3.2. Redox processes control 77
3.5.3.3. Temperature control 78
3.5.3.4. Physical mixing control 78
3.5.4. Interactions between physical and biogeochemical processes 79
3.5.5. Conclusions 80

3.6. References **82**

4. Chapter 4: Annually variability in mixing frequency of a shallow lake: implications for arsenic mobilization and transport ***87***

4.1. Abstract **87**

4.2. Introduction **88**

4.3. Methods **92**
4.3.1. Study site 92
4.3.2. Data collection 93
4.3.3. Data processing 95

4.4. Results **96**
4.4.1. Meteorology 96
4.4.2. Stratification and mixing events 98
4.4.3. Arsenic and dissolved oxygen 101

4.5. Discussion **104**
4.5.1. Main findings 104
4.5.2. Annual variability in meteorology 105
4.5.3. Annual variability in stratification and mixing 105
4.5.4. Annual variability in DO and arsenic 108
4.5.5. Conclusions 112

4.6. References **115**

5. Chapter 5: Conclusions ***120***

5.1. Main findings **120**
5.1.1. Summary 120
5.1.2. The importance of physical processes in biogeochemical processes 120

5.2. Implications **122**
5.2.1. Suggestions for current and future lake managers 123
5.2.2. The necessity of protecting lakes in developing countries 125

5.3. References **127**

A1. Appendix 1: Chapter 2 Supplement 128
A2. Appendix 2: Chapter 3 Supplement 134
A3. Appendix 3: Chapter 4 Supplement 136

Acknowledgements

I am very grateful to Rebecca Neumann, Jim Gawel, and Alex Horner-Devine for being such wonderful advisors and guiding me through this process. Becca, Jim, and Alex, thank you for investing your time and an incredible amount of patience into me while I navigated the ups and downs of grad school. Thank you for teaching me about your respective fields and for being willing to learn along with me as we all dove into the world of shallow lakes together. I greatly appreciated your encouragement during weekly meetings and your feedback, which was always constructive and helped me grow as a scientist and a person. Above all, I want to express my respect of your ability to care deeply about the world while maintaining an optimistic perspective. Holding this dichotomy is a skill I hope to learn and practice in the coming years.

None of this work would have been possible without the immense efforts of Erin Hull, Ken Burkart, and Marco Barajas. Fieldwork with you was a highlight of the research process and I am truly thankful for the laughs we shared and the friendships we developed during the numerous hours out on the lakes.

I would like to extend my heartfelt gratitude to the extraordinary community of graduate students who played an integral role in making this experience enjoyable and fulfilling. I am incredibly lucky to have gotten to learn from and work alongside members of two amazing research groups: the hydrobiogeochemistry group and the Environmental Fluid Mechanics (EFM) group. Yasmine Farhat, Nick Waldo, and Joel Eklof: I am so appreciative of the time we spent together, from hours in the lab making SOP videos or fixing the water system to drinking beer on a sailboat. To all of the EFM members past and present: thank you for your comradery in both science and life. It was truly a joy to get to know you all as people and to see the progression of the incredible research you worked on. Thank you also to the fishbowl and

treehouse communities, whose grounding presence significantly impacted both my professional and personal life during the past five years. I would not have made it through without the countless discussions, shared commiseration, and friendship you all provided. Thank you especially to Christine Baker, Michelle Hu, and Shelby Ahrendt, whose support and friendship I relied on heavily throughout various parts of this journey. I am extremely grateful for you.

To Henry and Nala, thank you for being my daily support system. Henry, I am constantly in awe of your selflessness and am so grateful for your patience and support. Nala, thank you for reminding me how to be silly and for never failing to make me smile even during the hardest of times. You were the best pandemic coworker I could have hoped for.

Lastly, I want to express my deep gratitude to my parents for creating a life where I have freedom in my pursuits; I hope I can use the privilege I've been afforded to do good in the world. Thank you for your unending support and for always emphasizing the importance of well-being and happiness above success.

List of Figures

Figure 1.1. *Flow chart showing some of the important controls on arsenic mobilization from lake sediments and distribution throughout lake water. 7*
Figure 2.1. *Map of Lake Killarney, displaying the location of the lake in the surrounding region (inset) and the three field measurement sites. 26*
Figure 2.2. *Meteorological data during the study period. Time series of: (a) daily mean air temperature, (b) daily mean wind speed, (c) hourly and daily maximum incoming shortwave (SW) radiation, and (d) weekly moving means of air temperature, sediment temperature and average water temperature. 27*
Figure 2.3. *(a) Lake temperatures; white dots indicate sensor placements. (b) Buoyancy frequency, N^2; black markers along the top axis indicate days when the lake experienced full convective overturning. (c) Hypolimnetic dissolved oxygen (DO) and water temperature measured by DO probe. 29*
Figure 2.4. *(a) Bottom and surface vertical turbulent intensity measured using the vertical beam on the acoustic Doppler current profiler (ADCP). (b) Mean weekly vertical turbulent intensity during convective and windy periods (see methods). Periods with no data indicate times when the ADCP was not deployed. 31*
Figure 2.5. *Linearly interpolated profiles of (a) dissolved oxygen (DO) from ~monthly water sampling, (b) dissolved arsenic (As) from ~monthly water sampling, and (c) dissolved arsenic concentrations from 2-week peeper deployments; the thick black line indicates the sediment water interface (SWI). (d) Upward vertical flux of dissolved arsenic from porewaters to above the SWI. 33*
Figure 2.6. *Summertime 2018 plots of (a) lake temperatures (white dots indicate sensor placements), (b) buoyancy frequency, N^2 (black markers indicate days when the lake experienced full convective overturning), (c) hypolimnetic dissolved oxygen (DO) and water temperature measured by DO probe (probe deployment depth was 2.5 m, or approximately 1 m above the lakebed), and (d) water column dissolved arsenic profiles (dots) and contours. 36*
Figure 2.7. *a) N^2 vs. bottom water DO and b) sediment temperature vs. bottom water DO. For (a) and (b), colored points are raw data, with color denoting the month of the year the sample was taken. Bottom water DO was binned into $2x10^{-3}$ s^{-2} and 3.3 °C bins and shown with black dots in (a) and (b), respectively. The unfilled data point in (a) indicates potentially inaccurate binned data, due to the relatively small number of data points being averaged at high N^2 values. c) Bottom water DO vs. aqueous dissolved arsenic concentrations and d) sediment temperature vs. aqueous dissolved arsenic concentrations. For c) and d): open and closed circles indicate porewater and bottom water concentrations, respectively; see Table A1.2 for statistics. 38*
Figure 2.8. *Schematic of processes that lead to high near-surface arsenic concentrations. 43*
Figure 3.1. *Site map of Lake Killarney, including the location of the lake within the Puget Sound in relation to nearby cities (inset), a bathymetric map, and the four field measurement sites. 64*
Figure 3.2. *Meteorological data from August 29 – September 4, 2019: (a) wind speed, (b) shortwave (SW) radiation, (c) the difference between air temperature and surface water temperature, and (d) the temperature difference in the top two thermistors in the water column (z = 3.0 and 3.5 m). Grey shading represents periods when the upper water column experienced unstable stratification, or when the difference between the top two thermistors was negative. 65*
Figure 3.3. *(a) Lake temperatures; white dots indicate placement of the thermistors and the white square indicates placement of the autosampler water intake point and the DO sensor within the water column. (b) Buoyancy frequency, N^2. (c) Vertical turbulent intensity; deployment error of the ADCP lead to non-physical data for the last 36 hours of the study. (d) Horizontal velocity magnitude. 67*
Figure 3.4. *Timeseries of (a) total arsenic (As), (b) surface and bottom water dissolved oxygen in black and blue, respectively, (c) total manganese (Mn) and total iron (Fe) in black and orange, respectively, and (d) surface and bottom water buoyancy frequency (N^2) in black and blue, respectively. Grey shading represents periods when the upper water column experienced unstable stratification. 69*
Figure 3.5. *Scatterplots of (a) bottom water total manganese (Mn) vs. bottom water total arsenic (As) and (b) bottom water total iron (Fe) vs. bottom water total As. 70*
Figure 3.6. *Timeseries of arsenic (As) residuals calculated from the 24-hour moving mean (left axis, black) overlayed with depth-averaged vertical turbulent intensity (right axis, blue). Grey shading represents periods when the upper water column experienced unstable stratification. 71*
Figure 4.1. *(a) Wind speed, (b) shortwave (SW) radiation, (c) air temperature, and (d) sediment and average water temperate. In (a) – (c), bold lines are daily moving means and background transparent lines are hourly data. 97*

Figure 4.2. *Thermistor timeseries in (a) 2018 and (b) 2019. Darker shades represent deeper depths in the water column.....98*
Figure 4.3. *(a) Hourly sediment – mean water temperature difference and (b) 24-hour moving mean of the sediment – air temperature difference for the summers of 2018 (blue) and 2019 (orange).....99*
Figure 4.4. *Number of mixing events each week from June 23 to October 26 for 2018 and 2019. Dots represent the last day of the week over which mixing events were summed.....100*
Figure 4.5. *Dissolved arsenic (As) concentrations from passive diffuser samplers: (a) bottom water, averaged from 5 to 20 cm above the sediment water interface (SWI) and (b) porewater, averaged from 5 to 20 cm below the SWI. Dots are plotted on the days that represent the middle of each passive diffuser deployment. Blue represents 2018 data and orange represents 2019 data in both panels. 101*
Figure 4.6. *(a) Dissolved oxygen (DO) and (b) dissolved arsenic (As) from monthly water column sampling. Solid lines are bottom water samples and dashed lines are surface water samples. Blue represents 2018 data and orange represents 2019 data in both panels.....103*
Figure 4.7. *Dry weight arsenic (As) concentrations in (a) phytoplankton and (b) zooplankton collected ~monthly. 111*
Figure A1.1. *Correlation of SeaTac and in situ air temperature data with linear fit (R^2 = 0.92, P < 0.01) and equation shown; linear fit of data was used to make a correction to the raw SeaTac air temperature data (Equation. A1.1). 128*
Figure A1.2. *Correlation of Washington State University (WSU) shortwave (SW) radiation measured at the Puyallup weather station and in situ SW radiation data (R^2 = 0.95, P < 0.01), showing that the data have a 1-1 relationship and no correction was needed. 129*
Figure A1.3. *Wind speed vs. surface vertical turbulent intensity, $(w')2$, where surface turbulent intensity measurements were averaged into 0.25 m s^{-1} wind speed bins. The dashed line at 1 m s^{-1} represents the threshold used to separate 'high' and 'low' wind values. 129*
Figure A1.4. *Hourly in situ wind speed data. 130*
Figure A1.5. *Top and bottom water column total arsenic concentrations.....130*
Figure A1.6. *Porewater peeper profiles representing seasonal differences in arsenic mobilization from the sediment and diffusion into bottom waters.....131*
Figure A1.7. *Nine-minute timeseries of vertical turbulent intensity, $(w')2$, with concurrent normalized sediment concentrations both from acoustic Doppler current profiler data. Data were taken at 2.88 m depth on October 25, 2018, during a convective overturning event. *Note that normalized concentration is unitless. 131*
Figure A1.8. *a) Dissolved and b) total arsenic concentrations profiles from ~monthly water sampling; black dots indicate sampling date and location within the water column. 131*
Figure A2.1. *Lake water density profiles on September 1 every 6 hours.....134*
Figure A2.2. *Dissolved arsenic (As), manganese (Mn), and iron (Fe) profiles 134*
Figure A2.3. *Scatterplots of (a) dissolved manganese (Mn) and dissolved arsenic (As) and (b) dissolved iron (Fe) and dissolved arsenic (As). 135*
Figure A2.4. *Water temperature timeseries from thermistors at 0.5, 1.0, and 1.5 m above the lakebed. 135*
Figure A3.1. *Difference in temperature between top and bottom thermistors (ΔT) used to define whether the lake water column was fully mixed vs. number of mixing events calculated from June 23 through October 31, the period of time when there is thermistor data in both summers, for 2018 and 2019.....136*
Figure A3.2. *Boxplots of (a, b) porewater and (c, d) bottom water dissolved arsenic concentrations from June 1 – October 31 in 2018 and 2019 from passive diffuser samples (n = 5 deployments in each summer). Middle lines on box plots represents median of data in plot. Note different scales for porewater and bottom water plots.....136*
Figure A3.3. *Hourly wind measurements for the month of March in 2018 and 2019.....137*

List of Tables

Table 2.1. *For three 10-day periods: average sediment temperature, mixing regime, average bottom water DO, $\Delta(DO)$, or the rate of change of bottom water DO [mg L^{-1} day^{-1}] during the 10 days, bottom water [As], and $\Delta(Bottom\ water\ As)$, or the change in bottom water dissolved arsenic concentration from the measurement prior to each period.* *39*

Table A1.1. *Arsenic speciation for water samples collected on five dates, where arsenite (As(III)) and arsenate (As(V)) are inorganic forms of arsenic and monomethylarsonic acid (MMA) and dimethylarsinic acid (DMA) are organic forms of arsenic.* *132*

Table A1.2. *Slope and statistics for relationships plotted in Fig. 2.7c (bottom water DO vs. both bottom water and porewater As) and Fig. 2.7d (sediment temperature vs. both bottom water and porewater As).* *133*

Table A3.1. *Monthly average air temperatures in 2018 and 2019 from January through May.* *137*

List of Equations

Equation A1.1. 128
Equation A1.2. 128

1. Chapter 1: Introduction

1.1. Shallow lakes

1.1.1. Global significance

Shallow lakes and ponds are globally abundant (Downing et al., 2006). Although the global estimate of shallow lake numbers and area coverage is still a topic of current research and debate, there is no uncertainty of their multifaceted importance, in global carbon cycles, in supporting biodiversity, and in the provision of numerous ecosystem services (Biggs et al., 2017; Holgerson and Raymond, 2016; Williams et al., 2004). Recent studies estimate that between 4 and 5.5 million km^2, translating to 3 to 4%, of the land surface is covered by standing waters (Downing et al., 2006; Verpoorter et al., 2014). Small, shallow lakes outnumber deep lakes 100:1 (Downing et al., 2006) and small lakes (< 10 km^2 in surface area) are estimated to constitute a large proportion, approximately 60%, of this overall area (Holgerson and Raymond, 2016).

Small lake processes have been shown to be extremely important in global freshwater processes (Downing et al., 2006) and gas cycling (MacIntyre et al. 2018). Because shallow lakes have a high perimeter to volume ratio, they generally have a high influx of terrestrial carbon, and a high carbon processing rate (Downing et al., 2008; Holgerson and Raymond, 2016). Further, shallow lakes support high levels of sediment respiration, which leads to bottom water anoxia and elevated production of methane. Recent large scale studies have found that shallow lakes produce more methane than larger lakes and contribute significantly to the total amount of carbon dioxide produced in inland standing waters (Holgerson and Raymond, 2016).

Shallow lakes have significant ecological importance and play a crucial role in supporting global biodiversity. Because small lakes are extremely heterogeneous, they are able to support a large and unique array of plant and animal species. Limited depths and increased sunlight

penetration allow for the growth of abundant aquatic vegetation, including submerged plants and floating macrophytes. Previous studies have established that macrophyte coverage is generally greater in small lakes than in larger lakes (Duarte et al., 1986). Macrophyte coverage enhances habitats and provides breeding grounds and food sources for a wide range of organisms, including fish, amphibians, birds, and invertebrates. As a result, shallow lentic systems often host greater species richness per unit area than large lakes; this was shown to be the case for waterfowl by Elmberg et al. (1994). At the regional and landscape level, small and shallow lakes are especially important in maintaining biodiversity and system stability. Williams et al. (2004) found that, in British lowlands, ponds exhibited the highest taxonomic richness and harbored the most unique and scarce species of macrophytes and invertebrates out of all types of small water bodies.

1.1.2. Physical and biogeochemical characteristics

Shallow lakes are distinct from deep lakes both in their morphology and in their biogeochemical and physical characteristics. Shallow lakes are extremely heterogeneous; because they generally have small watersheds, these systems each have unique chemical characteristics that are distinct to their regional geology and climate. Further, they are strongly affected by the local climate and their chemical and physical characteristics adjust quickly as meteorological conditions change. Although ‘shallow’ remains an ambiguous term in describing lake size and depth, there have been recent efforts to characterize and identify traits that distinguish shallow lakes, small lakes, and ponds from the general category of ‘lake’ (Richardson et al., 2022; Søndergaard et al., 2005). Patterns in water chemistry, gas flux, metabolism, vegetation coverage, and nutrient concentrations have been investigated to develop a mechanistic definition of these systems (Richardson et al., 2022).

Shallow lakes are often distinguished from deeper lakes not only by depth, but also through mixing regime. Although mixing characteristics tend to lie on a gradient, rather than in distinct categories, shallow lakes are often polymictic, meaning they mix multiple times throughout the year, whereas deeper lakes are more often monomictic or dimictic, meaning they have one or two distinct mixing periods per year, respectively (Lewis, 1983). Because monomictic and dimictic lakes exhibit longer periods of thermal stability than polymictic lakes, shallow lakes often have more complex thermal structures than larger lakes (Xenopoulos and Schindler, 2001).

The variation in external forcing mechanisms throughout the year controls the magnitude and frequency of lake mixing. In lakes without significant through-flow, wind shear and surface heat transfer are the predominant sources of mixing (Tuan et al., 2009). The importance of mixing forces varies with lake size; mixing in deep lakes is most often dominated by wind, whereas thermal convection increases in importance as lake size decreases (Read et al., 2012). Lake morphology and forcing factors can lead to significant differences in the degree and timescale of mixing between and within shallow, polymictic lakes. For example, a deeper polymictic lake will mix less frequently than a shallower polymictic lake, given similar external forcing and surface area. Further, meteorology can change the mixing patterns of individual lakes on an interannual timescale (MacIntyre et al., 2009, Ahmed et al., 2023). Mixing processes are important in overall lake functioning, as they regulate many biogeochemical processes, including gas and contaminant transfer, and environmental characteristics, such as temperature and oxygen.

1.1.3. Shallow, urban lakes

Urban lakes are often shallow and are susceptible to degradation in water quality due to anthropogenic impacts (Birch and McCaskie 1999). These systems are affected by their catchment, which often contains urban and suburban land, and can receive contaminants through overland flow as well as through aerial deposition. Eutrophication from nutrient loading, namely phosphorus and nitrogen, is a common problem in urban lakes and can cause these lakes to be unfit for human recreation (Gkelis et al., 2014; Kalaji et al., 2016). Historic industry in urban areas has also caused legacy contamination of many of these systems with metals such as arsenic, zinc, and copper (Gawel et al., 2014; Thapalia et al., 2010). In addition, new contaminants from anthropogenic sources have emerged in recent years and are still being discovered. Of note are perfluorinated alkylated substances (PFAS), polychlorinated biphenyls (PCBs), and polycyclic aromatic hydrocarbons (PAHs) (Simcik et al., 1997; Xiao et al., 2013).

Because urban lakes are prone to contamination and are heavily used by local populations, they pose potential health risks both to the aquatic ecosystems and to lake users. Urban lake contamination can affect lake residents and users in many ways. People harvesting biota from lakes, such as snails, crayfish, and finfish, can be exposed to pollutants through consumption of contaminated organisms (Hull et al., 2021). Other recreational activities, such as swimming or even recreating on the lake shore, can lead to direct human exposure to pollutants. Children and pets are at an increased risk for exposure through accidental water or sediment consumption. Lake residents who have properties in close proximity to contaminated water bodies can transfer toxins onto their own properties if lake water is used for lawn or garden irrigation. Because past limnological research has mainly focused on large lakes, rather than shallow lakes, the management of shallow, urban lakes is still lacking (Birch and McCaskie, 1999).

1.2. Arsenic contamination of lentic systems

Arsenic is a naturally occurring metalloid that is toxic to plants, animals, and humans. Arsenic contamination of lakes and other water bodies can originate from both natural and anthropogenic sources. The predominant natural sources of arsenic to the environment are volcanic activity and the accelerated weathering of minerals by geothermal activity, especially in areas where minerals are naturally enriched with arsenic (Smedley and Kinniburgh, 2002). Anthropogenic activities, including mining, smelting, and the historic application of arsenic-containing pesticides, have accelerated the release of arsenic into the environment in both urban and remote areas (Gawel et al., 2014; Rice et al., 2002).

Arsenic can exist in multiple organic and inorganic forms. Inorganic arsenic is largely present either as arsenite, As(III), or arsenate, As(V) (Smedley and Kinniburgh, 2002). Organic arsenic, which is produced by biological activity, is typically found in smaller amounts than inorganic arsenic and, as a result, is generally considered to be less significant (Smedley and Kinniburgh, 2002). Algae actively absorb arsenic from surrounding waters by mistaking arsenate, the oxidized form of inorganic arsenic, for phosphate (Sanders et al., 1989; Wang et al., 2013). In lakes, arsenite, the reduced form of arsenic, is often thought to be the dominant form of inorganic arsenic in the hypoxic porewater and bottom waters of lakes (Aggett and O'Brien, 1985; Keimowitz et al., 2005), whereas arsenate is thought to be present mainly in oxygenated surface waters. However, there are also studies that report the prevalence of arsenate in hypoxic regions of the lake, which is significant because this would indicate that there is a larger area of spatial overlap between primary producers and bioavailable arsenic than previously considered (Martin and Pedersen, 2002; Spliethoff et al., 1995, Andrade et al., 2010).

In contaminated lakes, arsenic can permeate the aquatic food web and harm ecosystem health and functioning. For instance, the presence of arsenic in lakes can alter the composition of phytoplankton and zooplankton communities, often resulting in reduced diversity and a shift towards more metal-tolerant species (Chen et al., 2015). Arsenic also affects fish in lakes by causing behavioral changes at low concentrations and fatality at higher concentrations (Kumari et al., 2017). Populations surrounding contaminated lakes can be heavily impacted, especially in areas where lakes are a source of drinking water and agricultural irrigation (Arain et al., 2009). Exposure to arsenic through consumption of contaminated water, or consumption of crops grown with contaminated water, can lead to the disruption of respiratory functions and other negative health effects in humans and animals (Arain et al., 2009). The harvesting of biota, including snails, crayfish, and finfish, from contaminated lakes is another exposure pathway and represents an especially large risk for subsistence fishers who rely on urban lakes as a food source (Hull et al. 2021).

Once arsenic builds up in the sediments of lakes, it remains in, and can continue to cycle through, the system indefinitely, or until the contaminated sediment is removed or covered by many years of natural deposition. Unfortunately, remediation techniques of arsenic in natural environments are generally costly and often have significant drawbacks (Singh et al., 2015). For example, removal of contaminated soils can lead to secondary contamination of the area where the soil is relocated and the addition of chemicals to immobilize arsenic in natural waters can have unforeseen negative environmental impacts. Because of these difficulties, it is necessary to be able to identify contaminated lakes that the pose the highest risk to surrounding communities and to gain understanding of how these systems function to inform management and remediation efforts.

1.3. Dissertation overview

Shallow, arsenic contaminated lakes represent an important environmental problem, especially in light of recent studies that demonstrate that these systems pose a greater health risk to their ecosystems and surrounding populations compared to deeper, contaminated lakes (Barrett et al., 2018; 2019; Hull et al., 2021). The goal of this dissertation is to further the understanding of the fate of arsenic in shallow lakes and of the physical and biogeochemical processes that control the transport of arsenic between the sediment, porewater, bottom waters, and surface waters. To this end, three studies were carried out utilizing data from 2018 and 2019, which was collected as part of an extensive field study conducted on Lake Killarney, a shallow, arsenic contaminated lake near Seattle, WA, USA. The results of these works elucidate how biogeochemical and physical factors, namely sediment temperature, dissolved oxygen, stratification, and lake mixing, affect concentrations of arsenic in lake bottom water and the distribution of arsenic throughout the water column (Fig. 1.1). Ultimately, we examine the mechanisms controlling the fate of arsenic in shallow lakes at daily to interannual timescales.

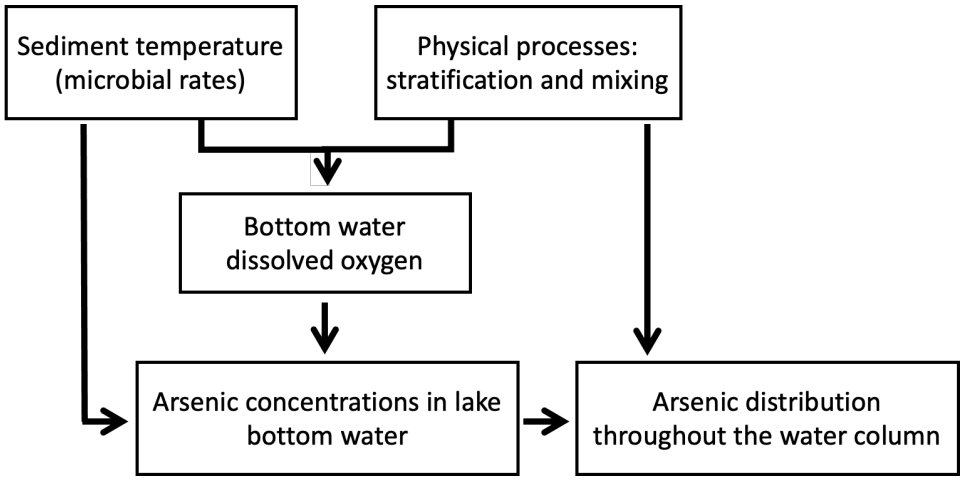

Figure 1.1. *Flow chart showing some of the important controls on arsenic mobilization from lake sediments and distribution throughout lake water.*

In Chapter 2, I examine the seasonality of physical and biogeochemical processes that modulate the concentrations and distribution of arsenic in Lake Killarney during a 17-month period. I describe and categorize seasonal patterns in these processes and in the resulting effects on the fate of arsenic. The cooccurrence of various conditions is required to maintain elevated arsenic concentrations in the lake water. Specifically, the results emphasize the importance of elevated temperatures in creating reducing conditions in the bottom water and show that intermittent mixing allows for the buildup of high levels of arsenic in the bottom water and occasional pulses of arsenic into surface waters.

Chapter 3 focuses on a weeklong period and examines the diel cycles observed in measured variables, including bottom water dissolved oxygen and bottom water total arsenic, iron, and manganese. Significantly, we show that nighttime thermal convection creates spikes in vertical turbulence that occur during periods of increasing arsenic concentrations. Timescale analysis shows that turbulent mixing must be present to create the diel arsenic signals. However, we also show that redox conditions in the hypolimnion likely control the near-bed availability of arsenic and contribute to the observed diel cycles.

Lastly, in Chapter 4, I investigate interannual variation in meteorological forcing, lake mixing frequency, and arsenic concentrations between the summers of 2018 and 2019. I show that summertime mixing frequency, rather than sediment temperature, controls flux rates of arsenic from sediment porewaters into lake bottom waters and ultimately, the uptake of arsenic into the base of the food web. Less frequent lake mixing leads to higher concentrations of arsenic in lake water and in plankton. These results have implications for the fate of arsenic in shallow lakes under future climate warming. Chapter 5 offers a summary of the work completed here and lays out implications for current and future lake managers. I also provide some final thoughts on

shallow lake research and on how we can appropriately value and protect the health of these important systems.

1.4. References

Aggett, J., & O'Brien, G. A. (1985). Detailed Model for the Mobility of Arsenic in Lacustrine Sediments Based on Measurements in Lake Ohakuri. *Environmental Science and Technology*, *19*(3), 231–238. https://doi.org/10.1021/es00133a002

Ahmed, S. S., Zhang, W., Loewen, M. R., Zhu, D. Z., Ghobrial, T. R., Mahmood, K., & van Duin, B. (2023). Stratification and its consequences in two constructed urban stormwater wetlands. *Science of the Total Environment*, *872*. https://doi.org/10.1016/j.scitotenv.2023.162179

Andrade, C. F., Jamieson, H. E., Kyser, T. K., Praharaj, T., & Fortin, D. (2010). Biogeochemical redox cycling of arsenic in mine-impacted lake sediments and co-existing pore waters near Giant Mine, Yellowknife Bay, Canada. *Applied Geochemistry*, *25*(2), 199–211. https://doi.org/10.1016/j.apgeochem.2009.11.005

Arain, M. B., Kazi, T. G., Baig, J. A., Jamali, M. K., Afridi, H. I., Jalbani, N., Sarfraz, R. A., Shah, A. Q., & Kandhro, G. A. (2009). Respiratory effects in people exposed to arsenic via the drinking water and tobacco smoking in southern part of Pakistan. *Science of the Total Environment*, *407*(21), 5524–5530. https://doi.org/10.1016/j.scitotenv.2009.07.012

Barrett, P. M., Hull, E. A., King, C. E., Burkart, K., Ott, K. A., Ryan, J. N., Gawel, J. E., & Neumann, R. B. (2018). Increased exposure of plankton to arsenic in contaminated weakly-stratified lakes. *Science of the Total Environment*, *625*, 1606–1614. https://doi.org/10.1016/j.scitotenv.2017.12.336

Barrett, P. M., Hull, E. A., Burkart, K., Hargrave, O., McLean, J., Taylor, V. F., Jackson, B. P., Gawel, J. E., & Neumann, R. B. (2019). Contrasting arsenic cycling in strongly and weakly stratified contaminated lakes: Evidence for temperature control on sediment–water arsenic fluxes. *Limnology and Oceanography*, *64*(3), 1333–1346. https://doi.org/10.1002/lno.11119

Biggs, J., von Fumetti, S., & Kelly-Quinn, M. (2017). The importance of small waterbodies for biodiversity and ecosystem services: implications for policy makers. In *Hydrobiologia* (Vol. 793, Issue 1, pp. 3–39). Springer International Publishing. https://doi.org/10.1007/s10750-016-3007-0

Birch, S., & McCaskie, J. (1999). Shallow urban lakes: A challenge for lake management. *Hydrobiologia*, *395–396*, 365–377. https://doi.org/10.1007/978-94-017-3282-6_31

Chen, G., Shi, H., Tao, J., Chen, L., Liu, Y., Lei, G., Liu, X., & Smol, J. P. (2015). Industrial arsenic contamination causes catastrophic changes in freshwater ecosystems. *Scientific Reports*, *5*, 1–7. https://doi.org/10.1038/srep17419

Downing, J. A., Prairie, Y. T., Cole, J. J., Duarte, C. M., Tranvik, L. J., Striegl, R. G., McDowell, W. H., Kortelainen, P., Caraco, N. F., Melack, J. M., & Middleburg, J. J. (2006). *The global abundance and size distribution of lakes , ponds , and impoundments*. *51*(5), 2388–2397.

Downing, J. A., Cole, J. J., Middelburg, J. J., Striegl, R. G., Duarte, C. M., Kortelainen, P., Prairie, Y. T., & Laube, K. A. (2008). Sediment organic carbon burial in agriculturally eutrophic impoundments over the last century. *Global Biogeochemical Cycles*, *22*(1). https://doi.org/10.1029/2006GB002854

Duarte, C. M., Kalff, J., & Peters, R. H. (1986). Patterns in biomass and cover of aquifer macrophytes in lakes. *Canadian Journal of Fisheries and Aquatic Sciences*, *43*(10), 1900–1908. https://doi.org/10.1139/f86-235

Elmberg, J., Nummi, P., Poysa, H., & Sjoberg, K. (1994). Relationships Between Species Number, Lake Size and Resource Diversity in Assemblages of Breeding Waterfowl. In *Source: Journal of Biogeography* (Vol. 21, Issue 1).

Gawel, J. E., Asplund, J. A., Burdick, S., Miller, M., Peterson, S. M., Tollefson, A., & Ziegler, K. (2014). Arsenic and lead distribution and mobility in lake sediments in the south-central Puget Sound watershed: The long-term impact of a metal smelter in Ruston, Washington, USA. *Science of the Total Environment*, *472*, 530–537. https://doi.org/10.1016/j.scitotenv.2013.11.004

Gkelis, S., Papadimitriou, T., Zaoutsos, N., & Leonardos, I. (2014). Anthropogenic and climate-induced change favors toxic cyanobacteria blooms: Evidence from monitoring a highly eutrophic, urban Mediterranean lake. *Harmful Algae*, *39*, 322–333. https://doi.org/10.1016/j.hal.2014.09.002

Holgerson, M. A., & Raymond, P. A. (2016). *Large contribution to inland water CO 2 and CH 4 emissions from very small ponds*. *9*(February). https://doi.org/10.1038/NGEO2654

Hull, E. A., Barajas, M., Burkart, K. A., Fung, S. R., Jackson, B. P., Barrett, P. M., Neumann, R. B., Olden, J. D., & Gawel, J. E. (2021). Human health risk from consumption of aquatic species in arsenic-contaminated shallow urban lakes. *Science of the Total Environment*, *770*, 145318. https://doi.org/10.1016/j.scitotenv.2021.145318

Kalaji, H. M., Sytar, O., Brestic, M., Samborska, I. A., Cetner, M. D., & Carpentier, C. (2016). Risk assessment of urban lake water quality based on in-situ cyanobacterial and total chlorophyll-a monitoring. *Polish Journal of Environmental Studies*, *25*(2), 655–661. https://doi.org/10.15244/pjoes/60895

Keimowitz, A. R., Zheng, Y., Chillrud, S. N., Mailloux, B., Jung, H. B., Stute, M., & Simpson, H. J. (2005). Arsenic redistribution between sediments and water near a highly contaminated source. *Environmental Science and Technology*, *39*(22), 8606–8613. https://doi.org/10.1021/es050727t

Kumari, B., Kumar, V., Sinha, A. K., Ahsan, J., Ghosh, A. K., Wang, H., & DeBoeck, G. (2017). Toxicology of arsenic in fish and aquatic systems. In *Environmental Chemistry Letters* (Vol. 15, Issue 1, pp. 43–64). Springer Verlag. https://doi.org/10.1007/s10311-016-0588-9

Lewis Jr., W. M. (1983). A Revised Classification of Lakes Based on Mixing. *Canadian Journal of Fisheries and Aquatic Sciences*, *40*(10), 1779–1787. https://doi.org/10.1139/f83-207

MacIntyre, S., Crowe, A. T., Cortés, A., & Arneborg, L. (2018). Turbulence in a small arctic pond. *Limnology and Oceanography*, *63*(6), 2337–2358. https://doi.org/10.1002/lno.10941

MacIntyre, S., Fram, J. P., Kushner, P. J., Bettez, N. D., O'Brien, W. J., Hobbi, J. E., & Kling, G. W. (2009). Climate-related variations in mixing dynamics in an Alaskan arctic lake. *Limnology and Oceanography*, *54*(6 PART 2), 2401–2417. https://doi.org/10.4319/lo.2009.54.6_part_2.2401

Martin, A. J., & Pedersen, T. F. (2002). Seasonal and interannual mobility of arsenic in a lake impacted by metal mining. *Environmental Science and Technology*, *36*(7), 1516–1523. https://doi.org/10.1021/es0108537

Read, J. S., Hamilton, D. P., Desai, A. R., Rose, K. C., Macintyre, S., Lenters, J. D., Smyth, R. L., Hanson, P. C., Cole, J. J., Staehr, P. A., Rusak, J. A., Pierson, D. C., Brookes, J. D., Laas, A., & Wu, C. H. (2012). *Lake-size dependency of wind shear and convection as controls on gas exchange*. *39*, 1–5. https://doi.org/10.1029/2012GL051886

Rice, K. C., Conko, K. M., & Hornberger, G. M. (2002). Anthropogenic sources of arsenic and copper to sediments in a Suburban Lake, Northern Virginia. *Environmental Science and Technology*, *36*(23), 4962–4967. https://doi.org/10.1021/es025727x

Richardson, D. C., Holgerson, M. A., Farragher, M. J., Hoffman, K. K., King, K. B. S., Alfonso, M. B., Andersen, M. R., Cheruveil, K. S., Coleman, K. A., Farruggia, M. J., Fernandez, R. L., Hondula, K. L., López Moreira Mazacotte, G. A., Paul, K., Peierls, B. L., Rabaey, J. S., Sadro, S., Sánchez, M. L., Smyth, R. L., & Sweetman, J. N. (2022). A functional definition to distinguish ponds from lakes and wetlands. *Scientific Reports*, *12*(1). https://doi.org/10.1038/s41598-022-14569-0

Sanders, J. G., Osman, R. W., & Riedel, G. F. (1989). Pathways of arsenic uptake and incorporation in estuarine phytoplankton and the filter-feeding invertebrates Eurytemora affinis, Balanus improvisus and Crassostrea virginica. *Marine Biology*, *103*(3), 319–325. https://doi.org/10.1007/BF00397265

Simcik, M. F., Zhang, H., Eisenreich, S. J., & Franz, T. P. (1997). *Urban Contamination of the Chicago/Coastal Lake Michigan Atmosphere by PCBs and PAHs during AEOLOS*. https://pubs.acs.org/sharingguidelines

Singh, R., Singh, S., Parihar, P., Singh, V. P., & Prasad, S. M. (2015). Arsenic contamination, consequences and remediation techniques: A review. In *Ecotoxicology and Environmental Safety* (Vol. 112, pp. 247–270). Academic Press. https://doi.org/10.1016/j.ecoenv.2014.10.009

Smedley, P. L., & Kinniburgh, D. G. (2002). A review of the source, behaviour and distribution of arsenic in natural waters. *Applied Geochemistry*, *17*(5), 517–568. https://doi.org/10.1016/S0883-2927(02)00018-5

Søndergaard, M., Jeppesen, E., & Jensen, J. P. (2005). Pond or lake: Does it make any difference? *Archiv Fur Hydrobiologie*, *162*(2), 143–165. https://doi.org/10.1127/0003-9136/2005/0162-0143

Spliethoff, H. M., Mason, R. P., & Hemond, H. F. (1995). Interannual Variability in the Speciation and Mobility of Arsenic in a Dimictic Lake. In *Environ. Sci. Techno* (Vol. 29). https://pubs.acs.org/sharingguidelines

Thapalia, A., Borrok, D. M., van Metre, P. C., Musgrove, M., & Landa, E. R. (2010). Zn and Cu isotopes as tracers of anthropogenic contamination in a sediment core from an Urban Lake. *Environmental Science and Technology*, *44*(5), 1544–1550. https://doi.org/10.1021/es902933y

Tuan, N. v., Hamagami, K., Mori, K., & Hirai, Y. (2009). Mixing by wind-induced flow and thermal convection in a small, shallow and stratified lake. *Paddy and Water Environment*, *7*(2), 83–93. https://doi.org/10.1007/s10333-009-0158-x

Verpoorter, C., Kutser, T., Seekell, D. A., & Tranvik, L. J. (2014). A global inventory of lakes based on high-resolution satellite imagery. *Geophysical Research Letters*, *41*(18), 6396–6402. https://doi.org/10.1002/2014GL060641

Wang, Z., Luo, Z., & Yan, C. (2013). Accumulation, transformation, and release of inorganic arsenic by the freshwater cyanobacterium Microcystis aeruginosa. *Environmental Science and Pollution Research*, *20*(10), 7286–7295. https://doi.org/10.1007/s11356-013-1741-7

Williams, P., Whitfield, M., Biggs, J., Bray, S., Fox, G., Nicolet, P., & Sear, D. (2004). Comparative biodiversity of rivers, streams, ditches and ponds in an agricultural landscape in Southern England. *Biological Conservation*, *115*(2), 329–341. https://doi.org/10.1016/S0006-3207(03)00153-8

Xenopoulos, M. A., & Schindler, D. W. (2001). The environmental control of near-surface thermoclines in boreal lakes. *Ecosystems*, *4*(7), 699–707. https://doi.org/10.1007/s10021-001-0038-8

2. Chapter 2: Seasonal patterns of mixing and arsenic distribution in a shallow, urban lake

This chapter was published previously as: Fung, S. R., Hull, E. A., Burkart, K., Gawel, J. E., Horner-Devine, A. R., & Neumann, R. B. (2022). Seasonal Patterns of Mixing and Arsenic Distribution in a Shallow Urban Lake. *Water Resources Research*, *58*(10). https://doi.org/10.1029/2022wr032564

2.1. Abstract

Arsenic, a neurotoxin and carcinogen, is a legacy contaminant in the sediments of many urban lakes and poses health risks to aquatic ecosystems and lake users. Arsenic uptake into the aquatic food web is enhanced in shallow, polymictic lakes compared to deep, seasonally stratified lakes. We present the results of a 17-month field study in Lake Killarney, a shallow, urban lake in Federal Way, Washington, USA, which examines the physical and biogeochemical mechanisms controlling arsenic mobilization and transport from sediment into lake waters, a prerequisite for arsenic uptake into the food web. In Lake Killarney, arsenic mobilization and transport into bottom waters occurred only when stratified conditions and elevated temperatures facilitated deoxygenation of bottom waters. Frequency of lake mixing varied seasonally and controlled the vertical distribution of arsenic in the water column. Convective mixing was the main contributor to elevated vertical turbulent intensity in the water column during periods of high arsenic mobilization, and thus to the upwards transport of arsenic from bottom waters. Maximum near-surface arsenic occurred when the lakebed sediment temperature was elevated and the water column was overturning frequently. This work clarifies the mechanisms that contribute to vertical arsenic transport in shallow lakes and provides a basis for identifying contaminated systems with the physical and biogeochemical conditions that promote transport of arsenic into near-surface water.

2.2. Introduction

Arsenic, a carcinogenic contaminant, has accumulated in the bottom sediments of lakes around the world due to a range of anthropogenic activities, such as mining, smelting, and the application of arsenic-containing pesticides (Gawel et al., 2014; Rice et al., 2002; Smedley & Kinniburgh, 2002). When arsenic is mobilized from sediments into overlying lake water, it can be taken up by primary producers (Barrett et al., 2018; Caumette et al., 2011) and move up the aquatic food web, including into organisms consumed by humans (Hull et al., 2021; Rahman et al., 2012). Both physical and biogeochemical lake processes control arsenic mobilization, transport, and concentration in lake water and thus control ecosystem and human exposure to arsenic. Recent findings show that conditions within shallow lakes, as opposed to deep lakes, facilitate rapid cycling of arsenic between the sediment and overlying lake water (Barrett et al., 2019), and enhance spatial overlap between oxygen-requiring biota and mobilized arsenic (Barrett et al., 2018; Hull et al., 2021).

According to lake mixing classifications, most shallow lakes are polymictic, meaning they circulate perennially and only stratify for short periods (Hutchinson & Löffler, 1956; Lewis Jr., 1983). Based on this reasoning, the water column in these systems is often assumed to remain largely well-oxygenated throughout the year (Martin & Pedersen, 2002). Because arsenic mobilization requires a reducing environment and dissolved arsenic is readily scavenged out of the water column under oxic conditions (Belzile & Tessier, 1990), arsenic concentrations are expected to be low in near-surface waters of shallow, well-mixed systems. However, there have been many documented observations of elevated dissolved arsenic concentrations in the surface water and ecosystems of shallow lakes (Barrett et al., 2019; Martin & Pedersen, 2002; Palmer et

al., 2019; Zhang et al., 2013); these observations conflict with the expected behavior of arsenic in polymictic systems.

In oxic conditions, inorganic arsenic is mainly present as arsenate, As(V), and is generally associated with oxide and oxyhydroxide minerals, including iron and manganese oxides (Smedley & Kinniburgh, 2002). Arsenite, As(III), is more prevalent in anoxic conditions and is generally more mobile due to the decrease in sorption area from the reductive dissolution of oxyhydroxide particles (Smedley & Kinniburgh, 2002). Although arsenic chemistry involves more complexities than discussed here (i.e. effects of pH on sorption equilibrium), the mobility of arsenic in many lake sediments, including those in this study (Barrett et al., 2019), is mainly controlled by redox state (Belzile & Tessier, 1990; Nikolaidis et al., 2004). Arsenic mobilization is a microbe-mediated process (Nickson et al., 2000); because microbial activity is moderated by both temperature (Ratkowsky et al., 1982) and redox state (Frindte et al., 2013), mobilization of arsenic sequestered in lake sediments into sediment porewater is sensitive to both of these factors. Multiple studies have shown that elevated temperatures, and the associated increase in microbial activity, can expediate the formation of reducing conditions and the mobilization of arsenic into porewater (Aurilio et al., 1994; Barrett et al., 2019; Weber et al., 2010). Once in the porewater, dissolved arsenic can diffuse upwards into lake bottom water (Barrett et al., 2019; Belzile & Tessier, 1990; Martin & Pedersen, 2002), driven by a vertical concentration gradient.

Arsenic will have a greater effect on the aquatic ecosystem if it moves from lake bottom water up into oxic, near-surface waters. Arsenic enters the aquatic food web through phytoplankton and other primary producers that mistakenly uptake As(V) instead of phosphate (Sanders et al., 1989; Wang et al., 2013). Once it is in the food web, arsenic can reach upper trophic level organisms, such as finfish and crayfish, posing health risks to communities who

harvest and consume organisms from these systems (Hull et al., 2021). Because oxic, near-surface waters are often the most favorable habitat in terms of light, carbon dioxide and nutrient content for phytoplankton (Clegg et al., 2007), it is important to understand how arsenic released from bottom sediment gets transported into near-surface waters.

Physical lake characteristics, such as depth and mixing regime, influence the movement of contaminants and other constituents throughout the water column (Boyce et al., 1991; Read et al., 2012; Rueda et al., 2008). Specifically, the strength and duration of stratification determines whether contaminants that diffuse into the bottom waters will be mixed into near-surface, oxygenated waters. Previous research has shown that the movement of arsenic into oxygenated waters occurs in shallow, polymictic lakes, but not in deep seasonally stratified lakes (Barrett et al., 2019). There have been many attempts to define and classify polymictic lakes over the years (Hutchinson & Löffler, 1956; Kirillin & Shatwell, 2016; Lewis Jr., 1983); lake depth, latitude and water clarity are some characteristics that have been widely accepted as predictive factors of lake mixing regime (Kirillin & Shatwell, 2016; Lewis Jr., 1983). In addition, recent studies have advanced the mechanistic understanding of important processes in polymictic lakes, including the timescales of stratification and mixing events (Woolway et al., 2017; Yang et al., 2019), the effects of meteorological forcing on mixing dynamics (Xing et al., 2014), the formation of hypoxia (Cortés et al., 2021; Jalil et al., 2018), and internal loading of nutrients (Wilhelm & Adrian, 2008). Despite advances in the understanding of polymictic lakes, the influence of physical processes on the distribution of sediment-based contaminants is still poorly understood. Turbulence near the sediment water interface (SWI) could have complex interactions with the biogeochemistry of the sediment, such as altering the redox state around the SWI, and the subsequent rates of mobilization of arsenic and transport from porewaters to bottom water.

Furthermore, bottom turbulence could greatly enhance vertical transfer of arsenic compared to that from molecular diffusion alone. As wind and surface heating and cooling control mixing and stratification dynamics of the water column, these forcing mechanisms are expected to influence the distribution of arsenic throughout the lake.

While previous studies have clearly identified that arsenic cycling and biotic exposure to arsenic are different in shallow and deep lakes (Barrett et al., 2018, 2019; Hull et al., 2021), it remains unclear how polymictic lake mixing mechanisms interact with biogeochemical conditions to influence the mobilization of arsenic from sediments into porewater and the subsequent transport of arsenic throughout the water column. In this study we use a combination of hydrodynamic and biogeochemical measurements to understand the processes that maintain high arsenic concentrations in the upper water column of a shallow, arsenic contaminated lake. To address the identified knowledge gaps, we collected a 17 month-long data set of biogeochemical and physical parameters in Lake Killarney, a shallow, urban lake southeast of Seattle, WA in the south-central Puget Sound Lowland region. The goal of our study was to examine how physical lake characteristics, such as frequency of lake mixing, moderate biogeochemical processes and the arsenic distribution in the water column. To this end, we analyzed meteorological data in conjunction with lake temperatures, water column stratification, water column and porewater arsenic concentrations, and turbulent intensity. We demonstrate how elevated turbulent intensity from convective overturning events is a key factor in the transport of arsenic from anoxic, hypolimnetic waters to the upper waters of the lake.

2.3. Methods

2.3.1. Study site

Lake Killarney is a eutrophic, arsenic-contaminated lake in Federal Way, WA, USA (47°17'8.60" N, 122°17'32.20" W, elevation 111 m.). The lake is small and shallow, with a maximum depth of 4.6 m, mean depth of 2.6 m, surface area of 0.14 km^2 and watershed area of 0.93 km^2 (Barrett et al., 2018; Gawel et al., 2014). Much of the shoreline is wind-sheltered by surrounding houses and trees. Lake Killarney is divided into a smaller, shallow basin in the north that connects to a larger, shallow basin in the south (Fig. 2.2.1). The southern basin, where sampling took place, has minimal macrophyte coverage and is considered to be an algae-dominated system. The fetch of the southern basin is ~500 m. The lakebed sediments contain high concentrations of legacy arsenic that result in elevated bulk water arsenic concentrations; previous studies have measured bottom sediment and surface water concentrations of up to 206 $\mu g\ g^{-1}$ and 30 $\mu g\ L^{-1}$, respectively (Barrett et al., 2018; Gawel et al., 2014). These high surface water arsenic concentrations contrast observations of low surface water arsenic concentrations (< 5 $\mu g\ L^{-1}$) in a nearby, deep, lake with a similar level of arsenic in the bottom sediments (Barrett et al., 2019). Lake Killarney does not have significant inflow or outflow and, in some years, has thin surface ice cover for a small portion of the winter months.

2.3.2. Chemical parameter data collection

Data were collected from June 2018 through October 2019 close to the deepest part of the lake, following Barrett et al. (2018; 2019). The lake depth at the sampling station was approximately 4 m but had slight seasonal variation.

Lake Killarney was sampled monthly during the summer, spring, and early fall (June - September 2018, May - October 2019) and every two months in the winter (October 2018 - April

2019), except in February 2019 due to ice-over of the lake. On each sampling day, profiles of temperature and dissolved oxygen (DO) were measured using a sonde (In-Situ smarTROLL MP equipped with an optical Rugged Dissolved Oxygen sensor); tubing attached to the sonde and a peristaltic pump was used to collect filtered (0.45 μm Geotech cartridge) and unfiltered water samples. Water samples were acidified with 1% HNO_3 (v/v) and analyzed for total and dissolved arsenic using inductively-coupled plasma mass spectrometry (ICP-MS) with standard quality control as described in Barrett et al. (2018). Replicate water samples were taken at a depth of 2.5 m on each sampling day. Average water column arsenic concentration from replicate samples is used in this study; the standard deviation for replicate arsenic samples was on average 2.8% of the measured average value. Barrett et al. (2019) conducted speciation of arsenic in Lake Killarney on water samples collected from 2016-2017. We assume that arsenic speciation within the water column during our 2018-2019 study period is roughly consistent with that measured during the 2016-2017 period for discussion purposes only. A DO sensor (HOBO U26, 0.2 mg L^{-1} accuracy, Onset Computer Corporation, Bourne, MA, USA) was deployed in early 2018 in the lower water column and used to measure DO and temperature at a frequency of 15 minutes. Deployment depth was 2.5 m, or approximately 1 m above the lakebed in 2018. No DO data were recorded between May 1, 2019 and July 31, 2019 due to a deployment error. Starting in August 2019, the probe location was refined and placed at 40 cm above the lakebed to more accurately measure near-bed oxygen dynamics.

Passive diffusive porewater samplers (peepers) were used to measure arsenic profiles across the sediment-water interface following sampling methods from prior studies (Barrett et al., 2019; Belzile & Tessier, 1990; Palmer et al., 2021). Peepers held 14 vials at a vertical spacing of 3.5 cm, seven vials below the SWI and seven above (see Fig. S2 from Barrett et al., 2019, for

diagram and further information). Replicate vials were deployed at each depth; average arsenic concentration from replicate peeper samples is used in this study; the standard deviation for replicate peeper samples was on average 13% of the measured average value. The 5 mL vials were filled with a deoxygenated reverse tracer solution (200 μM KBr) to gauge progress toward equilibrium with the surrounding waters (Thomas & Arthur, 2010). Vials were kept deoxygenated until deployment using sealed bags with oxygen scavengers. Peepers were deployed from a boat and an underwater camera was used to confirm correct placement. Deployments occurred monthly from March-October and once every two months during intermittent winter periods and were two weeks in length allow the vial solution to equilibrate with the surrounding porewaters. Retrieved samples were acidified with 1% HNO_3 (v/v) after being transported back to the lab and analyzed via ICP-MS for total arsenic. Bromide concentrations were measured with an ion-selective electrode (Oakton by Cole-Parmer, Combination Bromide Ion-Selective Electrode) and used to correct ICP-MS measurements according to methods outlined in Thomas and Arthur (2010). Bromide concentrations indicated that all samples had reached equilibrium and thus arsenic corrections were negligible.

2.3.3. Physical parameter data collection

An array of in situ instruments was deployed for the 17-month sampling period to obtain a data set of physical parameters at high temporal frequency, including meteorological data, temperature profiles, and mean water velocities and turbulence. Temperature sensors (a combination of HOBO Pro v2 and HOBO Tidbit v2, both with accuracy of ±0.2 °C, Onset Computer Corporation, Bourne, MA, USA) recorded water temperature profiles every 10 minutes. Sensors were calibrated in ice-water before deployment. The string of loggers was anchored to the lake bottom by a cinder block and held taut by one or more surface buoys. From

June 20 - December 14, 2018, the temperature string had seven sensors located at z = 0, 1, 1.5, 2, 2.5, 3, and 3.5 m, where z = 0 m is the lakebed. Since the lake is generally fully mixed during winter months (Barrett et al., 2018), the number of temperature sensors was decreased between December 14, 2018 - May 28, 2019 to three sensors with z = 0, 1.5, and 3 m. On May 28, 2019, we returned to the previous seven-sensor configuration and on August 7, 2019, we added an additional sensor to the temperature string at a height of 0.5 m above the bed. The bottom temperature sensor was mounted within the cinder block anchor; the cinder block and bottom sensor were submerged in the lake sediment and provided a measure of sediment temperature.

Meteorological data were measured on a small bare island in the main lake basin (Fig. 2.2.1). Wind data were collected with a Davis wind speed and direction smart sensor (Davis Instruments Corporation, Hayward, CA, USA) mounted 2.4 m above the ground. A compass was used for initial direction calibration and data were collected at a frequency of 10 minutes. The instrument's wind speed accuracy is ±1.1 m s^{-1} or ±5% of the reading, whichever is greater; for wind direction, it has an accuracy of ±7 degrees. We used average hourly and daily wind speed in our analyses, which have propagated errors of ±0.44 m s^{-1} and ±0.092 m s^{-1}, respectively. During summer of 2019, a Kipp-Zonen (Delft, Netherlands) CMP3 pyranometer was used to measure downwelling shortwave (SW) radiation. Air temperature measurements were made using a HOBO Tidbit v2 from August through October 2019.

Water velocities were measured using an acoustic Doppler current profiler (ADCP, Nortek Signature 1000). The ADCP was attached to an L-shaped bracket on an aluminum pole at the water surface and positioned down-looking to capture full water column dynamics. Deployments were approximately three months in duration, except for the winter deployment, when we were unable to recover the ADCP until five months after its deployment due to ice-over of the lake.

The ADCP was configured to record 10-minute 'bursts' of data in high resolution mode (HR) every hour at 8 Hz to allow the instrument's battery to last for the duration of its deployments.

2.3.4. Data processing

Five-minute air temperature data from the SeaTac weather station (19 km north of Lake Killarney) recorded by the University of Utah's Department of Atmospheric Sciences (MesoWest) was obtained for the whole study period because in situ air temperature was only measured for a portion of the study period. In situ and SeaTac data were compared (August-October 2019) and in situ data were used to make a minor correction to the SeaTac data (Fig. A1.1, Eqn. A1.1). Shortwave radiation was sourced from Washington State University AgWeatherNet's Puyallup station (11 km southwest of Lake Killarney) for the whole deployment period and compared to in situ shortwave radiation from summer 2019; there was a 1:1 relationship between these two data sources (Fig. A1.2), so no correction was made to the AgWeatherNet data presented in Fig. 2.2c.

Using interpolated vertical temperature profiles, we calculated density profiles (IOC et al., 2010) and buoyancy frequency (N^2) profiles to characterize lake stratification.

$$N^2[s^{-2}] = \frac{g}{\rho}\frac{\Delta\rho}{\Delta z} \quad (Eqn.\ 1)$$

Where $\Delta\rho/\Delta z$ is the vertical density gradient between adjacent thermistors, g is gravity, and ρ is the density at the mid-distance between adjacent thermistors. Vertical turbulent intensity was calculated from the ADCP vertical velocity data. High resolution vertical velocity data (4 cm vertical cell resolution) from the ADCP's vertical beam were de-spiked and used to calculate hourly time-averaged vertical turbulent intensity, $\overline{(w')^2}$, where $w' = w - \overline{w}$, w is the instantaneous vertical velocity measurements and $\overline{w}$ is the average vertical velocity in each 10-

minute data collection burst. Because the turbulence in the lake is assumed to be isotropic and the turbulent eddies are not large enough to be coherent throughout the volume encompassed by the slanted beams of the ADCP, our vertical turbulent intensity will be used as a measure of the amount of turbulence in each measurement bin. The respective contribution of wind and convective forcing to elevated $\overline{(w')^2}$ was calculated from hourly wind, stratification, and vertical water velocity data. Windy and convective periods were defined and used to calculate mean weekly windy and convective $\overline{(w')^2}$ values; windy periods were defined as hours with a mean wind speed greater than 1 m s^{-1}, as no relationship between surface $\overline{(w')^2}$ and wind was seen with wind speeds below 1 (Fig. A1.3). Convective periods were defined as hours with unstable near-surface stratification (negative near-surface density gradient). A paired *t*-test with a significance level of 5% was used to test the statistical difference between windy and convective $\overline{(w')^2}$ during summer months (June - October), when arsenic mobilization was greatest.

Peeper data were used to calculate arsenic flux across the SWI. Flux calculations were based on Fickian diffusion and are thus conservative estimates, as the diffusive boundary layer in lakes has been shown to end approximately 5 mm above the SWI (Wüest & Lorke, 2003). The samples directly on either side of the SWI were used to define the concentration gradient (*dC/dz*). Following Hemond and Fechner (2014), a conservative Fickian transport coefficient of $D = 10^{-5}\ cm^2\ sec^{-1}$ was used to calculate the flux. Peeper data were also used to examine the effect of sediment temperature on arsenic mobilization and diffusion; samples between 5 and 20 cm (n = 4) on either side of the SWI were averaged to get representative measures of bottom water and porewater dissolved arsenic concentrations. Sediment temperature data were averaged during the corresponding deployment periods for comparison to dissolved arsenic.

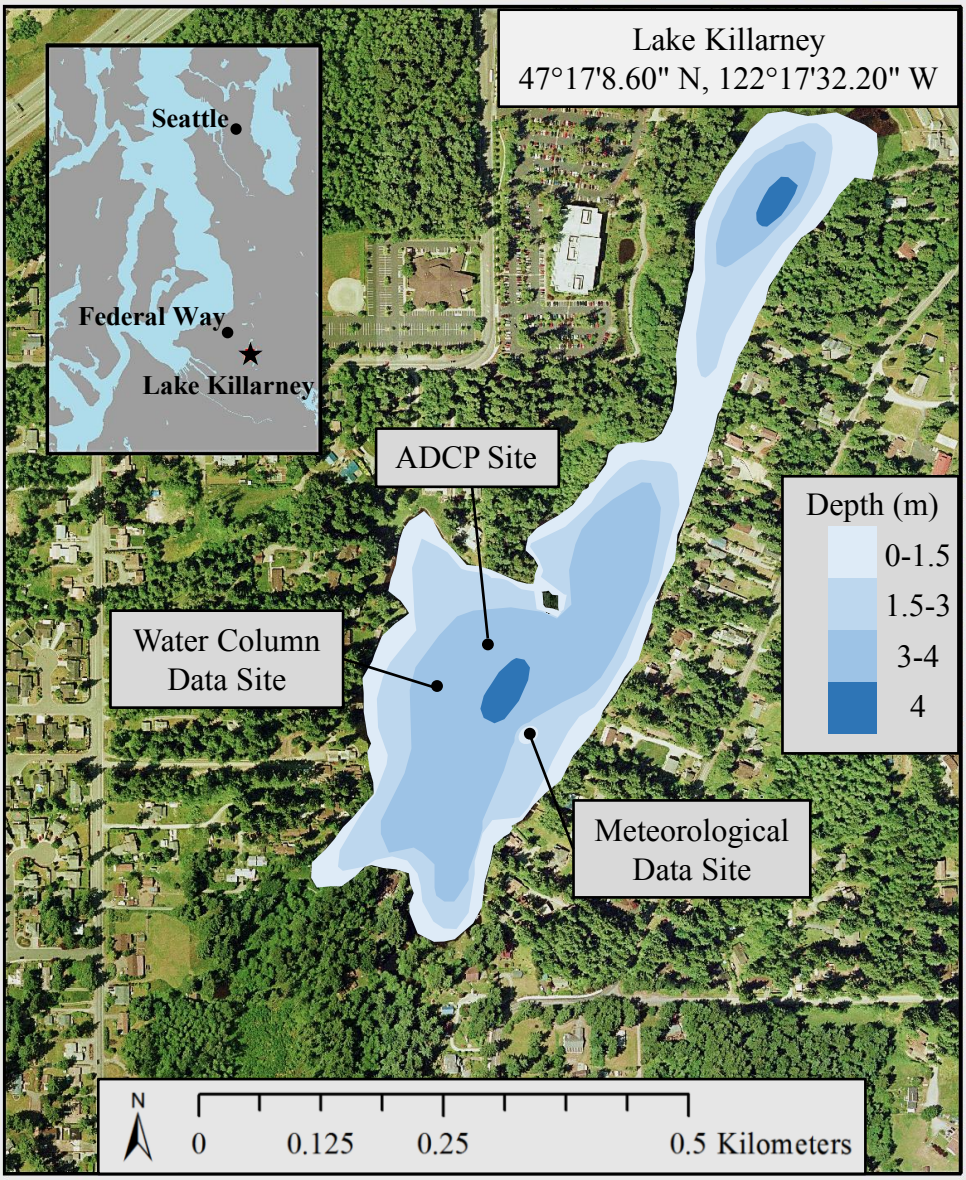

Figure 2.1. *Map of Lake Killarney, displaying the location of the lake in the surrounding region (inset) and the three field measurement sites.*

2.4. Results

2.4.1. Meteorological forcing

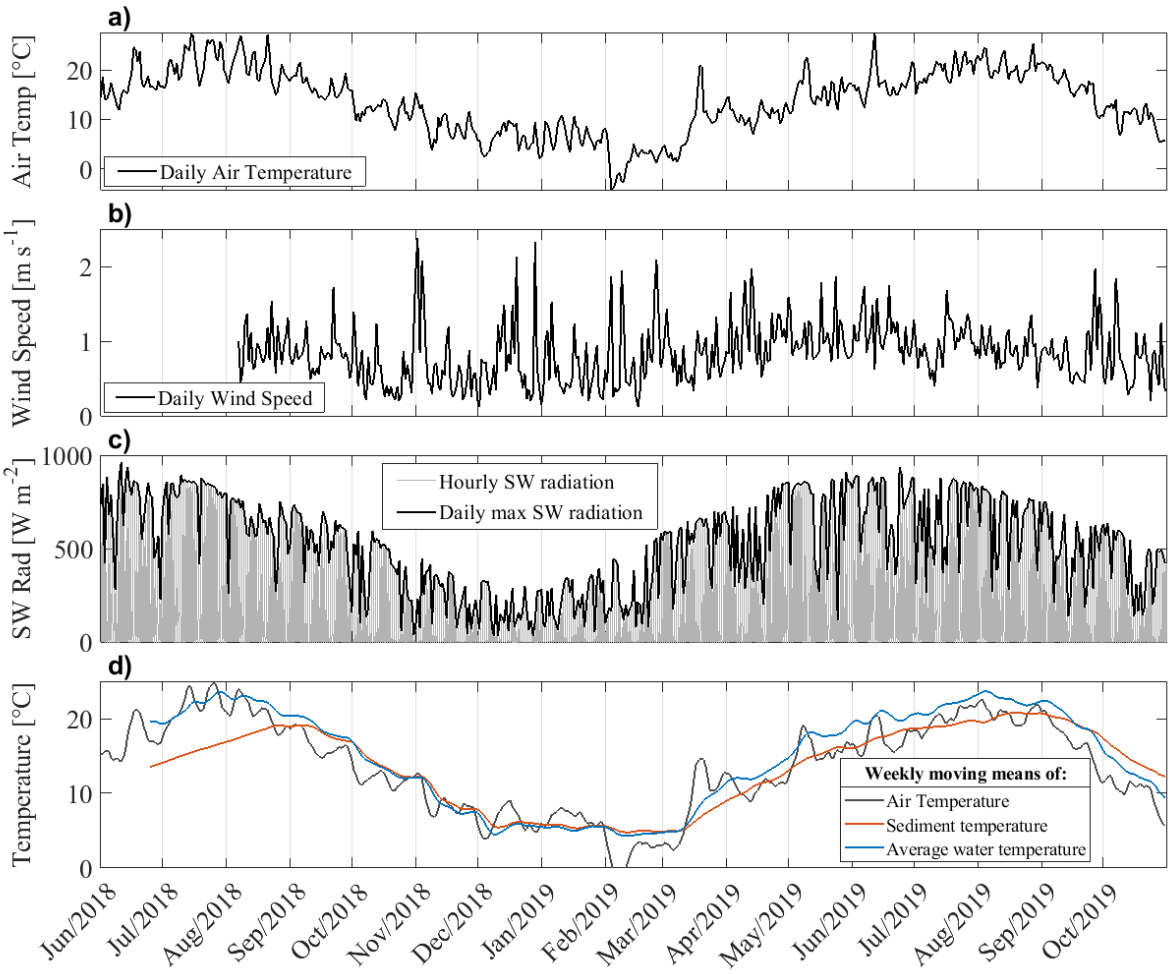

Figure 2.2. *Meteorological data during the study period. Time series of: (a) daily mean air temperature, (b) daily mean wind speed, (c) hourly and daily maximum incoming shortwave (SW) radiation, and (d) weekly moving means of air temperature, sediment temperature and average water temperature.*

The observational dataset captures two summer seasons (2018, 2019) as well as the fall, winter and spring in between. During this time, hourly wind speeds varied between 0 and 5.7 m s^{-1} (Fig. A1.4) with daily mean wind speeds reaching 2.4 m s^{-1} during fall storms (Fig. 2.2b). Incoming SW radiation peaked in mid-June and late June in 2018 and 2019, respectively, and the minimum SW radiation occurred in late December 2018 (Fig. 2.2c). Seasonal peaks in air and

water temperature lagged about a month behind that of incoming SW radiation, with patterns in air temperature leading those in water temperature by a few days to a week, depending on time of year. Air and water temperatures peaked in late July and early August in 2018 and 2019, respectively, and were at a minimum in February 2019 (Fig. 2.2d). Sediment temperature reached a maximum in early September in both 2018 and 2019, lagging approximately one month behind peaks in air and water temperature; sediment temperature tracked water temperature in the winter and was at a minimum during February 2019 (Fig. 2.2d). During the lake warming period (approximately March - August), the sediment was colder than the water and, in general, the air. However, the sediment either matched (2018) or became warmer (2019) than the average water temperature and warmer than the air temperature (both years) in early fall, presumably contributing to convection and mixing dynamics within the water column.

2.4.2. *Stratification and turbulence*

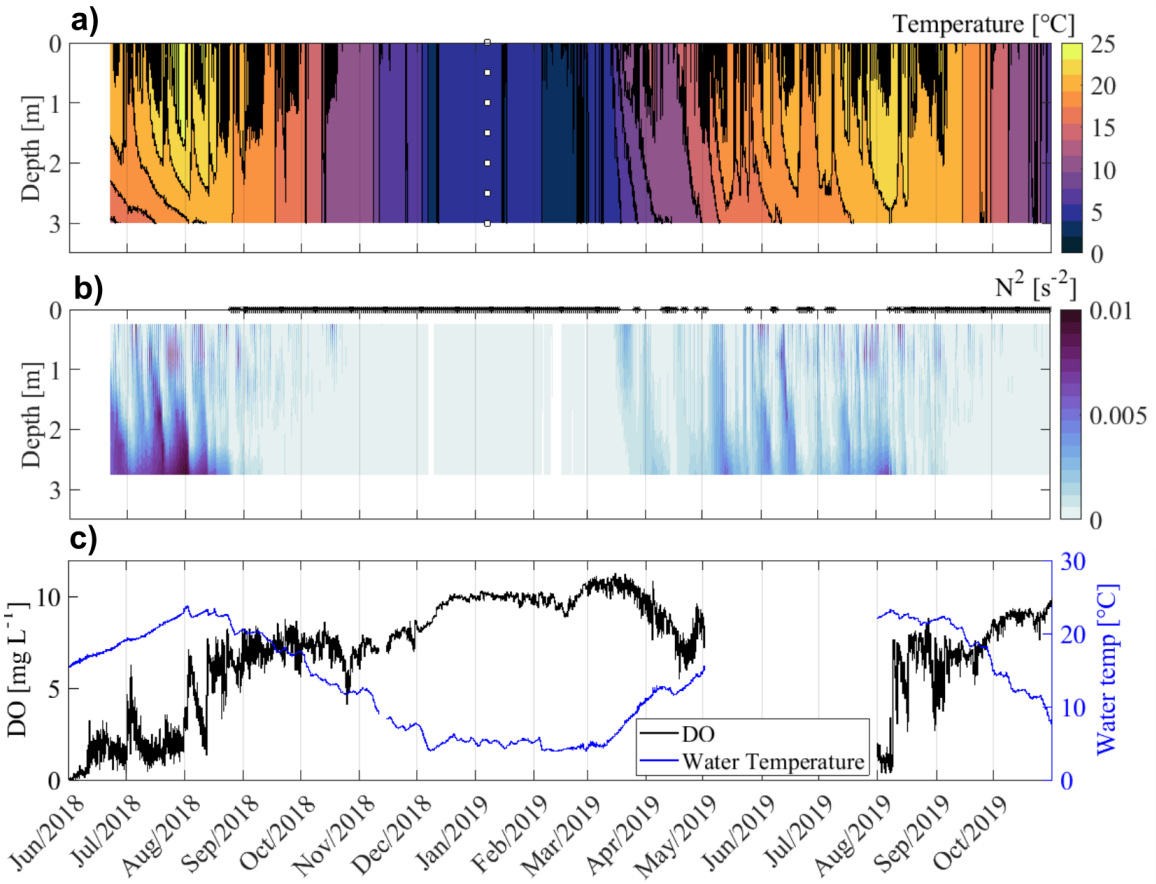

Figure 2.3. *(a) Lake temperatures; white dots indicate sensor placements. (b) Buoyancy frequency, N^2; black markers along the top axis indicate days when the lake experienced full convective overturning. (c) Hypolimnetic dissolved oxygen (DO) and water temperature measured by DO probe.*

Lake temperature structure and stratification are shown in Fig. 2.3a and 2.3b, respectively. Lake temperatures were consistently low (between 4 - 5 °C) from early December 2018 through early March 2019. The lake began to heat up in mid-March and had maximum surface temperatures from mid-July through mid-August in both summers. Water temperature homogenized and started cooling by late August. Strength of stratification (Fig. 2.3b) was seasonal, peaking in mid-summer (late July - early August) with N^2 values up to 0.01 s^{-2}. Summer stratification was episodic, where periods of stable stratification were interspersed with

mixing events that deepened the thermocline (Fig. 2.3a, 2.3b). Surface stratification set up most days, as shown in Fig. 2.6a and 2.6b. Stratification started to deteriorate in late summer and early fall, with weaker daytime stratification and full water column mixing occurring nightly. In the winter, N^2 values were small ($< 10^{-4}$ s^{-2}), indicating that the system remained well-mixed.

From these data, we identified three seasonal mixing patterns. From spring through mid-summer, the lake was stratified for week to month-long periods that were interspersed with episodic mixing events. From September through early November, the lake overturned frequently and generally exhibited a diel pattern of midday surface stratification and nightly convective mixing. During this late summer and early fall period, stratification was generally weaker (smaller N^2 values) than during the early summer period. Lastly, during winter months, the water column remained fully mixed, with occasional periods of weak surface stratification setting up midday.

Dissolved oxygen levels track patterns in stratification (Fig. 2.3c). During extended periods of stratification (June - July 2018), hypolimnetic DO was depleted and remained below 3 mg L^{-1}, except when a mixing event caused a temporary spike in bottom water DO (e.g. July 3, August 2, 2018 and August 9, 2019). In the late summer, when mixing was more frequent, DO concentrations oscillated daily, but were consistently higher (6 - 8 mg L^{-1}) than during spring and early summer. During the winter, DO concentrations were consistently elevated and ranged from mid to high-saturation (7 - 11 mg L^{-1}, where saturation ~ 12 mg L^{-1}).

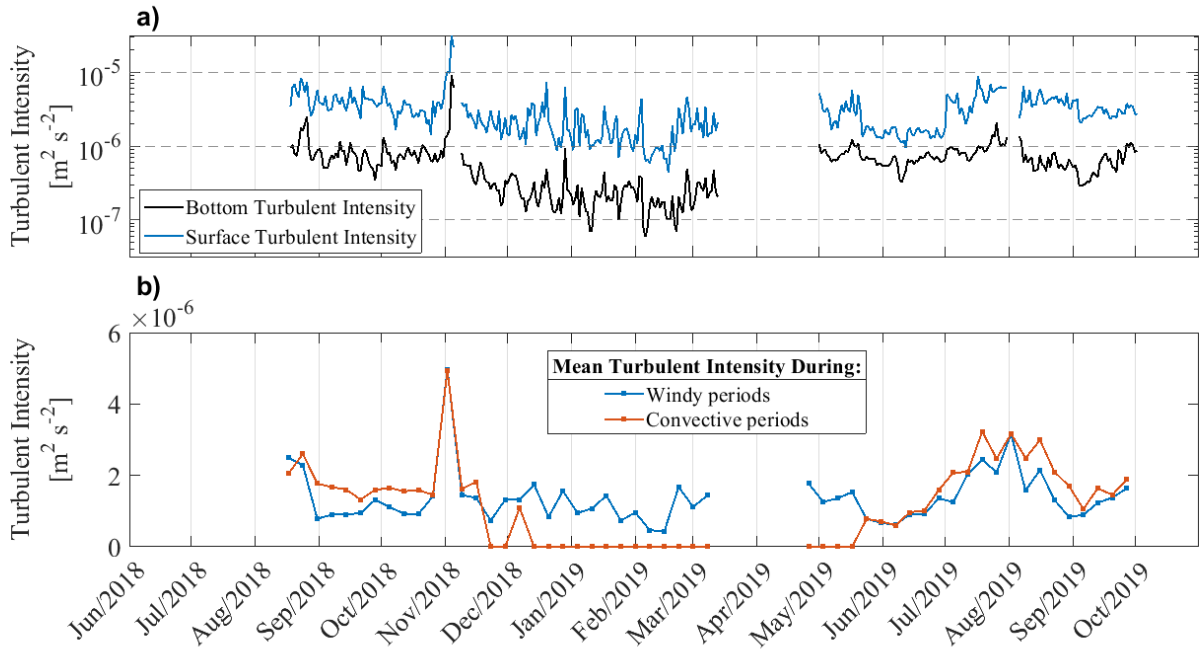

Figure 2.4. *(a) Bottom and surface vertical turbulent intensity measured using the vertical beam on the acoustic Doppler current profiler (ADCP). (b) Mean weekly vertical turbulent intensity during convective and windy periods (see methods). Periods with no data indicate times when the ADCP was not deployed.*

Turbulence in the water column varied seasonally, with average near-bottom turbulent intensity, $\overline{(w')^2}$, of ~1x10^{-6} during the spring, summer and fall and ~3x10^{-7} during winter. Further, time series of bottom and surface turbulent intensity show that near surface $\overline{(w')^2}$ was approximately one order of magnitude higher than bottom $\overline{(w')^2}$, indicating that the primary sources of turbulence production were at the surface (Fig. 2.4a). The similar short-term responses of near-surface and bottom turbulent intensity also point to common forcing mechanisms creating elevated turbulence throughout the whole water column; however, the lower values of $\overline{(w')^2}$ near the lake bottom demonstrate that $\overline{(w')^2}$ decreased with depth. To examine the forcing mechanisms driving turbulence production, $\overline{(w')^2}$ values were calculated during periods of high winds and during periods of convection (methods, Fig. 2.4b). During the summer and early fall, the mean daily turbulent intensity during convective periods was statistically higher than mean

daily turbulent intensity during windy periods (t = 5.99, df = 27 with P < 0.05), indicating that convective cooling was the leading cause of turbulent mixing during those periods. From mid-December through mid-May, no convective events were observed and convective $\overline{(w')^2}$ was zero. Instead, mixing during this period was forced solely by wind. The $\overline{(w')^2}$ spike that occurred at the beginning of November 2018 (Fig. 2.4a) represents a large storm event that resulted in both convection and high winds during the peak in $\overline{(w')^2}$ (Fig. 2.4b) and thus no singular forcing mechanism could be identified.

2.4.3. As and DO concentrations

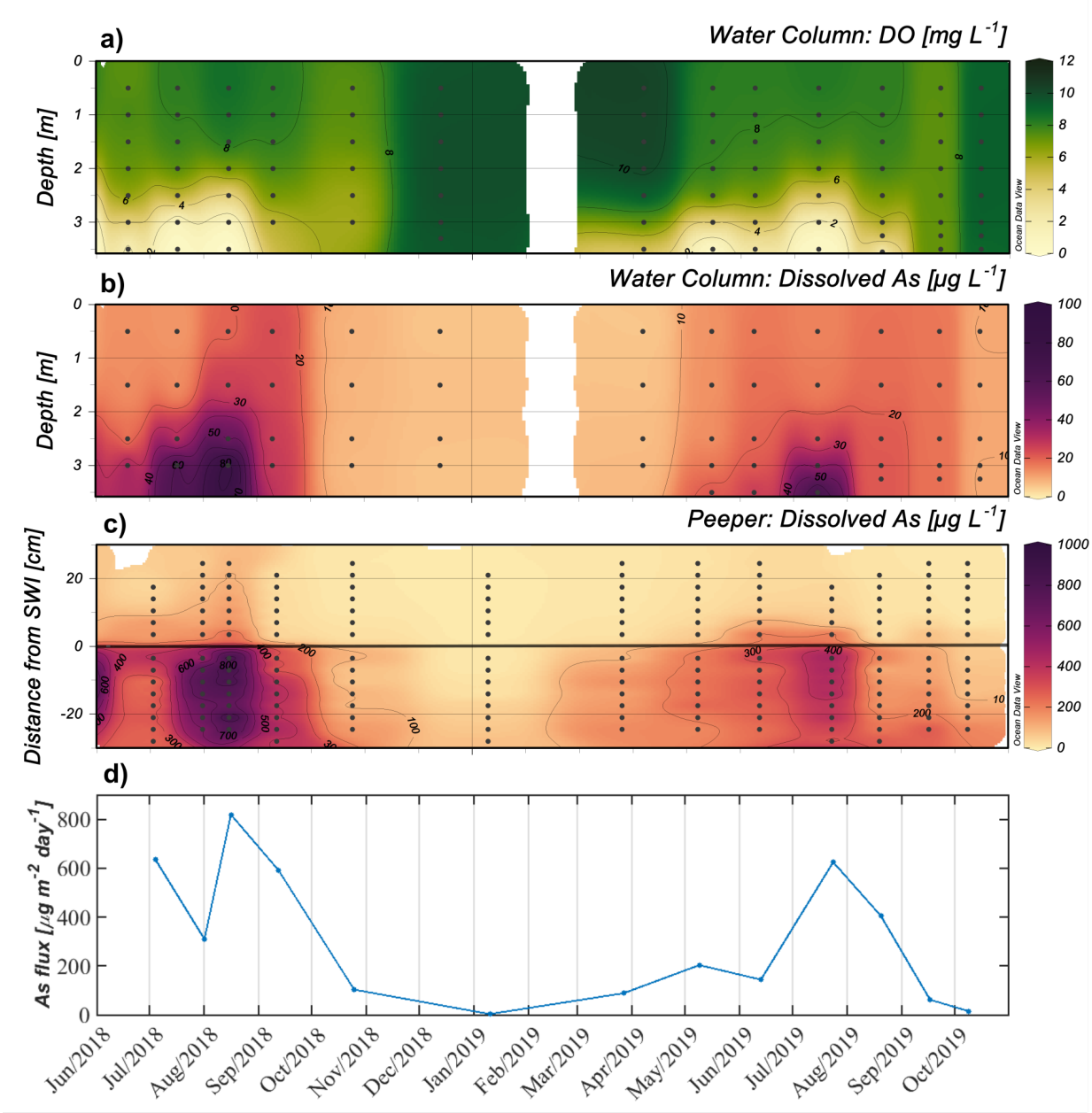

Figure 2.5. *Linearly interpolated profiles of (a) dissolved oxygen (DO) from ~monthly water sampling, (b) dissolved arsenic (As) from ~monthly water sampling, and (c) dissolved arsenic concentrations from 2-week peeper deployments; the thick black line indicates the sediment water interface (SWI). (d) Upward vertical flux of dissolved arsenic from porewaters to above the SWI. Note different y-scale for panel (c); positive values indicate measurements above the SWI and negative values indicate measurements in the sediment porewater. In panels a-c, black dots indicate sampling date and location. Date for peeper data (c and d) represents mid-point of the deployment. June 2018 values are interpolated between May 2018 data (not shown) and the first data point shown in this plot.*

We observe that aqueous arsenic concentrations were elevated (> 20 μg L^{-1}, defined as above background winter concentrations, which range from 5-13 mg L^{-1}) when bottom water DO was less than 4 mg L^{-1} (Fig. 2.5a and 5b); consequently, 4 mg L^{-1} was used as a threshold to identify time periods when the bottom water DO was low or high. In 2019, bottom water DO concentrations began to decrease in late spring (Fig. 2.5a) corresponding to the onset of lake heating and episodic periods of stratification (Fig. 2.3). Hypolimnetic anoxia continued to develop throughout the summer; its vertical extent peaked in mid-July, when bottom water was anoxic (< 1 mg L^{-1}, 1 m above the bed) and concentrations were low (< 4 mg L^{-1}) up to 1.5 m above the bed. By the end of September in both 2018 and 2019, when overturning was occurring nightly, water column DO was relatively high (> 6 mg L^{-1}) and largely homogenous.

Water column arsenic profiles (Fig. 2.5b) vary seasonally with concentrations ranging from background levels of ~5 μg L^{-1} during winter to a mid-summer peak of 89 μg L^{-1}. Data collected in 2016 and 2017 show that inorganic arsenic accounted for over 93% of the total water column arsenic throughout the seasons (Table A1.1). Arsenic was largely speciated as As(V) in the water column; specifically, As(V) accounted for an average of 76% of the inorganic arsenic and 73% of the total arsenic throughout the year (Table A1.1). Arsenic levels in the lake bottom water began to increase in late spring, about a month after the onset of reduced DO (Fig. 2.5a, Fig. 2.5b). Bottom water dissolved arsenic peaked in August and July; maximum values were 89 μg L^{-1} and 73 μg L^{-1} in 2018 and 2019, respectively. Bottom water dissolved arsenic remained elevated through August in 2018, while values in 2019 decreased after July. In near-surface waters (within 1.5 m of the surface), maximum levels of arsenic occurred in August and September, reaching 25 μg L^{-1} and 18 μg L^{-1} in 2018 and 2019, respectively (Fig. 2.5b). As seen most clearly during the August to September period in 2018, an increase in near-surface water

arsenic concentration coincided with a decrease in bottom water arsenic concentration (Fig. 2.5b, Fig. A1.5); this result suggests that mixing events distributed high concentration bottom waters throughout the lake and homogenized the water column.

Minimum porewater dissolved arsenic concentrations were < 10 μg L^{-1} in surficial sediments and < 80 μg L^{-1} in deeper sediments as observed in January 2019 (Fig. 2.5c, Fig. A1.6). Concentrations increased when sediment temperatures were elevated (Fig. 2.2d) and bottom water DO started to decrease; this pattern is visible in May 2019 (Fig. 2.5a, Fig. 2.5c). The initial increase in porewater concentrations was not captured in 2018, as concentrations were already elevated in June 2018 at the beginning of the measurement period. Porewater arsenic peaked in mid-summer, with values close to 1000 μg L^{-1} in 2018 and 500 μg L^{-1} in 2019. Bottom water and porewater arsenic maxima coincided, although the magnitude of concentrations in the bottom water was always lower than that in the porewater likely due to dilution of arsenic in the hypolimnion. Arsenic was elevated in the porewater for a longer period than it was in water above the SWI (Fig. 2.5b, Fig. 2.5c).

Peeper profiles, such as those plotted in Fig. 2.5c and Fig. A1.6, were used to calculate diffusive arsenic flux across the SWI (see methods). Arsenic flux out of the porewater peaked when porewater concentrations were at their highest (Fig. 2.5c, d). Flux values reached seasonal maxima in August of 2018, at 818 μg m^{-2} day^{-1}, and in July of 2019, at 623 μg m^{-2} day^{-1}. Timing of maximum flux values matched observations of high bottom water arsenic concentrations during these periods (Fig. 2.5b). By late summer, when mixing became more frequent (Fig. 2.3a) and oxygen concentrations started to increase (Fig. 2.3c), arsenic flux across the SWI started to decrease and was ~100 μg m^{-2} day^{-1} by mid-October in both years, which is below the mean flux of the data record, ~300 μg m^{-2} day^{-1}.

2.4.4. *Summertime patterns of stratification, As, and DO*

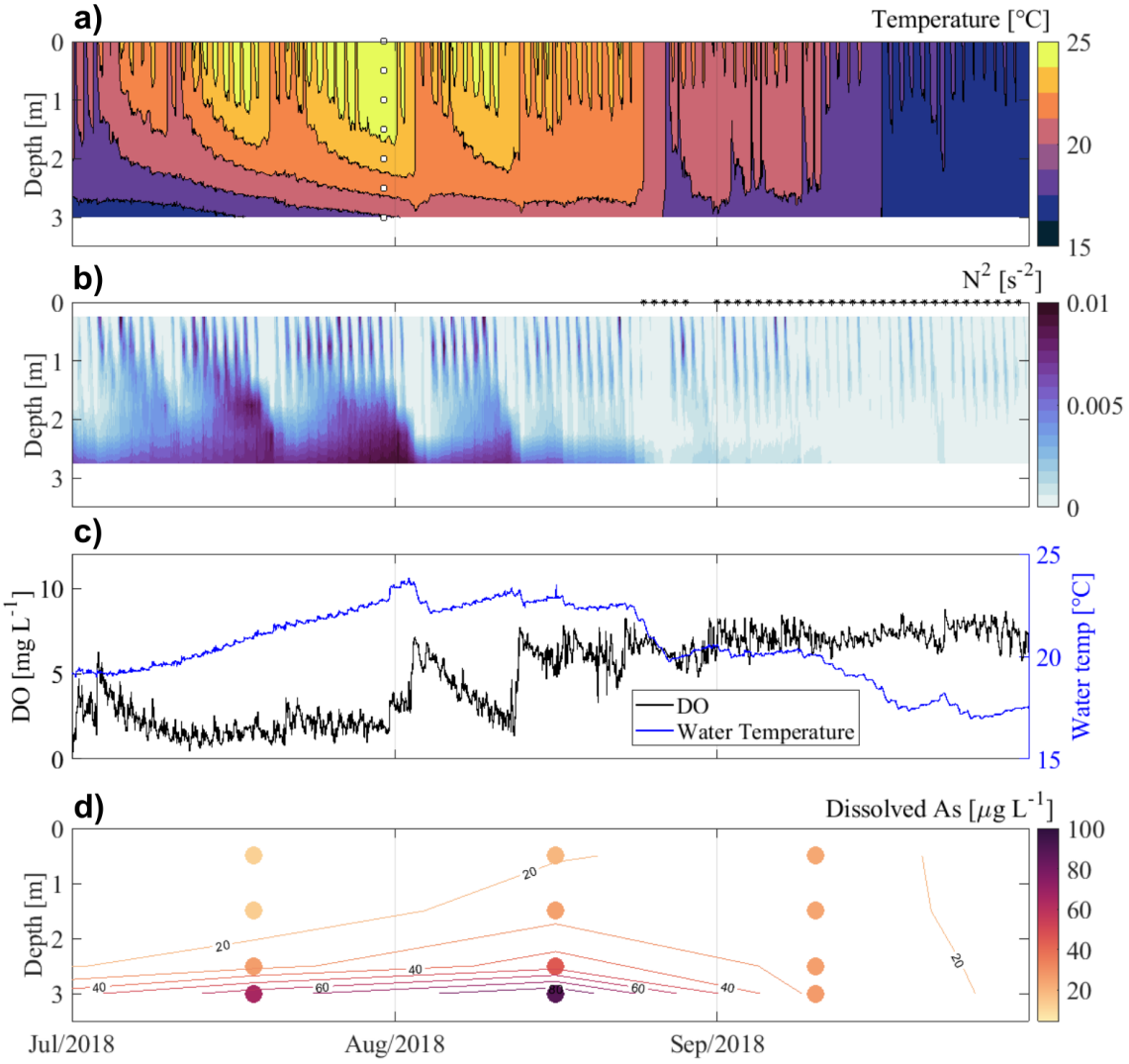

Figure 2.6. *Summertime 2018 plots of (a) lake temperatures (white dots indicate sensor placements), (b) buoyancy frequency, N^2 (black markers indicate days when the lake experienced full convective overturning), (c) hypolimnetic dissolved oxygen (DO) and water temperature measured by DO probe (probe deployment depth was 2.5 m, or approximately 1 m above the lakebed), and (d) water column dissolved arsenic profiles (dots) and contours.*

Arsenic concentrations in the lake water were highest from July through September (Fig. 2.5). In Fig. 2.6 we zoom in to this period in 2018, investigating how variations in temperature, stratification, and dissolved oxygen contributed to the observed distribution of arsenic in the water column. Lake heating occurred from early July through early August (Fig. 2.6a). During

this time, stratification set up in cycles, with strength of stratification increasing over approximately weeklong periods; periods of stratification were interrupted by intermittent mixing events (Fig. 2.6a, 2.6b). Bottom water stratification was relatively stable during the latter part of July, resulting in consistently low concentrations of bottom water DO ranging from 0.4 – 3.5 mg L^{-1} (Fig. 2.6c). Mixing events on August 2 and 13 resulted in bottom water DO spikes, indicating that the mixed layer deepened past a depth of 2.5 m, where the DO probe was located. Lake Killarney began to cool in late August; this cooling coincided with full mixing of the water column and homogenization of water temperatures, except during daytime heating (Fig. 2.6a). During September, daytime surface stratification weakened (Fig. 2.6b).

The distribution of arsenic throughout the water column varied during summer 2018 (Fig. 2.6d). In July, arsenic concentrations in the bottom water were elevated, but surface levels were low (< 20 µg L^{-1}). In August, concentrations increased throughout the water column and reached a bottom water maximum of ~90 µg L^{-1}. Surface water concentrations were elevated in August (> 20 µg L^{-1}) and stayed high through September. In contrast, bottom water concentrations decreased from August to September. Water column concentrations were homogenous in September and ranged from 23.4 – 26.6 µg L^{-1}.

2.4.5. Effects of sediment temperature and stratification on DO and As concentrations

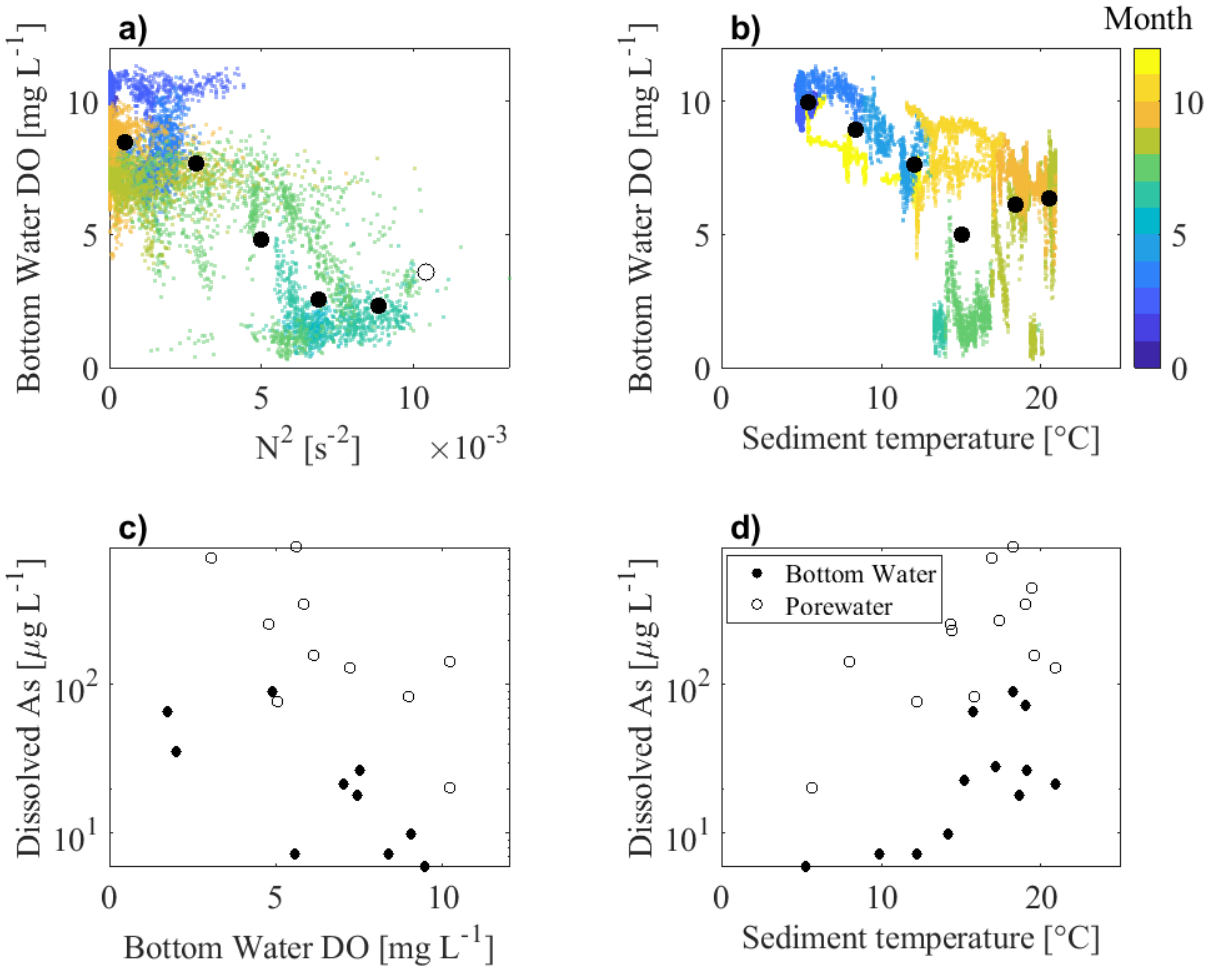

Figure 2.7. *a) N^2 vs. bottom water DO and b) sediment temperature vs. bottom water DO. For (a) and (b), colored points are raw data, with color denoting the month of the year the sample was taken. Bottom water DO was binned into 2x10^{-3} s^{-2} and 3.3 °C bins and shown with black dots in (a) and (b), respectively. The unfilled data point in (a) indicates potentially inaccurate binned data, due to the relatively small number of data points being averaged at high N^2 values. c) Bottom water DO vs. aqueous dissolved arsenic concentrations and d) sediment temperature vs. aqueous dissolved arsenic concentrations. For c) and d): open and closed circles indicate porewater and bottom water concentrations, respectively; see Table A1.2 for statistics.*

Stratification (N^2) was related to bottom water DO, where stronger stratification corresponded to lower DO concentrations (Fig. 2.7a). As seen in Fig. 2.3, weak stratification and high bottom water DO occurred during winter months, whereas stronger stratification and lower DO occurred during the summer. Bottom water DO also varied with sediment temperature (Fig.

2.7b); colder sediment temperature corresponded to greater bottom water DO concentrations. Low DO concentrations (< 4 mg L^{-1}) only occurred when bottom water temperatures were > 13 °C, but high DO concentrations also occurred in these warm temperature conditions. This behavior indicates that, during portions of the year with high temperatures, factors beyond temperature influenced DO.

As shown in Fig. 2.7c, lower DO corresponded to higher porewater and bottom water dissolved arsenic concentrations. Warmer temperatures were also associated with higher porewater and bottom water dissolved arsenic (Fig. 2.7d). Notably, bottom water arsenic concentrations were low (< 8 mg L^{-1}) when the sediment temperature was < 13 °C. Collectively, the results shown in Fig. 2.7 indicate that stratification, temperature, DO, and arsenic were interrelated, with stratification and temperature moderating DO and both temperature and DO impacting dissolved arsenic concentrations within the sediment porewater and lake water near the SWI.

Table 2.1. *For three 10-day periods: average sediment temperature, mixing regime, average bottom water DO,* $\Delta(DO)$*, or the rate of change of bottom water DO [mg* L^{-1} day^{-1}*] during the 10 days, bottom water [As], and* $\Delta(\text{Bottom water } [As])$*, or the change in bottom water dissolved arsenic concentration from the measurement prior to each period.*

	Sediment temperature [°C]	Mixing regime	DO [mg L^{-1}]	ΔDO [mg L^{-1} day^{-1}]	Bottom water [As] [μg L^{-1}]	Δ(Bottom water [As]) [μg L^{-1}]
Aug 2 – Aug 12, 2018	17.4	Stratified	4.2	-0.5	89.2	+ 23.8
September 1 – 11, 2018	19.1	Midday surface stratification; nightly full overturning	7.2	0.0	26.6	- 62.6
April 1 - April 11, 2019	9.6	Stratified	9.1	-0.1	7.2	+ 1.3

To parse out the previously observed relationships between temperature, bottom water DO, and arsenic concentrations (Fig. 2.7), we chose three 10-day periods out of the larger data set during which we examined physical and chemical lake characteristics (Table 2.1). Lake mixing

behavior and sediment temperature were at a steady state during each period, allowing us to look at how these factors affected rates of dissolved oxygen consumption and bottom water arsenic concentrations. Specifically, we look at how dissolved oxygen and arsenic concentrations change during periods of high sediment temperature and either stratification with episodic mixing (Table 2.1, August 2018) or diel overturning (Table 2.1, September 2018) as well as during periods of low sediment temperature and stratification with episodic mixing (Table 2.1, April 2019).

We observed that lake stratification combined with high temperatures facilitated the development of anoxic bottom waters and the build-up of dissolved arsenic in the hypolimnion (Table 2.1, August 2018). In contrast, high temperatures combined with frequent mixing led to constant, relatively high, DO concentrations and lower, but still elevated bottom water arsenic concentrations (Table 2.1, September 2018). The lake transitioned from being stratified to overturning nightly between the August and September periods; bottom water DO concentration increased by 3 mg L^{-1} while bottom water arsenic concentrations decreased by ~63 ug L^{-1}. We hypothesize that this decrease in bottom water arsenic concentration was caused by the mixing of hypolimnetic arsenic up into the upper water column combined with arsenic sequestration out of the oxic water column. During early spring, Lake Killarney experienced stratification, relatively low temperatures, and a slow rate of bottom water deoxygenation (Table 2.1, April 2019). These conditions suggest that the microbial rate of oxygen depletion was not fast enough at low temperatures to create reducing conditions in the bottom waters even during extended isolation of the hypolimnion. Early spring was thus characterized by high DO concentrations and low bottom water arsenic.

These data demonstrate that the co-occurrence of stratified conditions and warm temperatures was required for the development of elevated arsenic concentrations within bottom

water. Within the lakebed sediment, elevated temperatures facilitated arsenic mobilization into porewater (Fig. 2.7d). Elevated temperatures and sustained stratification allowed for the formation of low DO conditions in lake bottom waters (Fig. 2.6a, 2.6c), which allows arsenic mobilized from the sediment to diffuse into in the hypolimnion. In addition, low DO conditions minimize re-sequestration of dissolved arsenic back into the solid phase (Smedley & Kinniburgh, 2002). Contrastingly, if temperatures are not sufficiently high (April 2019) or mixing is frequent (September 2019), arsenic mobilization from sediment into porewater is minimized (Fig. 2.5c) and the lake bottom water will remain oxic (Fig. 2.5a), leading to low arsenic concentrations in bottom water.

2.5. Discussion

2.5.1. Summary

Our results clarify the conditions necessary for mobilization and transport of arsenic from lakebed sediment to near-surface lake water. We found that arsenic build up within the bottom water happened in the summertime and required the co-occurrence of stratified conditions and high sediment temperatures (Table 2.1). Transport of arsenic into near-surface waters depended on lake mixing. We observed three distinct mixing types: 1) multi-week periods of stratification interspersed with episodic mixing, 2) diel overturning, and 3) continuous mixing (Fig. 2.3). Mixing types 1 and 2 (episodic mixing and diel overturning) occurred during the summer when arsenic mobilization from sediment into porewater was greatest (June-October; Fig. 2.3, Fig. 2.5) and controlled the vertical profiles of dissolved oxygen and arsenic within the water column. From June through August, periods of stratification and elevated temperatures resulted in deoxygenation of lake bottom waters and the subsequent build-up of arsenic at the SWI (Fig. 2.5a, 2.5c). During September and October, the lake was characterized by a homogenous water

column with mid-saturation levels of oxygen and intermediate arsenic concentrations (Fig. 2.5). Highest near-surface arsenic concentrations occurred in August 2018 and September 2019, respectively. Finally, analysis of turbulence data demonstrates that thermal convection was the main source of vertical turbulent intensity in the bottom waters during summer months (Fig. 2.4b), and thus the dominant process driving the vertical transport of arsenic in the lake.

Through synthesis of the key findings summarized above, we find that the occurrence of elevated arsenic concentrations in near-surface waters of Lake Killarney required the coexistence of several environmental conditions and a specific sequence of biogeochemical and physical processes (Fig. 2.8). First, the sediment temperature had to be high enough to allow for sufficient microbial activity to both mobilize arsenic from sediment into porewater and consume oxygen within the water column (Fig. 2.8i). Additionally, stratification of the water column had to be sustained for long enough for bottom water oxygen levels to be reduced (Fig. 2.8, (1) and (2)) and allow dissolved arsenic mobilized from the sediments to build up within the hypolimnion. This stratification regime occurred from mid-May to early September during which time the lake remained stratified for periods ranging from a few days to 6 weeks. Lastly, full lake mixing was required to cause turbulent transport of arsenic to near-surface waters (Fig. 2.8ii and (3)). Full overturning was convection-driven (Fig. 2.8ii) and, from mid-May to early September, occurred episodically.

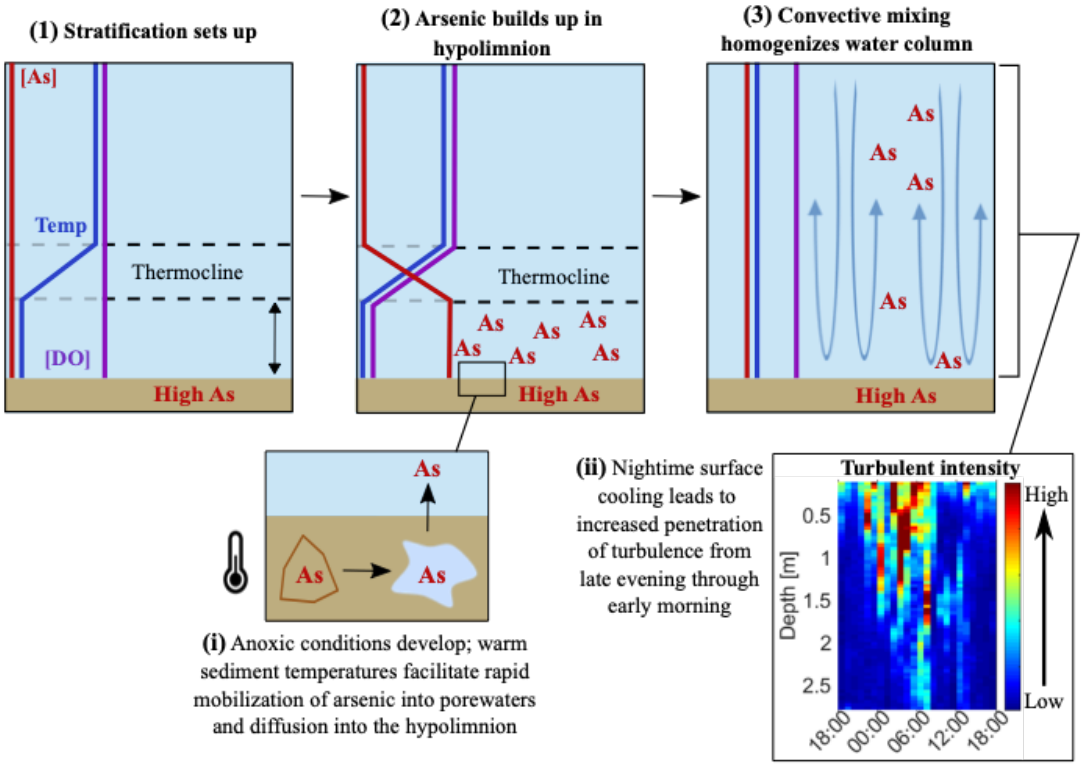

Figure 2.8. *Schematic of processes that lead to high near-surface arsenic concentrations. Red, blue, and purple profiles in three top panels represent dissolved arsenic, temperature, and dissolved oxygen levels, respectively, in the water column. Surface and bottom water are defined as above and below the thermocline, respectively. (1) Thermal stratification sets up; initially, dissolved oxygen concentration is high and dissolved arsenic concentration is low throughout the water column. (2) After a period of sustained stratification, dissolved oxygen depletes in the hypolimnion. Dissolved arsenic being mobilized from the sediments (i) diffuses into bottom waters and builds up in the hypolimnion. In the well-mixed surface layer, dissolved oxygen concentrations remain high and arsenic concentrations remain low. (3) A full lake convective mixing event (ii) homogenizes the water column and elevated turbulent intensity causes mixing of arsenic-loaded, hypoxic bottom waters into near-surface waters. Temperature, dissolved oxygen concentrations and arsenic concentrations are all intermediate.*

2.5.2. Dependence of arsenic mobilization on stratification, dissolved oxygen, and temperature

Arsenic mobilization, a microbially-mediated process, is sensitive to both temperature and redox conditions (Fig. 2.7). At high temperatures, increased rates of microbial respiration expedite the production of reducing conditions (Ratkowsky et al., 1982) and the mobilization of arsenic (Table 2.1) through elevated rates of microbe-mediated reductive dissolution of oxide

minerals (Aurilio et al., 1994; Nickson et al., 2000; Weber et al., 2010). We observed low bottom water DO and high bottom water arsenic only when the sediment temperatures were > 13 °C (Fig. 2.7). This finding confirms and refines the results from Barrett et al. (2019) in which temperature was shown to be a key control in the mobilization of arsenic into lake bottom water.

To create a low-DO environment, rates of microbial oxygen consumption must be fast enough to deoxygenate the hypolimnion during periods of stratification; in Lake Killarney, this situation only occurred in the summer when temperatures were high enough to support microbial activity at a rate that depleted oxygen (e.g., August 2018, Table 2.1) during the week to multi-week periods of stratification we observed. In contrast, when temperatures were cooler (e.g., April 2019, Table 2.1), the rate of oxygen consumption was slow (-0.11 mg L^{-1} day^{-1}), such that it would have taken ~three months for the hypolimnion to transition from full oxygen saturation to hypoxia. This pattern of anoxia development during transient summer stratification is likely important to the cycling of redox sensitive molecules in other shallow, temperate lakes. It is noteworthy that in lakes with different climate, hypoxia can form and support high aqueous arsenic concentrations during extended periods of wintertime ice cover despite cold temperatures (Palmer et al., 2019). Differences in the composition of microbial communities, which has been shown to vary in lakes across regions and according to environmental variations (Yannarell & Triplett, 2005), likely affects the relationship between temperature and oxygen consumptions rates. For example, microbes in arctic lake sediments may have special adaptations for thriving in cold environments (Ruuskanen et al., 2020) and thus could have high respiration rates at cold temperatures.

Despite sediment temperatures remaining high (> 13 °C) through September in both 2018 and 2019, dissolved arsenic concentrations began to decrease when nighttime convective mixing

became the norm (Fig. 2.2d, Fig. 2.3, Fig. 2.5b) and allowed for regular oxygenation of lake bottom waters. Oxic bottom water can facilitate oxidation of the sediment-water interface, transformation of dissolved Fe(II) into particulate Fe(III), and oxidation of arsenite into arsenate. All three of these processes facilitate arsenic sorption, which is a known mechanism for arsenic sequestration within Lake Killarney (Barrett et al., 2019). Significantly, these results show that lake mixing not only controls how arsenic released into bottom waters is distributed vertically throughout the water column, but also the residence time of arsenic within the water column. Because rates of arsenic scavenging and resorption are not well defined in natural systems, a closer examination into short term (daily and weekly) arsenic dynamics in lake waters is required for developing an understanding of the residence time of dissolved arsenic in the surface waters of lakes.

2.5.3. Vertical turbulent mixing of arsenic

During periods of elevated arsenic mobilization from sediment into porewater (June-October, Fig. 2.5c), convection was the largest source of elevated vertical turbulence (Fig. 2.4b). Studies on air-water gas exchange have similarly concluded that convection disproportionately controls vertical mixing in small lakes (MacIntyre & Melack, 1995; Read et al., 2012). Because these previous studies mainly focused on parsing out the effects of convection on the surface mixed layer, our observations expand these findings, showing that convection has a substantial effect not only on surface layer dynamics, but also on chemical processes within the lake sediment, porewater, and bottom water. Our results show that enhanced turbulent intensity near the SWI impacts the biogeochemistry and mobility of the sediment, and thus the mobilization of arsenic from sediment and diffusion into lake bottom waters. Resuspension of oxic surface sediment has been previously investigated as a potential source of increased dissolved arsenic concentrations

in shallow lakes through lab experiments (Linge & Oldham, 2002). In the field, reducing, and therefore arsenic-mobilizing, conditions have been shown to form 5-10 cm below the SWI (Martin & Pedersen, 2002) and our profiles of porewater arsenic suggest that reducing conditions may be present in Lake Killarney adjacent to the SWI, especially during summer months (Fig. 2.5c). Thus, depending on the degree to which sediment is resuspended, nightly convective overturning could cause regular resuspension of both oxic and anoxic sediments and porewater and greatly impact water column dissolved arsenic. Qualitative inspection of acoustic Doppler current profiler (ADCP) data show an increase in near bottom acoustic backscatter and bottom stress during periods of strong convectively driven $\overline{(w')^2}$, suggesting that convective plumes may indeed stir up easily erodible bed material (Fig. A1.7). Thus, arsenic transfer to near surface waters via re-suspension of sediments is probable in Lake Killarney due to its shallow depth and our observations of frequent full lake mixing during summer periods. However, our measurements show that almost all arsenic in bulk waters is dissolved (Fig. A1.8). It is possible that arsenic mixed into upper waters due to sediment resuspension at night settled out of the water column before sampling occurred during daylight hours; additional sampling of dissolved and total water column arsenic concentrations during lake convective mixing would be needed to confirm this hypothesis. Calculating the turbulent diffusivity of arsenic, a process beyond the scope of this study, is an avenue of investigation that should be further examined in order to understand how mixing processes contribute to the movement of arsenic from porewaters to the upper lake waters.

2.5.4. Seasonal patterns

Our observations suggest that trends in sediment heating and cooling strongly influenced water column stability, frequency of convective overturning, and the distribution of mobilized

arsenic in lake water. In Lake Killarney, air, water, and sediment temperature were relatively well coupled (Fig. 2.2d), in contrast to larger lakes where water temperature often lags patterns in air temperature (Arhonditsis et al., 2004; McCombie, 1959). This coupling in temperature, especially in 2019, indicates that frequent lake mixing and heat exchange with the atmosphere likely occurred. Importantly, the tight link between meteorological conditions, lake, and lakebed temperatures (Fig. 2.2) allows for prediction of the timing of arsenic release given the important role that temperature plays in the mobilization of arsenic, as demonstrated in Fig. 2.7, and reported previously by Barrett et al. (2019). The onset of arsenic release into hypolimnetic waters (Fig. 2.5b) occurred in June of 2018 and 2019, coinciding with the formation of periodic stratification (Fig. 2.3a), elevated sediment temperatures (Fig. 2.2d), and reduced bottom water DO (Fig. 2.5a). Buildup of other dissolved constituents resulting from low DO has been observed in hypolimnetic waters in other shallow lakes during periods of stratification with episodic mixing; for example, MacIntyre and Melack (1995, 1988) posited that high concentrations of bottom water methane were caused by infrequent deep water mixing events in a shallow tropical lake and Wilhelm and Adrian (2008) examined pulses in phosphorus caused by alternating stratification and mixing events.

Soon after sediment temperature peaked and began to steadily decrease (late August, Fig. 2.2d), full lake mixing became more frequent and the lake settled into a diel cycle of midday surface stratification and nighttime convective mixing (Fig. 2.3a, Fig. 2.6a). This timing demonstrates that the combination of warm bottom sediments and cool air temperatures facilitates nighttime overturning. Similar diel variability has been seen in other shallow lakes (Holgerson et al., 2016; MacIntyre et al., 2018) and has implications for gas efflux as well as mobilization and movement of sediment contaminants, as observed in our work. Bottom water

oxygen levels remained high (~7 mg L^{-1}) during these late summer months in Lake Killarney (Fig. 2.6), despite elevated sediment temperatures presumably supporting high biological demand for DO (Solanki et al., 2007). The elevated hypolimnetic DO concentrations during this warm period demonstrate the ability of convective mixing to not only induce rapid gas exchange at the air-water interface, as shown in Holgerson et al. (2016), but also to transport oxygen-rich surface water down to lake bottom waters. Further, high bottom water DO likely caused increased rates of adsorption and scavenging of arsenic from the water column (de Vitre et al., 1991) and led to the lower water column arsenic concentrations observed during September and October (Fig. 2.5b, Fig. 2.6d). During the winter, sediments were cold (< 13 °C), and the water column remained fully mixed (Fig. 2.3a), resulting in low levels of arsenic flux out of the sediment (Fig. 2.5d) and low water column concentrations (Fig. 2.5b). Findings in Barringer et al. (2011) likewise observed low levels of lake water dissolved arsenic in winter months.

2.5.5. Study implications

We observed and characterized seasonal patterns of the biogeochemical and physical processes that control the mobilization and distribution of arsenic in a shallow, temperate lake. Patterns of lake stratification and mixing are key factors in controlling bottom and surface water dissolved arsenic concentrations, especially during summertime periods of high arsenic mobilization from sediment into sediment porewaters. Because lake depth largely controls the degree of summer stratification and frequency of full lake mixing, these findings provide a mechanistic understanding for why legacy arsenic contamination leads to higher arsenic concentrations in near-surface waters of shallow, polymictic lakes compared to deep, dimictic lakes. Elevated arsenic concentrations in near-surface waters lead to uptake into the aquatic food web (Hull et

al., 2021); thus, our study explains the disparate impacts legacy arsenic contamination has on shallow and deep lake ecosystems in temperate climates.

Increased knowledge of the behavior of arsenic in shallow, temperate lakes is useful for lake management and hazard advisories and may be applicable in systems containing other redox-sensitive sediment contaminants. Because lake biota preferentially inhabit near-surface waters, we conclude that the greatest potential for arsenic entry into the food web occurs in temperate lakes where the highest surface water arsenic concentrations overlap with the peak growing season of primary producers. In contrast, high latitude polymictic lakes that experience highest aqueous arsenic concentrations in the winter (Palmer et al., 2019) have less potential for harmful ecosystem impacts. Classifying contaminated systems based on depth and strength of forcing mechanisms is needed to systematically determine which lakes are most sensitive to legacy arsenic. This study's contribution to the understanding of physical and biogeochemical factors controlling arsenic mobilization and mixing throughout shallow lakes could also aid in the development of a screening tool for efficiently identifying lakes of concern and choosing where to focus remediation efforts.

2.6. References

Arhonditsis, G. B., Brett, M. T., DeGasperi, C. L., & Schindler, D. E. (2004). Effects of climatic variability on the thermal properties of Lake Washington. *Limnology and Oceanography*, *49*(1), 256–270. https://doi.org/10.4319/lo.2004.49.1.0256

Aurilio, A. C., Mason, R. P., & Hemond, H. F. (1994). Speciation and Fate of Arsenic in Three Lakes of the Aberjona Watershed. In *Environ. Sci. Technol* (Vol. 28). https://pubs.acs.org/sharingguidelines

Barrett, P. M., Hull, E. A., Burkart, K., Hargrave, O., McLean, J., Taylor, V. F., Jackson, B. P., Gawel, J. E., & Neumann, R. B. (2019). Contrasting arsenic cycling in strongly and weakly stratified contaminated lakes: Evidence for temperature control on sediment–water arsenic fluxes. *Limnology and Oceanography*, *64*(3), 1333–1346. https://doi.org/10.1002/lno.11119

Barrett, P. M., Hull, E. A., King, C. E., Burkart, K., Ott, K. A., Ryan, J. N., Gawel, J. E., & Neumann, R. B. (2018). Increased exposure of plankton to arsenic in contaminated weakly-stratified lakes. *Science of the Total Environment*, *625*, 1606–1614. https://doi.org/10.1016/j.scitotenv.2017.12.336

Barringer, J. L., Szabo, Z., Wilson, T. P., Bonin, J. L., Kratzer, T., Cenno, K., Romagna, T., Alebus, M., & Hirst, B. (2011). Distribution and seasonal dynamics of arsenic in a shallow lake in northwestern New Jersey, USA. *Environmental Geochemistry and Health*, *33*(1), 1–22. https://doi.org/10.1007/s10653-010-9289-7

Belzile, N., & Tessier, A. (1990). Interactions between arsenic and iron oxyhydroxides in lacustrine sediments. *Geochimica et Cosmochimica Acta*, *54*(1), 103–109. https://doi.org/10.1016/0016-7037(90)90198-T

Boyce, F. M., Schertzer, W. M., Hamblin, P. F., & Murthy, C. R. (1991). *Behaviour of Lake Ontario with Reference to Contaminant Pathways and Climate Change*.

Caumette, G., Koch, I., Estrada, E., & Reimer, K. J. (2011). Arsenic speciation in plankton organisms from contaminated lakes: Transformations at the base of the freshwater food chain. *Environmental Science and Technology*, *45*(23), 9917–9923. https://doi.org/10.1021/es2025092

Clegg, M. R., Maberly, S. C., & Jones, R. I. (2007). Behavioral response as a predictor of seasonal depth distribution and vertical niche separation in freshwater phytoplanktonic flagellates. *Limnology and Oceanography*, *52*(1), 441–455. https://doi.org/10.4319/lo.2007.52.1.0441

Cortés, A., Forrest, A. L., Sadro, S., Stang, A. J., Swann, M., Framsted, N. T., Thirkill, R., Sharp, S. L., & Schladow, S. G. (2021). Prediction of Hypoxia in Eutrophic Polymictic Lakes. *Water Resources Research*, *57*(6). https://doi.org/10.1029/2020WR028693

de Vitre, R., Belzile, N., & Tessier, A. (1991). Speciation and adsorption of arsenic on diagenetic iron oxyhydroxides. *Limnology and Oceanography*, *36*(7), 1480–1485. https://doi.org/10.4319/lo.1991.36.7.1480

Frindte, K., Eckert, W., Attermeyer, K., & Grossart, H. P. (2013). Internal wave-induced redox shifts affect biogeochemistry and microbial activity in sediments: A simulation experiment. *Biogeochemistry*, *113*(1–3), 423–434. https://doi.org/10.1007/s10533-012-9769-1

Gawel, J. E., Asplund, J. A., Burdick, S., Miller, M., Peterson, S. M., Tollefson, A., & Ziegler, K. (2014). Arsenic and lead distribution and mobility in lake sediments in the south-central Puget Sound watershed: The long-term impact of a metal smelter in Ruston, Washington, USA. *Science of the Total Environment*, *472*, 530–537. https://doi.org/10.1016/j.scitotenv.2013.11.004

Hemond, H. F., & Fechner, E. J. (2014). *Chemical Fate and Transport in the Environment*. https://books.google.com/books?hl=en&lr=&id=zbRHAwAAQBAJ&oi=fnd&pg=PP1&dq=Hemond,+H.+F.,+and+E.+J.+Fechner.+2014.+&ots=Yl9QleF2ee&sig=k-PJeUuSdHDXwSURQUtd6CgQSV4#v=onepage&q=Hemond%2C%20H.%20F.%2C%20and%20E.%20J.%20Fechner.%202014.&f=false

Holgerson, M. A., Zappa, C. J., & Raymond, P. A. (2016). *Substantial overnight reaeration by convective cooling discovered in pond ecosystems*. *2*, 8044–8051. https://doi.org/10.1002/2016GL070206.Received

Hull, E. A., Barajas, M., Burkart, K. A., Fung, S. R., Jackson, B. P., Barrett, P. M., Neumann, R. B., Olden, J. D., & Gawel, J. E. (2021). Human health risk from consumption of aquatic species in arsenic-contaminated shallow urban lakes. *Science of the Total Environment*, *770*, 145318. https://doi.org/10.1016/j.scitotenv.2021.145318

Hutchinson, G. E., & Löffler, H. (1956). The Thermal Classification of Lakes. In *Joint Task Force One, on Biological Aspects of Atomic Bomb Tests* (Vol. 39).

IOC, SCOR, & IAPSO. (2010). *The international thermodynamic equation of seawater - 2010: Calculation and use of thermodynamic properties. Manual and Guides No. 56. Intergovernmental Oceanographic Commission, UNESCO (English).*

Jalil, A., Li, Y., Du, W., Wang, W., Wang, J., Gao, X., Khan, H. O. S., Pan, B., & Acharya, K. (2018). The role of wind field induced flow velocities in destratification and hypoxia

reduction at Meiling Bay of large shallow Lake Taihu, China. *Environmental Pollution*, *232*, 591–602. https://doi.org/10.1016/j.envpol.2017.09.095

Kirillin, G., & Shatwell, T. (2016). Generalized scaling of seasonal thermal stratification in lakes. In *Earth-Science Reviews* (Vol. 161, pp. 179–190). Elsevier B.V. https://doi.org/10.1016/j.earscirev.2016.08.008

Lewis Jr., W. M. (1983). A Revised Classification of Lakes Based on Mixing. *Canadian Journal of Fisheries and Aquatic Sciences*, *40*(10), 1779–1787. https://doi.org/10.1139/f83-207

Linge, K. L., & Oldham, C. E. (2002). Arsenic Remobilization in a Shallow Lake. *Journal of Environmental Quality*, *31*(3), 822–828. https://doi.org/10.2134/jeq2002.8220

MacIntyre, S., Crowe, A. T., Cortés, A., & Arneborg, L. (2018). Turbulence in a small arctic pond. *Limnology and Oceanography*, *63*(6), 2337–2358. https://doi.org/10.1002/lno.10941

MacIntyre, S., & Melack, J. (1995). *Vertical and horizontal transport in lakes : linking littoral, benthic, and pelagic habitats*. *14*(4), 599–615.

MacIntyre, S., & Melack, J. M. (1988). Frequency and depth of vertical mixing in an Amazon floodplain lake (L. Calado, Brazil). *SIL Proceedings, 1922-2010*, *23*(1), 80–85. https://doi.org/10.1080/03680770.1987.11897906

Martin, A. J., & Pedersen, T. F. (2002). Seasonal and interannual mobility of arsenic in a lake impacted by metal mining. *Environmental Science and Technology*, *36*(7), 1516–1523. https://doi.org/10.1021/es0108537

McCombie, A. M. (1959). Some Relations Between Air Temperatures and the Surface Water Temperatures of Lakes. *Limnology and Oceanography*, *4*(3), 252–258. https://doi.org/10.4319/lo.1959.4.3.0252

Nickson, R. T., Mcarthur, J. M., Ravenscroft, P., Burgess, W. G., & Ahmed, K. M. (2000). Mechanism of arsenic release to groundwater, Bangladesh and West Bengal. *Applied Geochemistry*, *15*(4), 403–413. https://doi.org/10.1016/S0883-2927(99)00086-4

Nikolaidis, N. P., Dobbs, G. M., Chen, J., & Lackovic, J. A. (2004). Arsenic mobility in contaminated lake sediments. *Environmental Pollution*, *129*(3), 479–487. https://doi.org/10.1016/j.envpol.2003.11.005

Palmer, M. J., Chételat, J., Jamieson, H. E., Richardson, M., & Amyot, M. (2021). Hydrologic control on winter dissolved oxygen mediates arsenic cycling in a small subarctic lake. *Limnology and Oceanography*, *66*(S1), S30–S46. https://doi.org/10.1002/lno.11556

Palmer, M. J., Chételat, J., Richardson, M., Jamieson, H. E., & Galloway, J. M. (2019). Seasonal variation of arsenic and antimony in surface waters of small subarctic lakes impacted by legacy mining pollution near Yellowknife, NT, Canada. *Science of the Total Environment*, *684*, 326–339. https://doi.org/10.1016/j.scitotenv.2019.05.258

Rahman, M. A., Hasegawa, H., & Lim, R. P. (2012). Bioaccumulation, biotransformation and trophic transfer of arsenic in the aquatic food chain. *Environmental Research*, *116*, 118–135. https://doi.org/10.1016/j.envres.2012.03.014

Ratkowsky, D. A., Olley, J., McMeekin, T. A., & Ball, A. (1982). Relationship between temperature and growth rate of bacterial cultures. *Journal of Bacteriology*, *149*(1), 1–5. https://doi.org/10.1128/jb.149.1.1-5.1982

Read, J. S., Hamilton, D. P., Desai, A. R., Rose, K. C., Macintyre, S., Lenters, J. D., Smyth, R. L., Hanson, P. C., Cole, J. J., Staehr, P. A., Rusak, J. A., Pierson, D. C., Brookes, J. D., Laas, A., & Wu, C. H. (2012). *Lake-size dependency of wind shear and convection as controls on gas exchange*. *39*, 1–5. https://doi.org/10.1029/2012GL051886

Rice, K. C., Conko, K. M., & Hornberger, G. M. (2002). Anthropogenic sources of arsenic and copper to sediments in a Suburban Lake, Northern Virginia. *Environmental Science and Technology*, *36*(23), 4962–4967. https://doi.org/10.1021/es025727x

Rueda, F. J., Schladow, S. G., & Clark, J. F. (2008). Mechanisms of contaminant transport in a multi-basin lake. *Ecological Applications*, *18*(8), A72–A88. https://doi.org/https://doi.org/10.1890/06-1617.1

Ruuskanen, M. O., Colby, G., St.Pierre, K. A., St.Louis, V. L., Aris-Brosou, S., & Poulain, A. J. (2020). Microbial genomes retrieved from High Arctic lake sediments encode for adaptation to cold and oligotrophic environments. *Limnology and Oceanography*, *65*(S1), S233–S247. https://doi.org/10.1002/lno.11334

Sanders, J. G., Osman, R. W., & Riedel, G. F. (1989). Pathways of arsenic uptake and incorporation in estuarine phytoplankton and the filter-feeding invertebrates Eurytemora affinis, Balanus improvisus and Crassostrea virginica. *Marine Biology*, *103*(3), 319–325. https://doi.org/10.1007/BF00397265

Smedley, P. L., & Kinniburgh, D. G. (2002). A review of the source, behaviour and distribution of arsenic in natural waters. *Applied Geochemistry*, *17*(5), 517–568. https://doi.org/10.1016/S0883-2927(02)00018-5

Solanki, V. R., Murthy, S. S., Kaur, A., & Raja, S. S. (2007). Variations in Dissolved Oxygen and Biochemical Oxygen Demand in Two Freshwater Lakes of Bodhan, Andhra. *Nature Environment and Pollution Technology*, *6*(4), 623–628.

Thomas, B., & Arthur, M. A. (2010). Correcting porewater concentration measurements from peepers: Application of a reverse tracer. *Limnology and Oceanography: Methods*, *8*(AUG), 403–413. https://doi.org/10.4319/lom.2010.8.403

Tuan, N. v., Hamagami, K., Mori, K., & Hirai, Y. (2009). Mixing by wind-induced flow and thermal convection in a small, shallow and stratified lake. *Paddy and Water Environment*, *7*(2), 83–93. https://doi.org/10.1007/s10333-009-0158-x

Wang, Z., Luo, Z., & Yan, C. (2013). Accumulation, transformation, and release of inorganic arsenic by the freshwater cyanobacterium Microcystis aeruginosa. *Environmental Science and Pollution Research*, *20*(10), 7286–7295. https://doi.org/10.1007/s11356-013-1741-7

Weber, F. A., Hofacker, A. F., Voegelin, A., & Kretzschmar, R. (2010). Temperature dependence and coupling of iron and arsenic reduction and release during flooding of a contaminated soil. *Environmental Science and Technology*, *44*(1), 116–122. https://doi.org/10.1021/es902100h

Wilhelm, S., & Adrian, R. (2008). Impact of summer warming on the thermal characteristics of a polymictic lake and consequences for oxygen, nutrients and phytoplankton. *Freshwater Biology*, *53*(2), 226–237. https://doi.org/10.1111/j.1365-2427.2007.01887.x

Woolway, R. I., Meinson, P., Nõges, P., Jones, I. D., & Laas, A. (2017). Atmospheric stilling leads to prolonged thermal stratification in a large shallow polymictic lake. *Climatic Change*, *141*(4), 759–773. https://doi.org/10.1007/s10584-017-1909-0

Wüest, A., & Lorke, A. (2003). Small-Scale Hydrodynamics in Lakes. *Annual Review of Fluid Mechanics*, *35*(1), 373–412. https://doi.org/10.1146/annurev.fluid.35.101101.161220

Xing, Z., Fong, D. A., Lo, E. Y., & Monismith, S. G. (2014). *Thermal structure and variability of a shallow tropical reservoir*. *59*(1), 115–128. https://doi.org/10.4319/lo.2014.59.01.0115

Yang, P., Fong, D. A., Lo, E. Y. M., & Monismith, S. G. (2019). Vertical mixing in a shallow tropical reservoir. *Limnology*, *20*(3), 279–296. https://doi.org/10.1007/s10201-019-00577-z

Yannarell, A. C., & Triplett, E. W. (2005). Geographic and environmental sources of variation in lake bacterial community composition. *Applied and Environmental Microbiology*, *71*(1), 227–239. https://doi.org/10.1128/AEM.71.1.227-239.2005

Zhang, N., Wei, C., & Yang, L. (2013). Occurrence of arsenic in two large shallow freshwater lakes in China and a comparison to other lakes around the world. *Microchemical Journal*, *110*, 169–177. https://doi.org/10.1016/j.microc.2013.03.014

3. Chapter 3: Short term arsenic cycling in a shallow, polymictic lake

3.1. Abstract

We observed repeated diel oscillations in arsenic (As) concentrations in the bottom waters of a shallow, temperate lake during a weeklong measurement period. Arsenic concentrations were highest during the morning or midday and lowest in the evening. In this work, we explore four mechanistic hypotheses to explain the diel As cycles based on the physical and biogeochemical processes that were investigated during the study. Despite pH being known to control As cycles in rivers, we determined that this mechanism was inconsistent with As dynamics observed in Lake Killarney. Instead, we found that Fe and Mn concentrations oscillated simultaneously with As concentrations and, thus, concluded that redox conditions adjacent to the lakebed controlled the near-bed availability of these three elements. However, based on timescale analysis, we determined that biogeochemical processes at the sediment water interface alone could not have led to the daily oscillations in bottom water concentrations. Rather, turbulence from convective mixing was necessary to transport dissolved species from the lakebed into bottom waters. Notably, we saw that the timing and intensity of peaks in convectively-driven turbulence were consistent with observed diel fluctuations in bottom water As. Our results indicate that physical mixing is key in controlling As transport and concentrations on diel timescales within shallow lakes. The daily cycling of redox-sensitive elements in shallow lakes and the potential physical controls on this phenomenon should be considered when designing sampling methods to assess the environmental health and water quality of contaminated sites.

3.2. Introduction

Arsenic (As) is a carcinogen and neurotoxin and is a global health concern (ASTDR, 2007). Although As is released by natural processes such as weathering of As-bearing minerals,

anthropogenic activities including smelting, mining, and the application of As-containing pesticides have greatly accelerated the release of As into natural waters (Smedley and Kinniburgh, 2002). Elevated As concentrations in natural systems can have a negative impact on the ecosystem and on surrounding communities (Chen et al., 2015; Jia et al., 2018). Arsenic concentrations are elevated in the sediments of many lakes in the south-central Puget Sound region, WA, USA, due to the historic contamination from local smelting activity (Gawel et al. 2014). Recent work has shown that there is elevated cancer risk associated with consumption of organisms from lakes in this region (Hull et al., 2021).

The mobility and cycling of As in lakes is controlled by biogeochemical and physical processes, including redox conditions, pH, temperature, and lake mixing regime. In lakes, As is stored in lakebed sediments sorbed onto or incorporated into solids, including iron (Fe) and manganese (Mn) oxide and oxyhydroxides (Smedley and Kinniburgh, 2002; Couture et al., 2010). Arsenite, or As(III), is the reduced form of inorganic As and is more readily found in hypoxic, reducing environments such as lakebed sediments (Aggett and O'Brien, 1985; Keimowitz et al., 2005). In lake surface waters and in other oxididizing environments, As is expected to be largely in the form of arsenate, or As(V) (Barrett et al. 2018; Hollibaugh et al., 2005). In neutral and alkaline conditions, pH can affect the adsorption and desorption of As onto minerals, such as metal oxides (Fuller and Davis, 1989; Dixit and Hering, 2003). Arsenic adsorption and desorption largely occur in the lakebed sediments, where there may be a mix of inorganic As species, i.e. As(V) and As(III) (Aggett and O'Brien, 1985; Couture et al., 2010); thus, pH may affect sorption process on both forms of inorganic As. In natural environmental conditions, trends in pH can have opposite effects on arsenite and arsenate (Dixit and Hering, 2003). For example, if pH increases in the circumneutral range, As(V) adsorption onto Fe

minerals is expected to decrease, whereas As(III) adsorption onto Fe minerals does not change significantly (Dixit and Hering, 2003). Further, the rates of formation and dissolution of Fe and Mn minerals are closely tied to redox conditions (Lovley, 1991; Muller et al., 2002). In anoxic and hypoxic conditions, microbe-mediated reductive dissolution of Fe and Mn minerals can release previously adsorbed and co-precipitated As into the sediment porewaters in dissolved form. Because microbial activity increases with temperature (Ratkowsky et al., 1982), the rate of As mobilization from the sediments into porewaters is accelerated in warmer conditions (Weber et al., 2010; Barrett et al., 2019). Once in dissolved form, lake depth, stratification, and frequency of lake mixing control the concentration and distribution of As in the lake water column (Fung et al., 2022). Although prior work has looked at how these various factors control seasonal trends in As concentrations in lake water (Martin and Pedersen 2002; Palmer et al. 2019; Fung et al. 2022), less is known about the short term dynamics of As in freshwater systems.

Diel oscillations in As concentrations have been observed and investigated in numerous rivers and streams, and studies show that As concentrations peak in the late afternoon or early evening and are at a minimum during the morning (Fuller and Davis, 1989; Nimick et al., 2003; Gammons et al., 2007). Nimick et al. (2003) summarized several of the mechanisms hypothesized to control diel As oscillations in rivers and streams and showed that some of them, including streamflow variability and Mn redox reactions, likely cannot explain the timing of the observed cycles. Rather, the body of literature on diel As cycles in rivers and streams points to photosynthesis-driven pH cycles and the corresponding adsorption and desorption of As onto and from substrate surfaces, particularly those of hydrous metal oxides (Fuller and Davis, 1989; Nimick et al., 2003), to explain the timing of these cycles in fluvial systems.

Unlike in rivers and streams, diel cycling of As in lakes has not been thoroughly examined, and existing observations are inconsistent. Gammons et al. (2007) found a lack of diel changes in As concentrations at their pond site, in contrast to their findings of clear diel oscillations at their stream sites. Dicataldo et al. (2011) observed a diel As cycle during a 24 hour sampling period in a wetland of the Great Salt Lake; however, despite the diel pH cycle in the wetland mimicking the pH cycles observed in river and stream studies, the timing of the As cycle observed in the wetland was opposite from what has been observed in fluvial systems (Dicataldo et al., 2011). Specifically, Dicataldo et al. (2011) found that the wetland exhibited maximum and minimum As concentrations in the early morning and late afternoon, respectively, exactly opposite to what has been widely observed in rivers and streams. There is not yet an established understanding of whether diel As cycling in lakes is common, nor is there an accepted explanation for what mechanisms control diel As cycling in lakes, where physical and biogeochemical processes diverge from those in rivers and streams.

Although short term oscillations in As concentrations have not been thoroughly studied in lacustrine systems, many studies show that diel cycling of other constituents occurs in lakes and that these cycles are often controlled by physical processes (Melack and Fisher, 1983; Holgerson et al., 2016). Specifically, nighttime convective mixing has been demonstrated to be a key mechanism in modulating the distribution of dissolved gasses (Ford et al., 2002; Andersen et al., 2017) on diel timescales, especially in shallow lakes. Because prior work has shown that lake mixing frequency plays a role in controlling the vertical distribution of As in shallow lakes on a seasonal timescale (Fung et al., 2022), it is possible that diel convective mixing may also affect As concentrations on shorter timescales.

Understanding the timescales of changes in As concentrations in contaminated lakes is necessary for designing sampling regimes that accurately represent water quality, environmental conditions, and the potential for negative ecosystem health impacts. Balistrieri et al. (2012) found that fish mortality rates can change drastically over a narrow range of toxicity metric values based on heavy metal concentrations, exposure time, and other environmental factors. The As toxicity threshold for fish has also been found to depend on concentration as well as exposure time and pattern (Chen et al., 2010). Further, increasing knowledge about the mechanisms behind short term As cycles is essential in the development of models that can be used to predict environmental and human health risk in As contaminated lakes. In this study, we present observations of repeated diel cycles in bottom water As concentrations in Lake Killarney, a shallow, temperate lake, from August 29 – September 5, 2019, a period when the lake experienced elevated surface water As concentrations (Fung et al., 2022). We discuss four mechanistic hypotheses for why these cycles occur and explore the timescales at which physical, chemical, and biological lake mechanisms act to influence the release of As from the lakebed and its vertical transport. Ultimately, we show how key physical and biogeochemical mechanisms interact to control As concentrations in lake bottom waters.

3.3. Methods

3.3.1. Study Site

Lake Killarney is a shallow, polymictic lake approximately 45 miles southeast of Seattle, WA. It has a mean depth of 2.6 m, an annual maximum depth of 4.6 m, and a surface area of 0.14 km^2 (Barrett et al., 2018; Gawel et al., 2014); the maximum lake depth fluctuates seasonally and was close to the seasonal minimum at 3.5 m during this study. There is no significant inflow or outflow. Lake waters are circumneutral to slightly alkaline; pH in August and September from

2015 to 2018 ranged from 6.0 to 8.7 and had an average of 7.2. Porewater pH was measured from 1.5 to 19.5 cm (n = 7) below the sediment water interface (SWI) in a sediment core collected in January 2018 (Barrett et al., 2019). Porewater pH throughout the core was in the circumneutral range (6.5 ± 0.1). Lake Killarney is in an urban environment and is wind-sheltered by the basin morphometry and densely-spaced houses and trees. Lake Killarney was contaminated with As by historic smelting operations in the region. Legacy As remains in the lake sediments at concentrations up to 206 μg g^{-1} and surface water As concentrations have been measured up to 30 μg L^{-1}, more than 2 orders of magnitude higher than the EPA limit of 0.14 μg L^{-1} for water containing organisms that people may consume (US EPA, 2009). Lake Killarney is considered to be eutrophic and had an average Secchi depth of ~2 m in August and September of 2019 (King County, 2015).

3.3.2. Data collection

From August 15 through October 11, 2019, an autosampler (ISCO model 3700, Teledyne ISCO, NE, USA) collected 500 ml unfiltered water samples in acid-washed bottles at a 6-hour frequency (02:00, 08:00, 14:00, and 20:00) from 40 cm above the lakebed near the deepest part of the lake (Fig. 3.1). The autosampler was set to flush the whole length of tubing before taking each sample. Deployments of the autosampler were 6 days in length. Upon collection, samples were acidified with 1% HNO_3 (v/v) and duplicate subsamples from each bottle were analyzed using inductively-coupled plasma mass spectrometry (ICP-MS) for total As and other metals, including total Fe and total Mn; quality control as described previously (Barrett et al., 2018) was followed in our analysis. Average concentrations of total metals from duplicate samples are reported here. Dissolved As profiles across the SWI were measured before and after the study period using passive diffusive porewater samplers. Deployments were approximately two weeks

in length, from August 14 – 27 and September 11 – 23, 2019; detailed methods on these deployments have been reported previously (Barrett et al., 2019; Fung et al., 2022).

Surface and bottom DO sensors (HOBO U26, 0.2 mg L^{-1} accuracy, Onset Computer Corporation, Bourne, MA, USA) were deployed at depths of 0.5 and 3.1 m (3 m and 0.4 m above the lakebed), respectively, and sampled at 15 minutes intervals. Water temperature profiles were recorded at 10-minute intervals using HOBO sensors (HOBO Pro v2 and HOBO Tidbit v2, accuracy of ±0.2 °C, Onset Computer Corporation, Bourne, MA, USA). Pre-deployment calibration in ice-water demonstrated that all sensors were within the accuracy range. The loggers were deployed every 0.5 m from z = 0 to 3.5 m above the lakebed and were attached to a nylon line that was held taut throughout the deployment by a bottom anchor and surface and sub-surface buoys. The bottom temperature sensor provided a measure of sediment temperature, as it was attached to the concrete block submerged in the sediment.

To measure water velocities and mixing characteristics, we deployed a down looking acoustic Doppler current profiler (ADCP; Nortek Signature 1000) at the water surface near the deepest part of the lake. From August 29 through mid-morning on September 3, the ADCP measured 10-minute bursts of data every hour operating. Horizontal velocity data were collected by the instrument's four slanted beams at a vertical resolution of 50 cm at 8 Hz. Vertical velocity data were collected by the ADCP's 5th, vertical beam operating on high resolution mode with a bin size of 4 cm and a sampling rate of 8 Hz. The configuration of the ADCP was changed on September 3 such that it continuously sampled until the end of the study period (September 5). Although horizontal velocity data quality was not affected by this configuration change, vertical velocities from the ADCP's 5th beam were non-physical and data after 11:00 on September 3 were excluded from the analysis. An air temperature sensor (HOBO Tidbit v2, accuracy of ±0.2

°C, Onset Computer Corporation, Bourne, MA, USA) was deployed for the duration of the study in a shaded housing 20 cm above the lake water at the ADCP site and measured every 10 minutes.

In situ meteorological data, including wind speed and shortwave (SW) radiation were recorded on a bare island in the lake's main basin, approximately 30 m away from the autosampler water collection site and 90 m away from the ADCP deployment site (Fig. 3.1). A pyranometer (Kipp-Zonen CMP3; Delft, Netherlands) measured downwelling SW radiation at a period of 10 minutes. A wind speed and direction sensor (accuracy of ±1.1 m s^{-1} and ±7° for wind speed and direction, respectively; Davis Instruments Corporation, Hayward, CA, USA) was mounted 2.4 m above ground and collected data at a period of 10 minutes. The wind direction sensor was calibrated upon deployment using a compass.

3.3.3. Data processing

Arsenic residuals were calculated to determine the variation in As concentrations: $[As]_{residual} = [As] - \overline{[As]}$, where $\overline{[As]}$ is a 24-hour moving mean As concentration.

Raw horizontal and vertical velocities from ADCP data were processed into hourly averages. Horizontal velocity magnitude, *U*, was calculated from the hourly east and north velocity components: $U = \sqrt{{Vel_{East}}^2 + {Vel_{North}}^2}$. High resolution vertical velocity data from each bin of the ADCP's 5th beam were de-spiked using a threshold of one standard deviation above the burst mean. De-spiked data were used to calculate hourly vertical turbulent intensities, $\overline{(w')^2}$, at each sample bin, where w' is the vertical velocity residual, $w' = w - \overline{w}$, and w and $\overline{w}$ are the instantaneous vertical velocities and the 10-min burst-average vertical velocities, respectively. To characterize stratification within the water column, we calculated density profiles (IOC et al., 2010) and buoyancy frequency (N^2) profiles, as described in Fung et al. (2022).

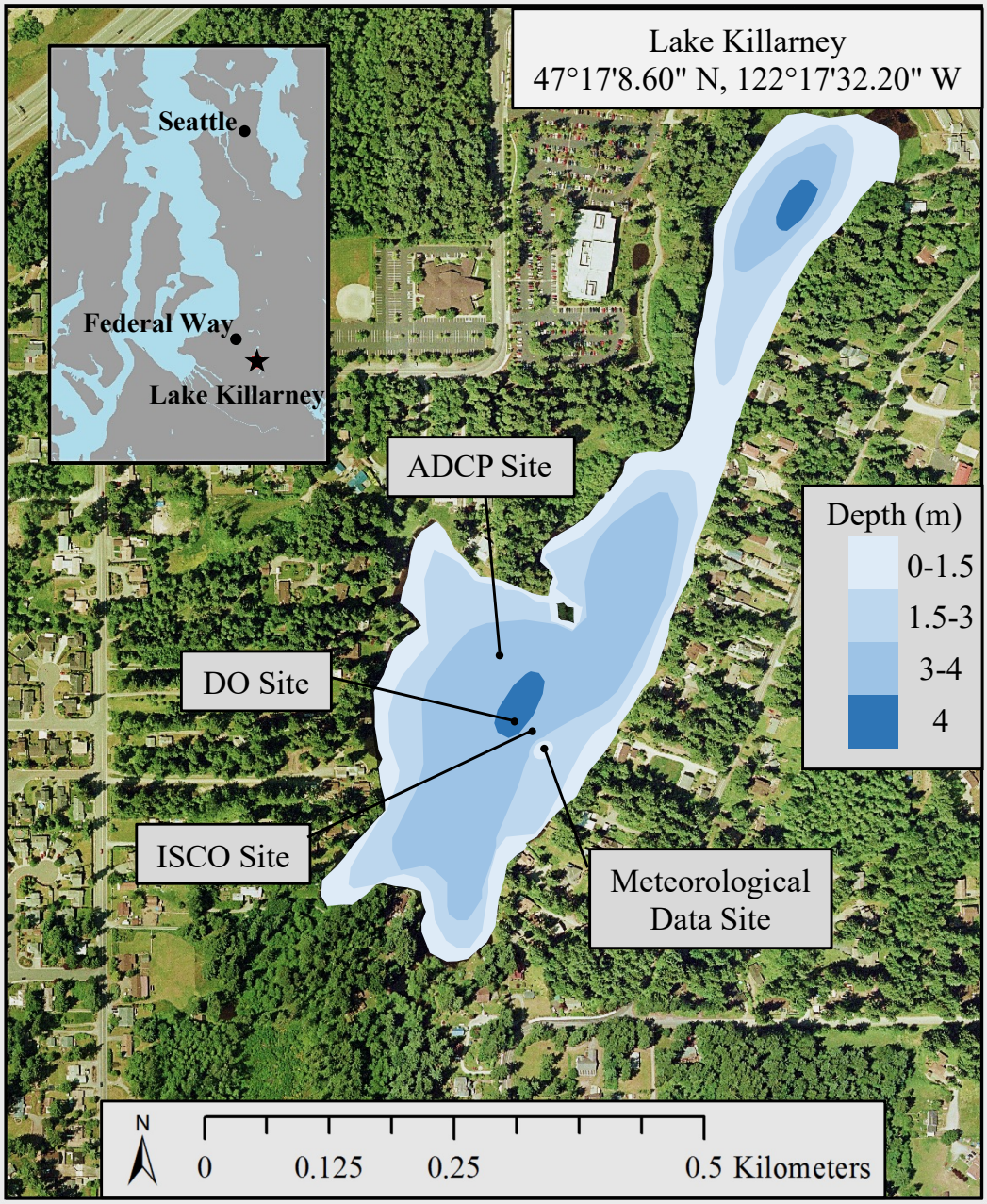

Figure 3.1. *Site map of Lake Killarney, including the location of the lake within the Puget Sound in relation to nearby cities (inset), a bathymetric map, and the four field measurement sites.*

3.4. Results

3.4.1. Meteorological conditions

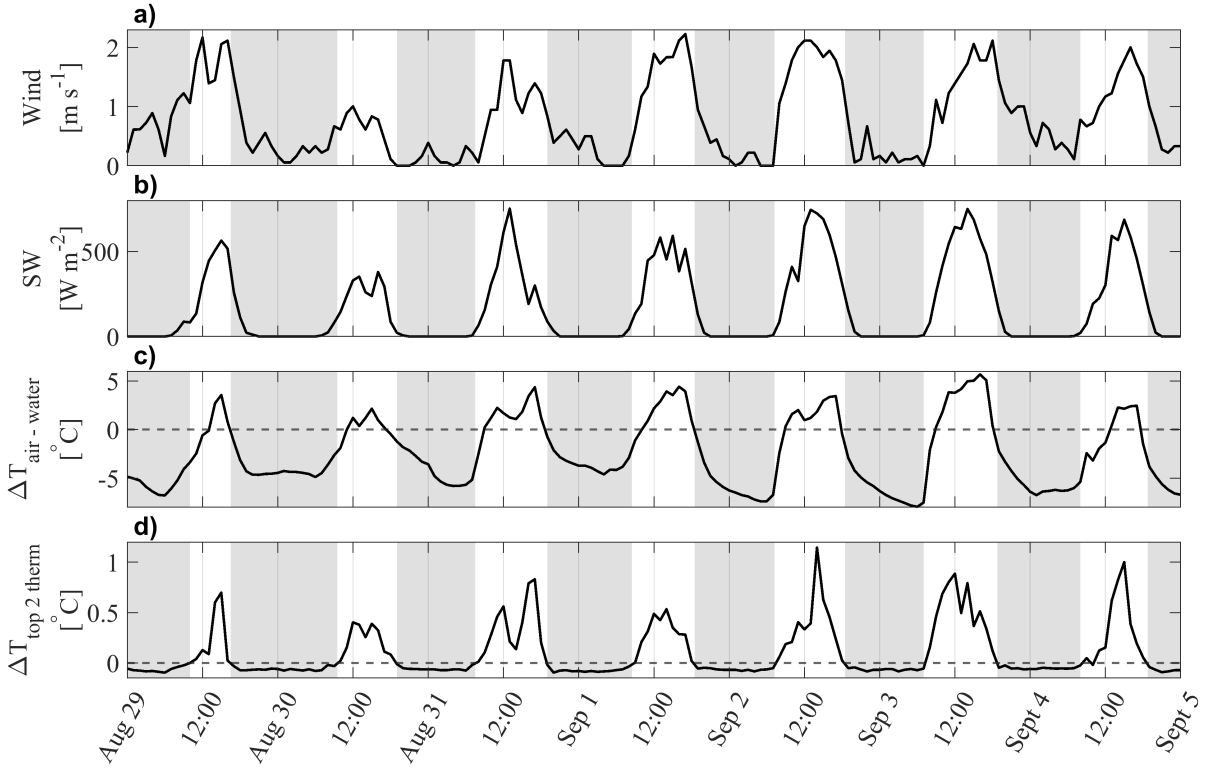

Figure 3.2. *Meteorological data from August 29 – September 4, 2019: (a) wind speed, (b) shortwave (SW) radiation, (c) the difference between air temperature and surface water temperature, and (d) the temperature difference in the top two thermistors in the water column (z = 3.0 and 3.5 m). Grey shading represents periods when the upper water column experienced unstable stratification, or when the difference between the top two thermistors was negative.*

Our observations documented diel patterns in wind speed, shortwave (SW) radiation, air-water temperature difference, and upper water column stability in Lake Killarney during the weeklong study period (Fig. 3.2). Hourly averaged wind speeds ranged from 0 – 2.2 m s^{-1}; wind speeds were low from the late evening through mid-morning and peaked midday to early afternoon (Fig. 3.2a). Shortwave radiation also peaked midday to early afternoon; daily maximum shortwave radiation was lowest during the first two days of the study, reaching 560 and 380 W m^{-2} on the first and second day, respectively, in comparison to the average daily

maximum of 705 W m^{-2} for the latter 5 days (Fig. 3.2b). During daytime heating, air temperatures were generally warmer than lake surface temperatures and surface water temperatures were warmer than water temperatures 0.5 m below the surface (Fig. 3.2c, d, unshaded regions). These conditions occurred in the late morning and afternoon and indicate stability of the upper water column. From evening through mid to late morning, the air-water temperature difference and temperature difference between the top two water column thermistors was negative (Fig. 3.2c, d, shaded regions). During these times, the upper water column was unstable and convective mixing induced deepening of the surface mixed layer. The largest negative air-water temperature differences occurred on September 2 and 3, with differentials of -7.4 and -8.0 °C, respectively. The mean air-water temperature difference during the study was -2.4 °C. The upper water column was unstable for longer than average on August 29 and 30, with 16 hours of stable surface stratification and 32 hours of unstable surface stratification. During the latter four days of the study, there was, on average, 11.3 hours of unstable stratification and 12.7 hours of stable stratification.

3.4.2. Stratification and mixing

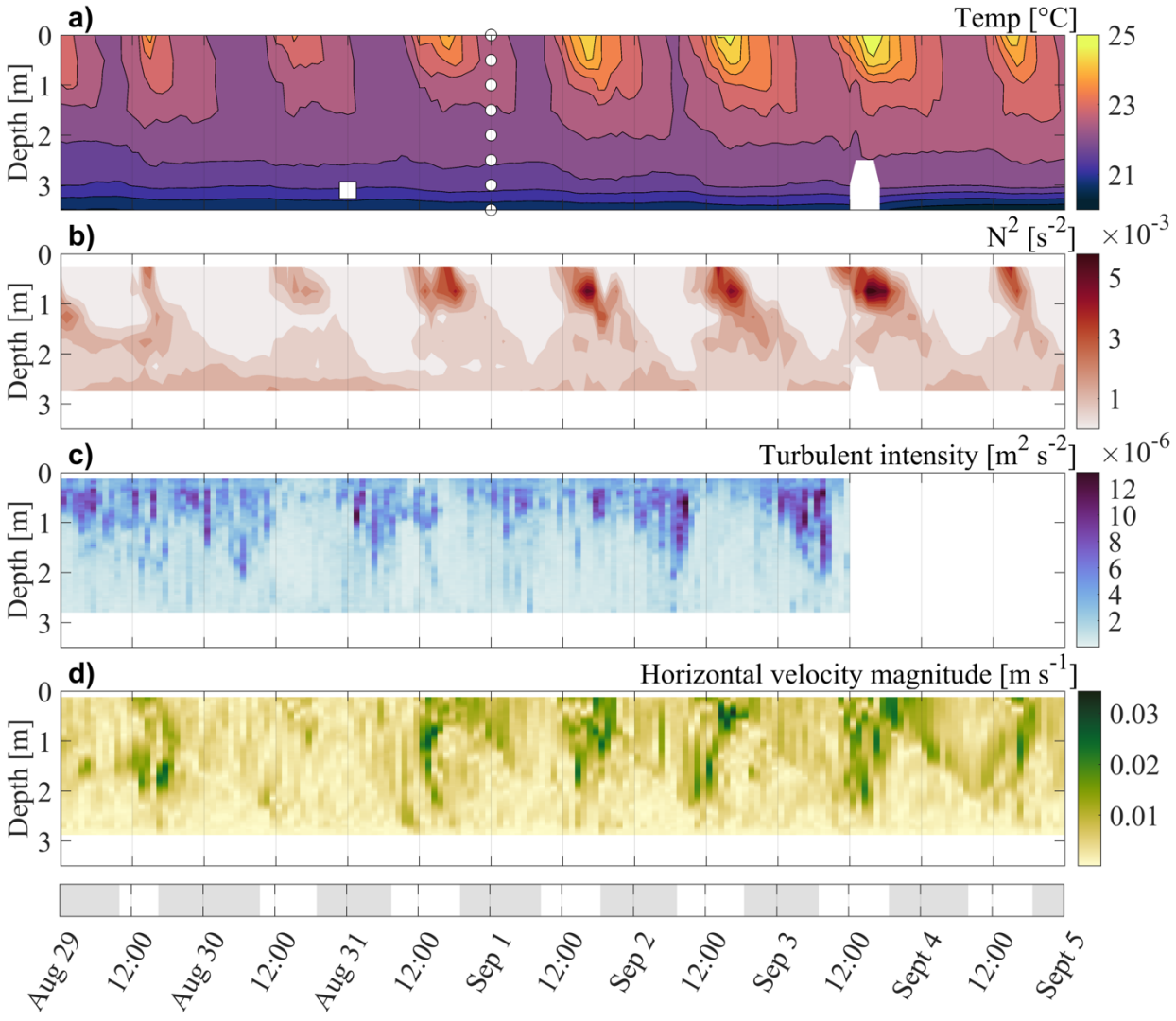

Figure 3.3. *(a) Lake temperatures; white dots indicate placement of the thermistors and the white square indicates placement of the autosampler water intake point and the DO sensor within the water column. (b) Buoyancy frequency, N^2. (c) Vertical turbulent intensity; deployment error of the ADCP lead to non-physical data for the last 36 hours of the study. (d) Horizontal velocity magnitude.*

Lake Killarney exhibited diel patterns in temperature, stratification, vertical turbulent intensity and horizontal velocity (Fig. 3.3). Stratification set up late morning and generally increased in strength through the afternoon, with surface water buoyancy frequency reaching up to 6×10^{-3} s^{-2} in the mid-afternoon (Fig. 3.3b). A transient thermocline formed daily in the top or

middle of the water column during daytime surface stratification. Surface structure began to break down in the late evening and, on most days, the surface mixed layer deepened to a depth of approximately 2 m by the morning. Water density varied approximately linearly with depth to the lake bottom from the evening until onset of heating the following day (Fig. A2.1).

In general, vertical turbulence was low from midday through late evening. Starting in the evening, the strength of vertical turbulent intensity increased in the surface waters; these elevated magnitudes of vertical turbulence then progressed downward into the water column during the night and early morning, indicative of penetrative convection (Fig. 3.3c). Horizontal velocities were generally greatest from midday to early evening (Fig. 3.3d); these high horizontal flow speeds reached maximum depth when horizontal velocities initially became elevated (> 1 cm s^{-1}) on each day. As the strength of surface stratification increased throughout the afternoon, elevated horizontal velocities became constrained to lake surface waters. In the late evening, horizontal velocities tapered off and remained low until wind speed again increased the following day (Fig. 3.2a, Fig. 3.3d).

There were several exceptions to the observed diel patterns in mixing metrics during the weeklong study. On August 29, vertical turbulent intensity was elevated in the surface waters for the entire day (Fig. 3.3c); however, this turbulent energy did not penetrate as deeply into the water column as the rest of the study days, when $\overline{(w')^2}$ exhibited diel patterns as described above. Further, horizontal velocities were low throughout August 30, when afternoon wind speeds were reduced relative to the rest of the study days.

3.4.3. As, Mn, Fe, and DO

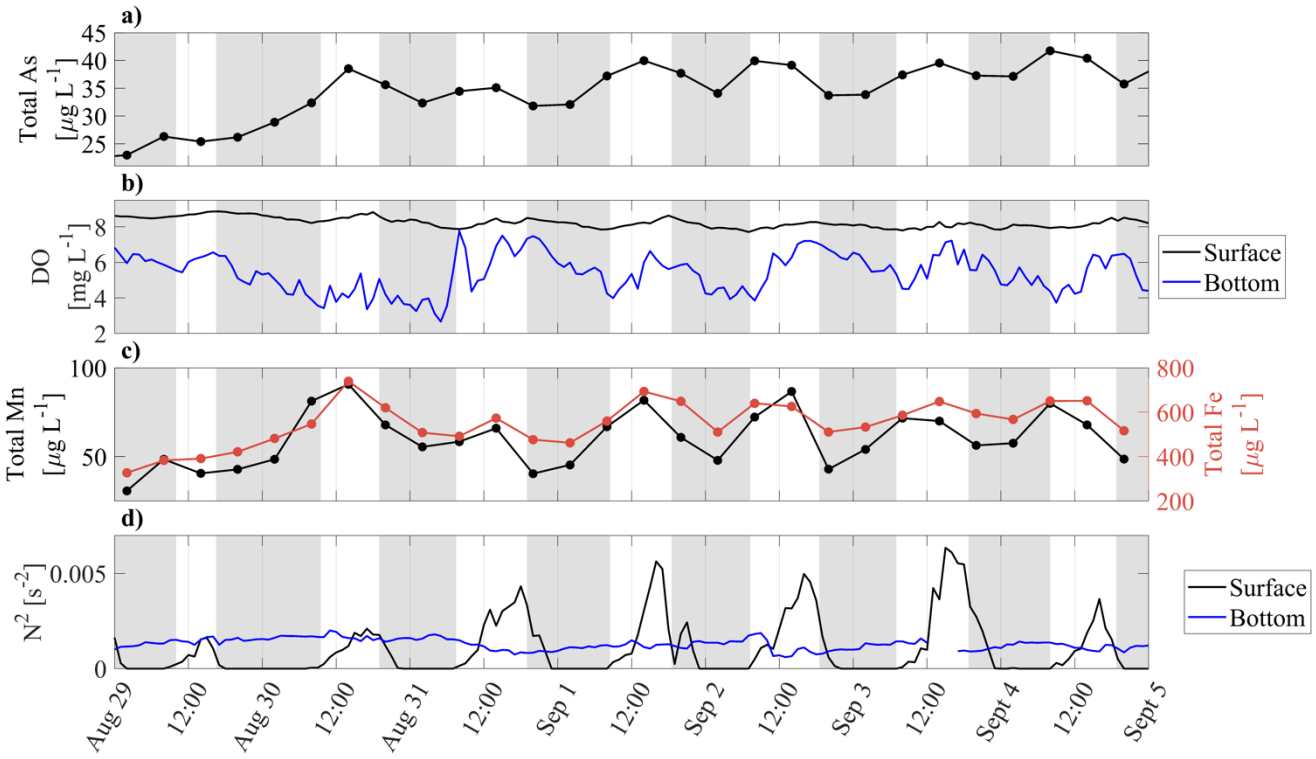

Figure 3.4. *Timeseries of (a) total arsenic (As), (b) surface and bottom water dissolved oxygen in black and blue, respectively, (c) total manganese (Mn) and total iron (Fe) in black and orange, respectively, and (d) surface and bottom water buoyancy frequency (N^2) in black and blue, respectively. Grey shading represents periods when the upper water column experienced unstable stratification.*

Lake Killarney exhibited diel signals in surface stratification and in bottom water total As, Mn, and Fe from August 30 through the end of the study week (Fig. 3.4). Patterns in As, Mn, and Fe were similar, with concentrations of all three elements increasing from nighttime through morning or midday and decreasing from midday through the evening (Fig. 3.4a, c). Bottom water DO exhibited opposite temporal cycles, with maximum concentrations (~7 mg L^{-1}) occurring in the early or mid-afternoon and minimum concentrations (~4 mg L) occurring in the mid-morning. Surface water buoyancy frequency, calculated at a depth of 0.75 m, exhibited a diel signal on all days with stronger daily variation the latter 5 days of the study. As observed in Fig. 3.3b, surface buoyancy frequency peaked mid-afternoon, during surface heating, and was

negligible at night, during periods of convectively-driven mixing (Fig. 3.4d). Bottom water buoyancy frequency, calculated at a depth of 2.75 m, was relatively constant during the study week with a mean magnitude of 1.3×10^{-3} s^{-2}.

Both physical and biogeochemical signals during the first two days were aberrant from the diel signals that were present during the rest of the week. From August 29 through midday on August 30, total As concentrations monotonically increased and almost doubled from 23.0 µg L^{-1} to 38.5 µg L^{-1} (Fig. 3.4a). Total Mn and Fe also increased from 31 µg L^{-1} to 91 µg L^{-1} and 327 µg L^{-1} to 740 µg L^{-1}, respectively (Fig. 3.4c). Inversely, the concentration of bottom water DO was 6.8 mg L^{-1} at the beginning of the sampling period and decreased monotonically through 5 am on August 30 to 2.7 mg L^{-1} (Fig. 3.4b). Maximum surface buoyancy frequency was lower on August 29 and 30 than during the rest of the study, only reaching 1.6×10^{-3} s^{-2} and 2.1×10^{-3} s^{-2}, respectively, corresponding to lower solar forcing on these two days (Fig. 3.2b, Fig. 3.4d).

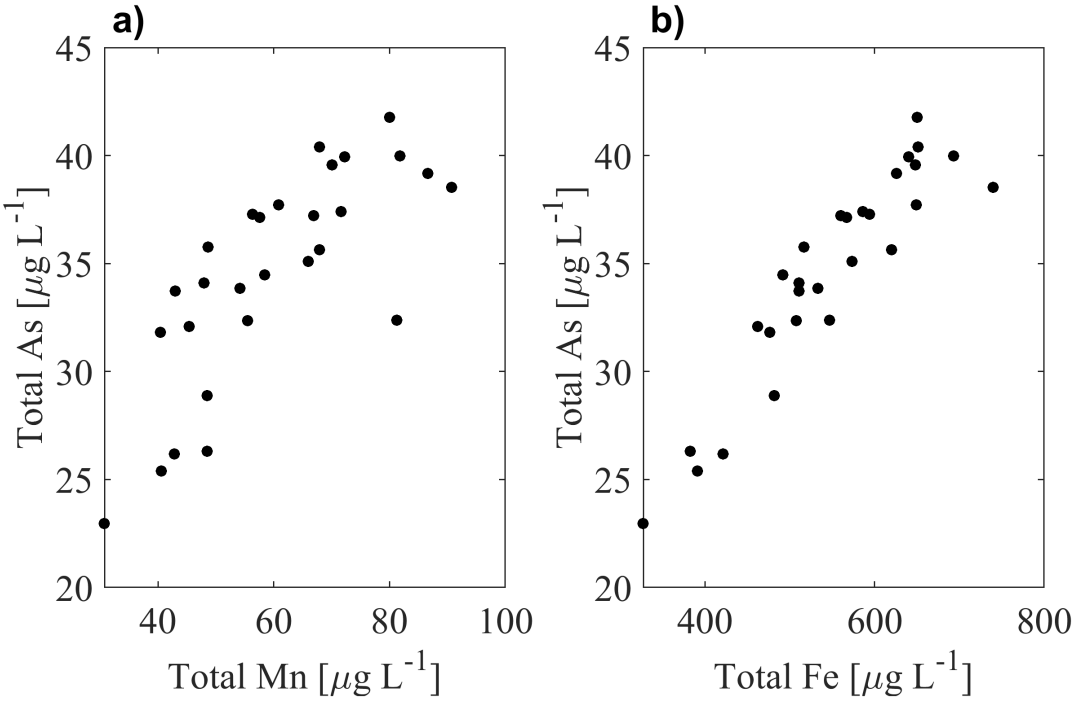

Figure 3.5. *Scatterplots of (a) bottom water total manganese (Mn) vs. bottom water total arsenic (As) and (b) bottom water total iron (Fe) vs. bottom water total As.*

Bottom water total Fe ($R^2 = 0.86$, $P < 0.05$) and total Mn ($R^2 = 0.59$, $P < 0.05$) were both positively correlated with bottom water total As (Fig. 3.5a, b), indicating that Mn- and Fe-oxide formation and dissolution are strongly tied to As mobilization in Lake Killarney. The relationship between Fe and As in the lake bottom water was similar to that in the region directly adjacent to the SWI, as indicated by passive sampler data from just before and after our study (Fig. 3.5b, Fig. A2.2, Fig. A2.3). The slope of the linear relationship between Fe and As in the bottom waters during our study week was 0.05 [µg As L^{-1}/ µg Fe L^{-1}]. Dissolved Fe and As from the passive sampler data also exhibited a comparable linear correlation with a slope of 0.03 [µg As L^{-1}/ µg Fe L^{-1}] (Fig. A2.3). While there was a linear correlation between Mn and As in both bottom water data during our study and in passive sampler data (Fig. 3.5a, Fig. A2.3), the slopes of these regressions differed noticeably, at 0.62 [µg As L^{-1}/ µg Mn L^{-1}] and 0.24 [µg As L^{-1}/ µg Mn L^{-1}] for passive sampler data and bottom water data, respectively.

3.4.4. Physical control on As trends

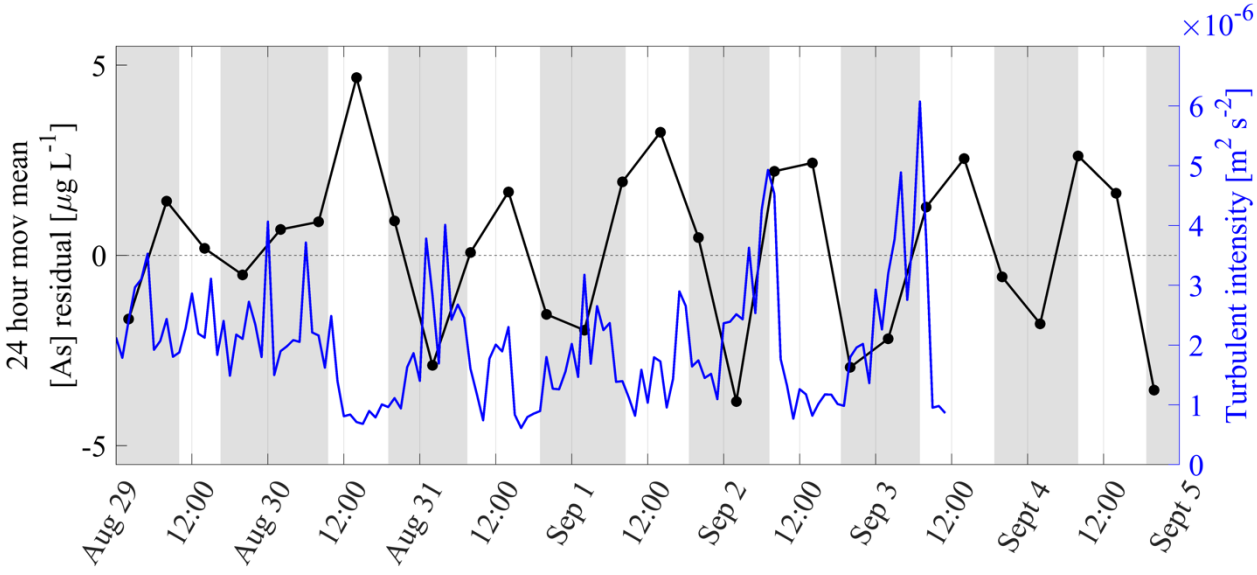

Figure 3.6. *Timeseries of arsenic (As) residuals calculated from the 24-hour moving mean (left axis, black) overlayed with depth-averaged vertical turbulent intensity (right axis, blue). Grey shading represents periods when the upper water column experienced unstable stratification.*

Depth-averaged vertical turbulent intensity, $\overline{(w')^2}$, ranged an order of magnitude from $6x10^{-7}$ m^2 s^{-2} to $6x10^{-6}$ m^2 s^{-2} during the study week (Fig. 3.6). As can also be observed in Fig. 3.3c, there was a diel cycle in vertical turbulence from August 30 to September 3, where $\overline{(w')^2}$ magnitudes began increasing in the evening and reached a peak in the early or mid-morning (Fig. 3.6). Vertical turbulent intensity was generally low from late morning through early evening. In contrast to the diel patterns observed during most of the study week, there were consistently high magnitudes of depth-averaged $\overline{(w')^2}$ from August 29 through midday on August 30 (Fig. 3.6). Mean depth-averaged vertical turbulent intensity was $2.1x10^{-6}$ m^2 s^{-2} during convective periods (gray shaded regions), with peaks exceeding $4x10^{-6}$ m^2 s^{-2} on most days. In contrast, mean $\overline{(w')^2}$ was only $1.4x10^{-6}$ m^2 s^{-2} during periods when surface stratification was stable (unshaded regions). This indicates that unstable stratification and convective mixing plays a large role in creating the observed elevated $\overline{(w')^2}$.

The diel signal in As concentrations observed in Fig. 3.4 is also visible in Fig. 3.6, with peaks in As concentrations occurring either at the 8 am or 2 pm sampling. From August 31 through September 4, there was a near-zero (-0.06 μg L^{-1}) mean As residual. Contrastingly, As residuals were positive overall on August 29 and 30, with an average residual of 0.82 μg L^{-1} (Fig. 3.6). Although precise resolution of the timing is challenging due to the relatively long As sampling interval, As concentrations appear to have begun increasing during, or shortly after, peaks in vertical turbulence, the majority of which occurred during periods when there was unstable stratification in the lake surface waters (Fig. 3.6).

3.5. Discussion

We found that a shallow, temperate lake exhibited diel cycles in bottom water total As concentrations over six days of our weeklong study. There are several physical, biological, and chemical mechanisms that could play a role in creating these cycles. Below, we discuss our observations of the physical and biogeochemical processes occurring during our study week. Based on our findings and on previous literature, we offer potential hypotheses for what may control the diel As cycles in Lake Killarney and evaluate the plausibility of each hypothesis.

3.5.1. Biogeochemical conditions

During the latter six days of the study, there were diel cycles in bottom water DO, total As, total Mn, and total Fe (Fig. 3.4). Peak As concentrations occurred early morning or midday and minimum concentrations occurred in the evening or nighttime (Fig. 3.4a). Bottom water DO increased during daytime periods of elevated shortwave radiation, which can likely be attributed to photosynthetic production of oxygen. Because this observation indicates that there were primary producers residing 40 cm above the lakebed, where the DO sensor was sampling, we can infer that these primary producers were also taking up As in this bottom water region and that the diel As cycle may impact uptake rates. DO concentrations decreased from late evening through the early morning showing that respiration dominated nighttime DO trends, as opposed to convective mixing and associated overnight reaeration as seen in some shallow lakes (Holgerson et al., 2016). Patterns in bottom water DO have the potential to impact the location of the oxycline, or the location where redox conditions transition from being fully reducing in the lakebed sediment to the more oxidizing in the hypolimnion. The oxycline has been shown to oscillate up and down based on rates of microbial respiration and oxygen dynamics (Beck and Bruland, 2000). Consequently, it is possible that the bottom water DO cycles observed in Lake

Killarney may impact the location of the oxycline on daily timescales. Because DO and pH generally exhibit synchronous cycles due to their linkage in photosynthesis and respiration reactions (Andersen et al., 2017), we can infer that pH in the bottom waters of Lake Killarney was likely lower in the early morning after nighttime respiration and higher in the late afternoon following daytime photosynthesis. This expected cycle parallels the pH cycle observed widely in natural waters, including in lentic (Carling et al. 2011; Dicataldo et al., 2011) and lotic (Fuller and Davis, 1989; Balistrieri et al., 2012) systems.

Total Fe and Mn concentrations had significant positive correlations with total As concentrations; all three elements had synchronized oscillations, suggesting that their behaviors were likely controlled by a common process (Fig. 3.4, Fig. 3.5). Barrett et al. (2019) reported that between 40 – 70% of the As in the sediment of Lake Killarney is adsorbed or co-precipitated with mineral phases and is available to be released into porewaters due to desorption and microbial reduction processes. The tight coupling of Fe, Mn, and As cycles observed in Lake Killarney is consistent with this previous study and suggests that the reduction of Fe and Mn minerals lead to the mobilization of these readily available pools of As. Profiles of dissolved Fe, Mn, and As from passive samplers measured before and after our study week provide additional evidence of the coincident production of dissolved species, especially of Fe and As, which both peak around the SWI (Fig. A2.2). Of note, Mn does not show as visible of a peak in concentration where Fe and As concentrations peak (Fig. A2.2). This result may indicate that Mn is less important than Fe in controlling the mobility of As in Lake Killarney, as is the case in other lake sediments (Muller et al., 2002; Couture et al., 2010). Simultaneous release of As and Fe has been documented in previous studies (Muller et al., 2002; Couture et al., 2010). The similarity in the ratios of Fe and As in the porewaters and the bottom waters (Fig. 3.5, Fig. A2.3)

indicates that the Fe and As measured by the autosampler represent dissolved species transported up from the SWI.

Dicataldo et al. (2011) also observed concurrent peaks in Mn and As and postulated that formation and dissolution of Mn oxyhydroxides and associated sorption of As onto these solids created the daily As cycles they documented in a wetland of the Great Salt Lake. In contrast to our observations, Dicataldo et al. (2011) did not observe a correlation between dissolved Fe and As; this lack of relationship could be due to their study site's sediment composition or other environmental conditions, such as redox potential, that could preclude the formation of Fe-As complexes. The observations of concurrent Mn and As oscillations in Lake Killarney and in the wetland studied by Dicataldo et al. (2011) are contrary to what has been documented in rivers, where Mn and As exhibit diel cycles that are 12 hours offset from each other (Nimick et al, 2003; Barringer et al., 2007). The offset of Mn and As cycles in rivers is likely due to the opposing effect that pH has on the adsorption of positively charged molecules, or cations, and negatively charged molecules, or anions. Specifically, increasing pH is expected to decrease anion adsorption, such as arsenate, and increase cation adsorption, such as manganese, Mn^{2+}.

3.5.2. Physical processes

We observed diel patterns in stratification and lake mixing. Peaks in depth-averaged vertical turbulent intensity were largely coincident with periods of unstable surface stratification and indicative of convective mixing (Fig. 3.3c, Fig. 3.6). These findings are consistent with previous studies that have demonstrated the importance of convective mixing in overall lake mixing processes, especially as lake depth decreases (Read et al., 2012). In our prior work, convective mixing was shown to be a key factor in modulating the vertical distribution of As in Lake Killarney on monthly timescales (Fung et al., 2022); this study expands on our previous findings

by demonstrating how diel lake mixing may impact short timescale As dynamics in shallow lakes. Although we don't have measurements of surface water As during this study, we know from sparser, seasonal data that surface water As was elevated during this time (Fung et al., 2022), indicating that diel mixing processes not only brought As from the near bed up into bottom waters, but also into near-surface waters.

3.5.3. Hypotheses

3.5.3.1. pH control

Diel As cycles caused by fluctuations in pH have been widely reported in rivers and streams (Fuller and Davis, 1989; Nimick et al., 2003; Gammons et al., 2007). In these studies, As concentrations reach a maximum in the late afternoon shortly following daily maximum pH. The As cycle observed in Lake Killarney is opposite of, or 12 hours offset from, the timing of cycles seen in fluvial systems. Specifically, As appears to reach the daily high in Lake Killarney approximately when it is at the daily low in rivers. However, pH cycles in Lake Killarney are expected to be photosynthetically-controlled, and thus to be synchronous with photosynthetically-controlled pH cycles observed in rivers and streams. Because the early-morning peaks in As in Lake Killarney occurred approximately 12 hours before the expected late afternoon daily peak in pH, it is reasonable to deduce that pH cycles, and associated sorption and desorption processes, do not modulate either the increases or decreases in As concentration we documented in Lake Killarney. Dicataldo et al. (2011) observed that filtered, or dissolved, As concentrations in a wetland decreased with increasing pH and also concluded that pH could not be controlling the As cycling in their study.

Further, As adsorption onto, and desorption off of, iron-oxides occurs in hypoxic or anoxic lakebed sediments where As(III) is likely to be present. Since pH does not alter As(III)

sorption equilibrium with Fe oxides in near-neutral or slightly alkaline conditions (Dixit and Hering, 2003), it is likely that pH does not have a large effect on As cycles in shallow lakes. As noted before, pH has a disparate effect on cations, such as Mn, and anions, such as As. Thus, our observation of concurrent Mn and As cycles provides further evidence that these cycles are not controlled by pH.

3.5.3.2. Redox processes control

Reducing conditions support microbe-mediated reductive dissolution of oxide and oxyhydroxide minerals in lakebed sediments and the release of As that is adsorbed and coprecipitated with these minerals (Muller et al., 2002; Nikolaidis et al., 2004). Redox conditions at the SWI moderate rates of mineralization of Fe and Mn and the sequestration of dissolved As by adsorption onto or coprecipitation with these minerals (Couture et al., 2010). If cycling in redox conditions controlled As cycling in Lake Killarney, we would expect the lowest DO during the early morning, before and during observed increases in As concentrations. Because lake bottom water exhibited diel DO cycles that reached a minimum DO concentration, and thus maximum reducing potential, during the early morning, it is possible that redox processes at the SWI supported the diel As cycles observed in Lake Killarney. We hypothesize that as DO concentrations within bottom waters oscillated, it altered the redox environment along the sediment surface and potentially within near surface sediment depths. When DO concentrations were low during the early morning periods, stronger reducing conditions were established in surface and near-surface sediment. These reducing conditions would allow for Fe, Mn and As to persist in their dissolved form within the sediment and diffuse across the SWI up into the hypolimnion at higher concentrations. In contrast, when DO concentration were high during the

afternoon and evening, more oxidizing conditions were established in surface and near-surface sediment, causing greater precipitation of Fe and Mn minerals and arsenic sequestration.

3.5.3.3. Temperature control

Temperature is known to be a key factor in the release of As from lakebed sediments, especially over monthly to seasonal timescales (Weber et al., 2010; Barrett et al., 2019; Fung et al., 2022). Elevated temperatures are expected to increase rates of microbial activity (Ratkowsky et al., 1982); in turn, high rates of microbial activity support the mobilization of As by expediting the production of reducing conditions and increasing rates of microbe-mediated reductive dissolution of oxide minerals, including Fe and Mn-oxides (Aurilio et al., 1994). However, during our weeklong study, sediment and bottom water temperatures were coolest in the morning when As concentrations were increasing and warmest in the afternoon when As concentrations were decreasing (Fig. A2.4, Fig. 3.4a), opposite to what would be expected if temperature contributed to the observed oscillations in As. Thus, temperature variation can be ruled out as a contributor to diel As cycles in Lake Killarney; if anything, this opposition in temperature cycles likely damps the magnitude of the observed cycles.

3.5.3.4. Physical mixing control

Mixing processes in lakes are responsible for the vertical transport of constituents, including gasses, nutrients and contaminants (Boyce et al., 1991; Rueda et al., 2008). Previous research has shown that stratification and mixing dynamics are important for controlling seasonal patterns in As in Lake Killarney (Barrett et al., 2019; Fung et al., 2022) and in other lakes (Hollibaugh et al., 2005). Specifically, it was shown in Fung et al. (2022) that convective processes dominated lake mixing during the summertime and, in turn, controlled the vertical distribution of As within the lake water column on a monthlong to seasonal timescale. If mixing processes were responsible

for the observed diel As cycles, we would expect to see elevated levels of turbulence shortly preceding and during periods of increasing As concentration. Importantly, our observations fit this timing; peaks in vertical turbulent intensity generally occurred during the early morning and aligned with periods of increasing As concentrations, indicating that convective mixing likely transported pulses of dissolved metals (As, Fe, and Mn) from the lakebed up into the hypolimnion (Fig. 3.6).

There were generally low levels of vertical turbulent intensity from midday through the evening when As concentrations were decreasing, indicating that that turbulent transport of dissolved species may have been reduced during this time. Previous research has demonstrated that As redistribution into littoral sediments occurs in Lake Killarney (Hull et al., 2021); we expect that the observed diel decreases in As concentration in the hypolimnion are due, in part, to redistribution of dissolved As throughout the rest of the lake due to lateral processes such a wind and thermally driven circulation.

3.5.4. Interactions between physical and biogeochemical processes

While it is possible that redox processes at the SWI contributed to the diel cycles we observed in bottom water As, the hypothesized variability in dissolved As at the lakebed surface had to get transported to 0.4 m above the lakebed where the ISCO sampler was collecting water. Using a conservative Fickian transport coefficient for As, $D = 10^{-9}$ m^2 s^{-1} (Hemond and Fechner, 2014), and an equation for approximate diffusion time based on an integrated diffusive flux equation, $t \approx {x^2}/{2D}$, we estimate that it would take 3.9 years for As to travel 0.4 m by chemical diffusion alone. Thus, we can conclude that biogeochemical processes at the SWI alone could not have led to the observed daily cycles. Rather, a turbulent mixing mechanism must have acted in tandem to transport the As released at the lakebed into the bottom water. Estimating a

timescale for As transport via turbulent diffusion, rather than Fickian diffusion, provides a more realistic result. Using a range in diffusivities that would be reasonable to expect in a shallow lake experiencing convection, 10^{-5} to 10^{-2} m^2 s^{-1} (Lorke, 1998), yields a time range of 13 seconds to 3.5 hours for As to be transported 0.4 m. Thus, the timing and expected intensity of the convectively-driven turbulence can explain the observed diel fluctuations in As concentration.

While sediment bed redox cycles alone could not generate the observed water column fluctuations, the timing of DO oscillations was consistent with that of the As peaks and we anticipate that the presumed redox oscillations controlled the near-bed availability of dissolved As and thus contributed to the observed fluctuations. We posit that reducing conditions in the surface sediment strengthened during nighttime respiration, leading to an increase in near-bed availability of dissolved metals. Concurrently, turbulence was generated when nighttime cooling of the lake surface water set up unstable surface stratification (Fig. 3.2d, Fig. 3.3c). As surface water became cooler and denser than the water below it, fluid descended in the water column and generated turbulent kinetic energy via negative buoyancy production. Turbulent plumes penetrated 2-3 meters below the water surface on most days (Fig 3.3c). Because As concentrations were elevated near the lake bottom, turbulence from the convective plumes generated an upward turbulent diffusive flux that transported dissolved As up from the SWI into the bottom water. These results demonstrate the key role that physical mechanisms play in modulating As mobilization and transport in shallow lakes at a short timescale.

3.5.5. Conclusions

Although 24-hour As cycles are widely documented in rivers and streams (Fuller and Davis, 1989; Nimick et al., 2003; Gammons et al., 2007), there are few observations of these cycles occurring in lakes. Our measurements of repeated diel As cycles over six days in a shallow lake

provide an important example of this phenomenon and suggest that diel cycling of redox-sensitive elements may occur in a wider range of environments than previously identified. This study adds to our understanding of As cycling in lakes by demonstrating that mixing processes can modulate As concentrations on diel timescales in addition to seasonal timescales as shown previously (Fung et al., 2022). Further, this study demonstrates that primary producers likely take up As in near-bottom lake water (0.4 m above the lakebed) in shallow lakes.

We hypothesize that short timescale oscillations in bottom water As concentration likely occur in As-contaminated, shallow, temperate lakes that undergo diel patterns of stratification and mixing during the summertime. The potential for daily cycling should be considered when designing sampling methods to assess the environmental health and water quality of sites with and without known sources of contamination. For example, using sampling methods that provide an in situ integration of dissolved metal concentrations over day to weeklong periods, rather than point samples, may provide a better representation of the conditions to which aquatic organisms are exposed (Balistrieri et al., 2012). This work shows that physical processes exert the dominant control on As mobilization and transport in shallow lakes on short timescales, despite our initial assumption that biogeochemical conditions, such as pH and temperature, determine these As dynamics in lake bottom waters. We suggest that future studies on this topic should include a comprehensive investigation of the mixing and stratification dynamics, in addition to the biogeochemical conditions.

3.6. References

Agency for Toxic Substances and Disease Registry (ATSDR). (2007). Toxicological Profile for Arsenic (Update). Atlanta, GA: U.S. Department of Public Health and Human Services, Public Health Service.

Aggett, J., & O'Brien, G. A. (1985). Detailed Model for the Mobility of Arsenic in Lacustrine Sediments Based on Measurements in Lake Ohakuri. *Environmental Science and Technology*, *19*(3), 231–238. https://doi.org/10.1021/es00133a002

Andersen, M. R., Kragh, T., & Sand-Jensen, K. (2017). Extreme diel dissolved oxygen and carbon cycles in shallow vegetated lakes. *Proceedings of the Royal Society B: Biological Sciences*, *284*(1862). https://doi.org/10.1098/rspb.2017.1427

Aurilio, A. C., Mason, R. P., & Hemond, H. F. (1994). Speciation and Fate of Arsenic in Three Lakes of the Aberjona Watershed. In *Environ. Sci. Technol* (Vol. 28). https://pubs.acs.org/sharingguidelines

Balistrieri, L. S., Nimick, D. A., & Mebane, C. A. (2012). Assessing time-integrated dissolved concentrations and predicting toxicity of metals during diel cycling in streams. *Science of the Total Environment*, *425*, 155–168. https://doi.org/10.1016/j.scitotenv.2012.03.008

Barrett, P. M., Hull, E. A., Burkart, K., Hargrave, O., McLean, J., Taylor, V. F., Jackson, B. P., Gawel, J. E., & Neumann, R. B. (2019). Contrasting Arsenic cycling in strongly and weakly stratified contaminated lakes: Evidence for temperature control on sediment–water arsenic fluxes. *Limnology and Oceanography*, *64*(3), 1333–1346. https://doi.org/10.1002/lno.11119

Barrett, P. M., Hull, E. A., King, C. E., Burkart, K., Ott, K. A., Ryan, J. N., Gawel, J. E., & Neumann, R. B. (2018). Increased exposure of plankton to arsenic in contaminated weakly-stratified lakes. *Science of the Total Environment*, *625*, 1606–1614. https://doi.org/10.1016/j.scitotenv.2017.12.336

Barringer, J. L., Bonin, J. L., Deluca, M. J., Romagna, T., Cenno, K., Alebus, M., Kratzer, T., & Hirst, B. (2007). Sources and temporal dynamics of arsenic in a New Jersey watershed, USA. *Science of the Total Environment*, *379*(1), 56–74. https://doi.org/10.1016/j.scitotenv.2007.03.006

Beck, N., & Bruland, K. W. (2000). *Diel Biogeochemical Cycling in a Hyperventilating Shallow Estuarine Environment* (Vol. 23, Issue 2).

Boyce, F. M., Schertzer, W. M., Hamblin, P. F., & Murthy, C. R. (1991). *Behaviour of Lake Ontario with Reference to Contaminant Pathways and Climate Change*.

Carling, G. T., Fernandez, D. P., Rudd, A., Pazmino, E., & Johnson, W. P. (2011). Trace element diel variations and particulate pulses in perimeter freshwater wetlands of Great Salt Lake, Utah. *Chemical Geology*, *283*(1–2), 87–98. https://doi.org/10.1016/j.chemgeo.2011.01.001

Chen, G., Shi, H., Tao, J., Chen, L., Liu, Y., Lei, G., Liu, X., & Smol, J. P. (2015). Industrial arsenic contamination causes catastrophic changes in freshwater ecosystems. *Scientific Reports*, *5*, 1–7. https://doi.org/10.1038/srep17419

Chen, W. Y., Tsai, J. W., Ju, Y. R., & Liao, C. M. (2010). Systems-level modeling the effects of arsenic exposure with sequential pulsed and fluctuating patterns for tilapia and freshwater clam. *Environmental Pollution*, *158*(5), 1494–1505. https://doi.org/10.1016/j.envpol.2009.12.021

Couture, R. M., Gobeil, C., & Tessier, A. (2010). Arsenic, iron and sulfur co-diagenesis in lake sediments. *Geochimica et Cosmochimica Acta*, *74*(4), 1238–1255. https://doi.org/10.1016/j.gca.2009.11.028

Dicataldo, G., Johnson, W. P., Naftz, D. L., Hayes, D. F., Moellmer, W. O., & Miller, T. (2011). Diel variation of selenium and arsenic in a wetland of the Great Salt Lake, Utah. *Applied Geochemistry*, *26*(1), 28–36. https://doi.org/10.1016/j.apgeochem.2010.10.011

Dixit, S., & Hering, J. G. (2003). Comparison of As(V) and As(III) sorption onto iron oxide minerals: Implications for arsenic mobility. *Environmental Science and Technology*, *37*(18), 4182–4189. https://doi.org/10.1021/es030309t

Ford, P. W., Boon, P. I., & Lee, K. (2002). Methane and oxygen dynamics in a shallow floodplain lake: the significance of periodic stratification. In *Hydrobiologia* (Vol. 485).

Fuller, C. C., & Davis, J. A. (1989). *Influence of coupling of sorption and photosynthetic processes on trace element cycles in natural waters*.

Fung, S. R., Hull, E. A., Burkart, K., Gawel, J. E., Horner-Devine, A. R., & Neumann, R. B. (2022). Seasonal Patterns of Mixing and arsenic Distribution in a Shallow Urban Lake. *Water Resources Research*, *58*(10). https://doi.org/10.1029/2022wr032564

Gammons, C. H., Grant, T. M., Nimick, D. A., Parker, S. R., & DeGrandpre, M. D. (2007). Diel changes in water chemistry in an arsenic-rich stream and treatment-pond system. *Science of the Total Environment*, *384*(1–3), 433–451. https://doi.org/10.1016/j.scitotenv.2007.06.029

Gawel, J. E., Asplund, J. A., Burdick, S., Miller, M., Peterson, S. M., Tollefson, A., & Ziegler, K. (2014). Arsenic and lead distribution and mobility in lake sediments in the south-

central Puget Sound watershed: The long-term impact of a metal smelter in Ruston, Washington, USA. *Science of the Total Environment*, *472*, 530–537. https://doi.org/10.1016/j.scitotenv.2013.11.004

Hemond, H. F., & Fechner, E. J. (2014). *Chemical Fate and Transport in the Environment*. https://books.google.com/books?hl=en&lr=&id=zbRHAwAAQBAJ&oi=fnd&pg=PP1&dq=Hemond,+H.+F.,+and+E.+J.+Fechner.+2014.+&ots=Yl9QleF2ee&sig=k-PJeUuSdHDXwSURQUtd6CgQSV4#v=onepage&q=Hemond%2C%20H.%20F.%2C%20and%20E.%20J.%20Fechner.%202014.&f=false

Holgerson, M. A., Zappa, C. J., & Raymond, P. A. (2016). *Substantial overnight reaeration by convective cooling discovered in pond ecosystems*. *2*, 8044–8051. https://doi.org/10.1002/2016GL070206.Received

Hollibaugh, J. T., Carini, S., Gürleyük, H., Jellison, R., Joye, S. B., LeCleir, G., Meile, C., Vasquez, L., & Wallschläger, D. (2005). Arsenic speciation in Mono Lake, California: Response to seasonal stratification and anoxia. *Geochimica et Cosmochimica Acta*, *69*(8), 1925–1937. https://doi.org/10.1016/j.gca.2004.10.011

Hull, E. A., Barajas, M., Burkart, K. A., Fung, S. R., Jackson, B. P., Barrett, P. M., Neumann, R. B., Olden, J. D., & Gawel, J. E. (2021). Human health risk from consumption of aquatic species in arsenic-contaminated shallow urban lakes. *Science of the Total Environment*, *770*, 145318. https://doi.org/10.1016/j.scitotenv.2021.145318

IOC, SCOR, & IAPSO. (2010). *The international thermodynamic equation of seawater - 2010: Calculation and use of thermodynamic properties. Manual and Guides No. 56. Intergovernmental Oceanographic Commission, UNESCO (English).*

Jia, Y., Wang, L., Li, S., Cao, J., & Yang, Z. (2018). Species-specific bioaccumulation and correlated health risk of arsenic compounds in freshwater fish from a typical mine-impacted river. *Science of the Total Environment*, *625*, 600–607. https://doi.org/10.1016/j.scitotenv.2017.12.328

Keimowitz, A. R., Zheng, Y., Chillrud, S. N., Mailloux, B., Jung, H. B., Stute, M., & Simpson, H. J. (2005). Arsenic redistribution between sediments and water near a highly contaminated source. *Environmental Science and Technology*, *39*(22), 8606–8613. https://doi.org/10.1021/es050727t

King County. (2015, December 15). *Lake Information Page - King County*. https://green2.kingcounty.gov/smalllakes/LakePage.aspx?SiteID=21#WaterQualityData

Lorke, A. (1998). *Investigation of turbulent mixing in shallow lakes using temperature microstructure measurements*.

Lovley, D. R. (1991). Dissimilatory Fe(III) and Mn(IV) Reduction. In *MICROBIOLOGICAL REVIEWS* (Vol. 55, Issue 2).

Martin, A. J., & Pedersen, T. F. (2002). Seasonal and interannual mobility of arsenic in a lake impacted by metal mining. *Environmental Science and Technology*, *36*(7), 1516–1523. https://doi.org/10.1021/es0108537

Melack, J. M., & Fisher, T. R. (1983). Diel oxygen variations and their ecological implications in Amazon floodplain lakes. In *Arch. Hydrobiol* (Vol. 98).

Müller, B., Granina, L., Schaller, T., Ulrich, A., & Wehrli, B. (2002). P, As, Sb, Mo, and other elements in sedimentary Fe/Mn of Lake Baikal. *Environmental Science and Technology*, *36*(3), 411–420. https://doi.org/10.1021/es010940z

Nikolaidis, N. P., Dobbs, G. M., Chen, J., & Lackovic, J. A. (2004). Arsenic mobility in contaminated lake sediments. *Environmental Pollution*, *129*(3), 479–487. https://doi.org/10.1016/j.envpol.2003.11.005

Nimick, D. A., Gammons, C. H., Cleasby, T. E., Madison, J. P., Skaar, D., & Brick, C. M. (2003). Diel cycles in dissolved metal concentrations in streams: Occurrence and possible causes. *Water Resources Research*, *39*(9). https://doi.org/10.1029/2002WR001571

Palmer, M. J., Chételat, J., Richardson, M., Jamieson, H. E., & Galloway, J. M. (2019). Seasonal variation of arsenic and antimony in surface waters of small subarctic lakes impacted by legacy mining pollution near Yellowknife, NT, Canada. *Science of the Total Environment*, *684*, 326–339. https://doi.org/10.1016/j.scitotenv.2019.05.258

Ratkowsky, D. A., Olley, J., McMeekin, T. A., & Ball, A. (1982). Relationship between temperature and growth rate of bacterial cultures. *Journal of Bacteriology*, *149*(1), 1–5. https://doi.org/10.1128/jb.149.1.1-5.1982

Read, J. S., Hamilton, D. P., Desai, A. R., Rose, K. C., Macintyre, S., Lenters, J. D., Smyth, R. L., Hanson, P. C., Cole, J. J., Staehr, P. A., Rusak, J. A., Pierson, D. C., Brookes, J. D., Laas, A., & Wu, C. H. (2012). *Lake-size dependency of wind shear and convection as controls on gas exchange*. *39*, 1–5. https://doi.org/10.1029/2012GL051886

Rueda, F. J., Schladow, S. G., & Clark, J. F. (2008). Mechanisms of contaminant transport in a multi-basin lake. *Ecological Applications*, *18*(8), A72–A88. https://doi.org/https://doi.org/10.1890/06-1617.1

Smedley, P. L., & Kinniburgh, D. G. (2002). A review of the source, behaviour and distribution of arsenic in natural waters. *Applied Geochemistry*, *17*(5), 517–568. https://doi.org/10.1016/S0883-2927(02)00018-5

U.S. Environmental Protection Agency (USEPA). (2001). *Technical Fact Sheet: Final Rule for Arsenic in Drinking Water.* EPA 815-F-00-016. https://nepis.epa.gov/Exe/ZyPdf.cgi?Dockey=20001XXE.txt

Weber, F. A., Hofacker, A. F., Voegelin, A., & Kretzschmar, R. (2010). Temperature dependence and coupling of iron and arsenic reduction and release during flooding of a contaminated soil. *Environmental Science and Technology*, *44*(1), 116–122. https://doi.org/10.1021/es902100h

4. Chapter 4: Annually variability in mixing frequency of a shallow lake: implications for arsenic mobilization and transport

4.1. Abstract

Analysis of physical and biogeochemical data collected during the 2018 and 2019 summers revealed stark interannual differences in summertime lake mixing frequency and in arsenic concentrations in a shallow, polymictic lake. We find that mixing frequency controls arsenic flux both indirectly, through the moderation of bottom water DO, and directly, through the turbulent transport of arsenic throughout the water column. Lower mixing frequency in 2018 led to a greater degree of hypoxia in the hypolimnion and greater arsenic flux from porewaters into bottom waters. The lake water column mixed more often in 2019, which resulted in more oxygenated bottom waters and lower arsenic concentrations, overall. Averaged over the summertime periods, bottom water and porewater arsenic concentrations were approximately two times greater in 2018 than in 2019. Meteorology did not vary greatly between the summers. We found that the observed interannual variation in mixing frequency could likely be attributed to colder sediment temperatures, and a more stable thermal structure, in 2018 compared to 2019. There were higher rates of arsenic flux into bottom waters in 2018 than in 2019, even though the sediment temperatures were colder in the prior year. Consequently, our annual comparison demonstrates that sediment temperature did not have the expected effect on arsenic concentrations, despite temperature being a known control on arsenic mobilization rates in natural environments. Ultimately, this study shows that hydrologic controls play a dominant role in regulating rates of arsenic flux into the lake water. We also demonstrate that multiyear studies are necessary for determining the potential ranges of contaminant levels in the water and biota of shallow lakes and, thus, for informing management efforts.

4.2. Introduction

Arsenic contamination of aquatic systems is a growing concern worldwide, particularly in lakes that serve as sources of food and recreation for surrounding communities. Arsenic, a naturally occurring element, can be introduced into water bodies in elevated concentrations through anthropogenic activities including mining and smelting (Gawel et al., 2014; Smedley and Kinniburgh, 2002). When arsenic is deposited into lakes, it is stored as a legacy contaminant in the lakebed sediments adsorbed to, or coprecipitated with, minerals, including iron and manganese oxides and oxyhydroxides (Smedley and Kinniburgh, 2002; Couture et al., 2010). Contaminated lake sediments act as a long term source of arsenic to the system and represent a health risk to the aquatic food web and to humans who utilize the lake (Chen et al., 2015; Jia et al., 2018). Recent findings show that processes in shallow lakes, as opposed to in deep lakes, support high levels of ecosystem exposure to arsenic and that physical mechanisms, including summertime mixing, are key in producing the spatial overlap of arsenic with lake biota (Barrett et al., 2019; Fung et al., 2022).

Interannual variability is a ubiquitous feature of many environmental processes and characteristics in lakes, including thermal structure (Masunaga and Komuro, 2020), anoxia dynamics, (Ladwig et al., 2021), nutrient input and cycling (Powers et al., 2014), phytoplankton community makeup (Hoyos and Comín, 1999), and contaminant levels (Spliethoff et al., 1995). These variables are interrelated and thus, likely interact to create interannual patterns in overall lake behavior. The extent of variability of these parameters may also depend on lake characteristics, such as its location, depth, and mixing regime. For example, shallow lakes, which have greater connectivity to the atmosphere due to their high surface area to volume ratios, are generally more susceptible to large interannual fluctuations in physical and biogeochemical

variables compared to deeper lakes with more stable water columns and larger volumes. Of interest in this study is the interannually variability of arsenic in a shallow, polymictic lake. We hypothesize that year-to-year fluctuations in arsenic concentrations depend on physical and biogeochemical processes, including redox conditions, temperature, and summertime lake mixing.

The oxygen content of lake bottom waters regulates the flux of redox-sensitive species, including nutrients, such as phosphorus, and contaminants, such as arsenic, from lakebed porewaters into the hypolimnion (Andrade et al., 2010; Giles et al., 2016). For example, Wang et al. (2008) show that the oxygen content of water directly above the sediment water interface (SWI) is the largest regulator of phosphorous concentrations in lake bottom water. The mobility of arsenic in lakebed sediments is controlled by the balance of mobilization and sequestration processes, which both depend on the redox conditions of the porewater and the overlying water. Arsenic is mobilized via microbe-mediated reductive dissolution of iron and manganese minerals, which occurs in the anoxic porewaters of the sediment (Couture et al., 2010). Sequestration of dissolved arsenic may then occur at the redox front, or the location where near-surface porewater or bottom waters become oxic, due to readsorption to, and coprecipitation with, oxidized iron and manganese minerals (Couture et al., 2010; Muller et al., 2002; Nikolaidis et al., 2004). The redox front can migrate vertically on diel to seasonal timescales (Smith et al., 2011), and the location of the oxycline may control whether dissolved arsenic will spatially overlap with turbulence before reaching the oxic zone. Ultimately the location of the redox front in relation to the end of the diffusive boundary layer, or the ~1 mm layer above the SWI in which molecular diffusion is the dominant transport mechanism (Wüest and Lorke, 2003), could potentially modulate the degree to which arsenic is transported into the lake water column.

Because full lake mixing transports oxic surface waters to the near-bed region, it is likely that summertime mixing frequency of shallow lakes may impact the location and characteristics of the redox front.

The stratification and mixing behavior of shallow, polymictic lakes has been found to modulate arsenic mobilization and control transport at both diel and seasonal timescales (Fung et al., 2022; Fung et al., in prep). Specifically, previous studies show that physical processes affect arsenic both indirectly, through the regulation of biogeochemical lake properties, including the oxygen content and temperature of the near-bed region, and directly, through turbulent transport of dissolved arsenic and resuspension of arsenic-containing sediments (Fung et al., 2022; Linge & Oldham, 2002; Palmer et al., 2021). Because polymictic lakes can experience annual variation in the frequency of summertime mixing events (MacIntyre et al., 2009; Ahmed et al., 2022), it is likely that these physical mechanisms can impact year-to-year differences in lake water arsenic. Multiple factors, including patterns in meteorological and climate forcing, can affect the summertime mixing frequency of shallow lakes (MacIntyre et al., 2009; Ahmed et al., 2022). Air temperature is a strong predictor of thermal stratification in lakes and annual variation in air temperature has been shown to impact the strength and duration of stratification in shallow lakes (Ahmed et al., 2022; Wilhelm and Adrian, 2008). For example, Wilhelm and Adrian (2008) found that their shallow study lake exhibited the longest periods of stable stratification during the two hottest summers of their four-year study. Further, conditions during initial seasonal warming, including wind and air temperature, may impact overall summertime stratification and mixing behaviors in shallow lakes (MacIntyre et al., 2009).

Sediment temperature plays a large role in regulating the mobilization and transport of nutrients and contaminants stored in the lakebed. In addition to surface forcings such as solar

heating and wind, the temperature of lakebed sediments and the sediment-water heat flux can also have a significant impact on the stability of lake water columns (Fang and Stefan, 1996). Sediment heat flux plays an especially large role in regulating the mixing behavior of shallow lakes because the sediment interacts directly with a large proportion of the lake water volume (Masunaga and Komuro, 2020). Further, solar radiation can penetrate to, and directly heat, sediments of shallow lakes, making the lakebed a large seasonal heat reservoir in these systems (Fang and Stefan, 1996; Likens and Johnson, 1969). Previous work has shown that incorporating the sediment heat flux is necessary to accurately model stratification and mixing dynamics of shallow lakes, but not deep lakes (Tsay et al., 1992). Sediment temperature dynamics can also influence the vertical flux of dissolved nutrients and metals from lake porewaters into bottom waters. Golosov and Ignatieva (1999) found that a negative sediment-water temperature difference, or sediment that is warmer than overlaying water, can lead to convective instabilities in lake porewaters and elevated fluxes of nutrients from porewaters into the hypolimnion.

The fate of arsenic in lakes will likely be impacted by both direct and indirect effects of climate change, including increasing temperatures and alterations in lake mixing regime. Climate change is expected to alter the temperature regime and mixing behavior of lakes (Golosov et al., 2012). In general, lakes are expected to warm and experience increases in water column stability. For temperate, polymictic lakes, warming may lead to longer periods of stratification and fewer mixing events in the summertime. Although the impact of climate change on lake mixing regimes has been the topic of many observational and modeling studies, the effect of mixing regime shift on lake contaminants, including heavy metals, has not been thoroughly examined. It is essential to understand the underlying drivers of interannual variability in arsenic concentrations to effectively manage contaminated lakes, particularly in light of the potential

impacts of climate change on lake processes. In this study, we report annual variation in arsenic concentrations in Lake Killarney, a shallow, polymictic lake, between the summers of 2018 and 2019. Specifically, we examine the effects of summertime mixing frequency on the spatial distribution of arsenic. Through this analysis, we aim to elucidate the mechanisms that can predict year-to-year variability in the behavior of arsenic in shallow lakes. The patterns in arsenic concentrations in the warmer of the two summers in this study provides insight into how arsenic may behave in similar systems with future climate change.

4.3. Methods

4.3.1. Study site

This study was conducted at Lake Killarney, an urban lake in Federal Way, WA, USA (47°17'8.60"N, 122°17'32.20"W, elevation 111 m). Lake Killarney is small and shallow, with a mean depth of 2.6 m, an annual maximum depth of 4.6 m, and a surface area of 0.14 km^2 (Barrett et al., 2018; Gawel et al., 2014). Secchi depth from June through October in 2018 and 2019 ranged from ~1.5 – 2.3 m (King County, 2015). Because it is in a temperate climate, summers are relatively dry and the lake depth generally declines from late spring until the onset of fall precipitation. Lake Killarney is polymictic; full lake mixing during the summertime occurs on daily to monthly timescales (Fung et al., 2022). The lake is divided into two basins (Fig. 2.1). During most summers, the channel connecting the basins becomes very shallow (< 0.5 m) and has heavy macrophyte growth. Sampling was conducted in the larger, southern basin, which has a fetch of ~500 m. Lakebed sediments contain legacy As contamination with dry weight concentrations up to 206 $\mu g\ g^{-1}$ (Barrett et al., 2018; Gawel et al., 2014). Previous studies have documented elevated arsenic concentrations in lake water and plankton during summer months in Lake Killarney (Barrett et al., 2018, 2019; Fung et al., 2022; Hull et al., 2021). Arsenic

concentrations at the base of the food web in Lake Killarney have been reported to be highest from June through September (Barrett et al., 2019). Elevated arsenic levels have also been measured in higher trophic level biota, including snails and finfish (Hull et al., 2021). The shoreline of Lake Killarney is wind sheltered by bordering by houses and trees. The lake has no significant inflow or outflow.

4.3.2. Data collection

We collected meteorological, physical, and biogeochemical data during the summers of 2018 and 2019. Summertime was operationally defined as June 1 to October 31, the period when elevated arsenic concentrations have been previously documented in the water column of Lake Killarney (Barrett et al., 2019; Fung et al., 2022).

In situ wind speed, air temperature, and shortwave (SW) radiation were measured during a portion of the study. Wind speed and SW radiation were measured on a small, bare island in the lake's main basin (Fig. 2.1). A wind sensor (Davis wind speed and direction smart sensor; Davis Instruments Corporation, Hayward, CA, USA) was deployed 2.4 m above ground and collected wind speed data at an accuracy of ±1.1 m s^{-1} every 10 minutes. Downwelling SW radiation was measured using a pyranometer (Kipp-Zonen; Delft, Netherlands) at a 10 min period. Air temperature was measured ~0.25 m above the water surface near the lake's deepest point with a HOBO Tidbit v2 (accuracy of ±0.2°C, Onset Computer Corporation, Bourne, MA, USA) at a 10 minute period. External meteorological data were obtained for the entire study period and corrected using comparisons with in situ data during periods of overlapping data availability. Hourly wind and SW radiation data were sourced Washington State University AgWeatherNet's Puyallup station (11 km southwest of Lake Killarney) and 5-minute air temperature data were sourced from the SeaTac weather station (19 km north of Lake Killarney).

A thermistor array (HOBO Pro v2 and HOBO Tidbit v2, accuracy of ±0.2°C) was deployed on June 22, 2018 and recorded water temperature profiles at a 10 minute period for the remainder of the study. For the majority of the study, the temperature string had seven thermistors located at z = 0, 1, 1.5, 2, 2.5, 3, and 3.5 m, where z = 0 m is the lakebed; an additional sensor was added at z = 0.5 m at the end of the study period, from August 7 through October 31, 2019. The string of loggers was held taut by a cinderblock on the bottom and one or more buoys on the top. The bottom thermistor was submerged in the sediment and serves as a measure of sediment temperature.

Monthly water column sampling took place near the deepest part of the lake from June through October in both 2018 and 2019. Profiles of dissolved oxygen (DO) were measured with a sonde (HOBO U26, 0.2 mg L^{-1} accuracy, Onset Computer Corporation, Bourne, MA, USA) at a vertical resolution of 0.5 m. The oxygen probe was calibrated before each sampling day in deoxygenated water. Filtered water samples (0.45 μm Geotech cartridge) were collected at a subset of sampling depths (n = 4 or 5 depending on lake depth at sampling). Filtered water samples were acidified with 1% HNO3 (v/v) after the samples were transported back to the lab. Inductively-coupled plasma mass spectrometry (ICP-MS) was used to measure dissolved As concentrations; standard quality control as described in Barrett et al. (2018) was followed in our analysis.

Passive diffuser samplers, or peepers, were used to measure profiles of dissolved arsenic from 25 cm below the sediment water interface (SWI) to 25 cm above the SWI. Samplers held replicate columns of 14 vials at a 3.5 cm vertical resolution. Vials were filled with reverse tracer solution (200 μM KBr); after all deployments, analysis of the tracer solution indicated that the vials had reached equilibrium with the surrounding environment. Comprehensive information on

peeper configuration and deployment techniques have been previously reported; see Barrett et al. (2019) and Fung et al., (2022) for further information. Five ~monthly deployments occurred during each summer of our study and were each approximately two weeks long. Analysis of arsenic concentrations from the peeper vials followed the methodology used for water column samples, as described above and in Barrett et al. (2019).

Plankton tows were done near the deepest part of the lake on monthly sampling days. Duplicate phytoplankton and zooplankton vertical tows were taken in the upper 2 – 3 m of the lake; a 20 mm and 153 mm mesh net was used for phytoplankton and zooplankton tows, respectively. Biomass samples were stored on ice in acid-washed polypropylene bottles and were processed in the lab the same day as collection. Phytoplankton samples were first filtered through a 153 mm mesh net to remove zooplankton; following filtration, all samples were separately collected on a 5 mm polycarbonate membrane filters (Millipore) and desiccated overnight in a drying oven set to 60 °C. Total As concentrations in plankton samples were determined by a total digestion followed by ICP-MS, as described in detail by Barrett et al. (2018).

4.3.3. Data processing

Mixing events were defined as days when the lake underwent full mixing. Because temperature gradients could not be detected within the accuracy of the thermistor ($\pm$0.2℃), mixing events were determined to occur when the temperature difference between the bottom and top thermistors reached < 0.2 ℃ during a given day. The bottom thermistor was functionally defined as the thermistor at a height of 1.0 m since the thermistor 0.5 m off of the bed was not deployed until August 7, 2019. We also conducted a sensitivity analysis by calculating the number of mixing events during each summer with temperature thresholds ranging from 0.05 to 1 ℃ at

intervals of 0.05 °C. Changing the temperature threshold did not change the ratio of the number of mixing events in 2018 to the number of mixing events in 2019. Differences between the sediment temperature and mean water temperature, $\Delta T_{Sed-water}$, and the sediment temperature and air temperature, $\Delta T_{Sed-air}$, were calculated using hourly data. Daily moving means of SW radiation, wind speed, air temperature, and $\Delta T_{Sed-air}$ were calculated for visualization purposes, as hourly data obscured trends.

Arsenic concentrations were averaged from 5 to 20 cm below and above the SWI from each peeper deployment to get a measure of porewater and bottom water As, respectively. Surface and bottom water DO and arsenic were defined at the upper and lowermost measurement depths where arsenic was measured.

4.4. Results

4.4.1. Meteorology

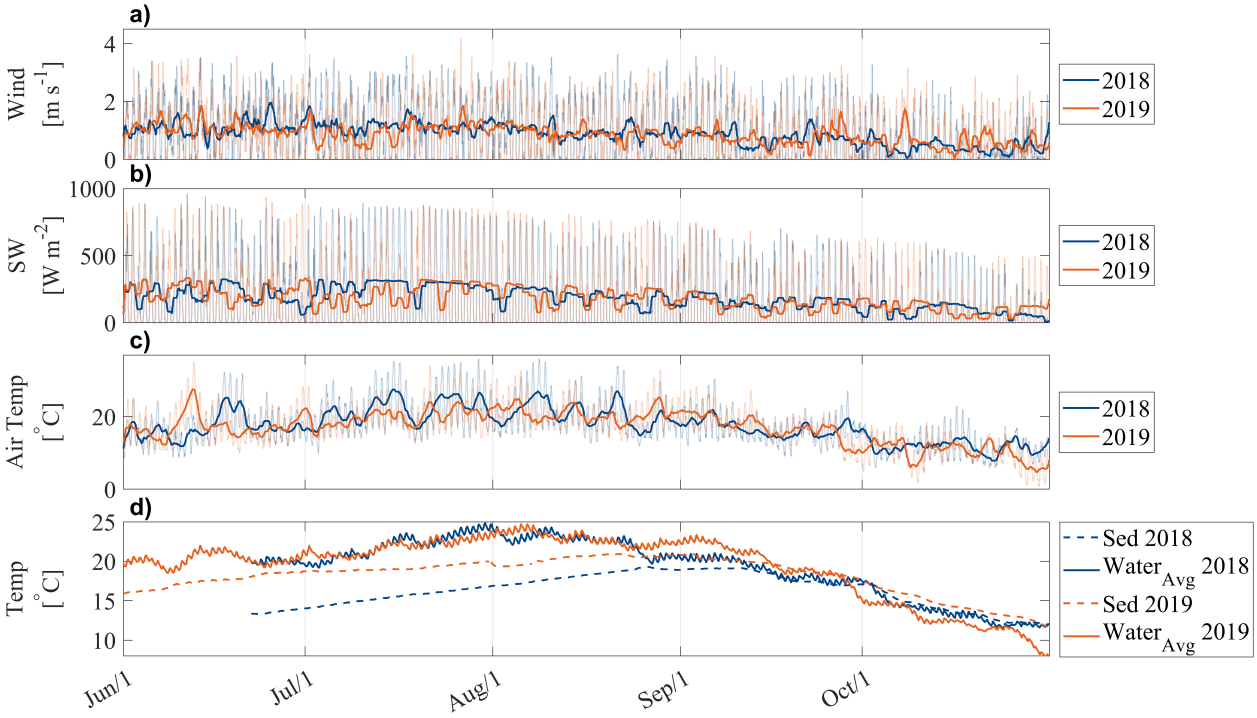

Figure 4.1. *(a) Wind speed, (b) shortwave (SW) radiation, (c) air temperature, and (d) sediment and average water temperate. In (a) – (c), bold lines are daily moving means and background transparent lines are hourly data.*

From June 1 to October 31, hourly wind speed ranged from 0 to 3.6 m s^{-1} in 2018 and from 0 to 4.2 m s^{-1} in 2019 (Fig 4.1a). The mean hourly wind speed was similar during both summers (0.88 m s^{-1} and 0.86 m s^{-1} in 2018 and 2019, respectively); variation in wind speed was large in both years, with a common standard deviation of 0.9 m s^{-1}. In both years, solar forcing was greatest in June and July and then steadily tapered off during the remainder of the summer (Fig 4.1b). Average hourly SW radiation during the summertime period was 180 W m^{-2} in 2018 and 176 W m^{-2} in 2019; maximum hourly SW radiation was 960 and 933 W m^{-2} in 2018 and 2019, respectively (Fig 4.1b). Air temperature was highest in late July and early August in both summers. In 2018, hourly air temperature ranged from 5.9 to 36.0 ℃ and was 17.6 ℃ on average. Air temperature was slightly colder in 2019, especially during late summer (Fig 4.1c). Mean hourly 2019 air temperature was 17.0℃, on average and had a range of 0.8 to 35.1℃. Average water temperature peaked simultaneously with air temperature, around late July in 2018 and early August in 2019 (Fig 4.1d). From June 22 through October 31, when we have thermistor data for both summers, the average mean water temperature was 19.3℃ in both years. In contrast to the similarity in water temperature, sediment temperature was much colder in 2018 than in 2019, especially through mid-summer (Fig 4.1d). Mean sediment temperature was 16.2℃ in 2018 and 18.3℃ in 2019. On July 1, the sediment temperature was 4.7℃ greater in 2018 than it was in 2019. Peak sediment temperature occurred in in late August in 2018 and early September 2019, approximately a month after the peak in air and water temperatures in the respective year (Fig 4.1c, d).

4.4.2. Stratification and mixing events

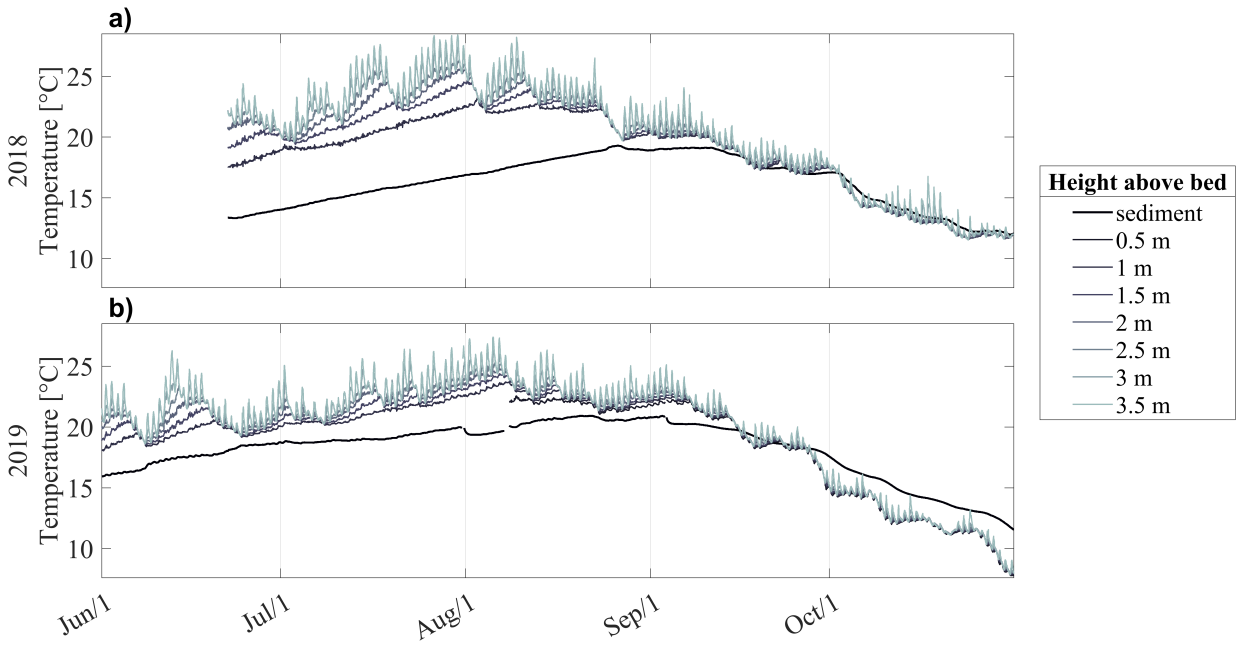

Figure 4.2. *Thermistor timeseries in (a) 2018 and (b) 2019. Darker shades represent deeper depths in the water column.*

The thermistor timeseries in Fig 4.2 show lake temperature structure throughout the summers of 2018 and 2019. Higher temperature gradients, or larger spread between the various thermistors, indicate greater strength in water column stratification. Stratification was strongest from June through early August in both summers, the period when all lake temperatures were increasing, overall (Fig 4.2). At the end of the warming period, all temperatures peaked, with the exception of sediment temperature. Surface water temperature exhibited a maximum of 28.4 and 27.4℃ in 2018 and 2019, respectively. Temperatures then cooled through the end of October and stratification became weaker (Fig 4.2). In mid- to late August, the temperature structure largely collapsed. Although there was still daytime heating and diel upper water column stratification, temperature in the water column homogenized almost nightly during this late summer period. During early October of 2018 and mid-September of 2019, the sediment temperature became warmer than the water temperature, with the exception of daytime surface water heating in 2018.

Lake temperatures were at a minimum at the end of our study and reached 11.5 and 7.8°C in 2018 and 2019, respectively. Because the water column was largely homogenous during this early fall period, the temperature minimums occurred throughout the water column. Colder water temperatures in the early fall of 2019 are consistent with observations of colder air temperatures in October of 2019, when compared to 2018 (Fig 4.1c, Fig 4.2).

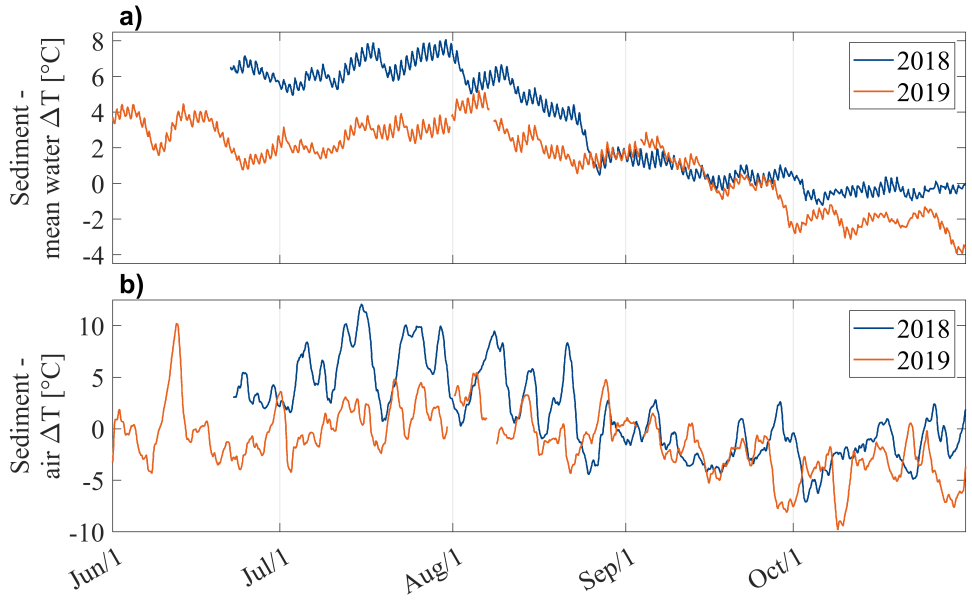

Figure 4.3. *(a) Hourly sediment – mean water temperature difference and (b) 24-hour moving mean of the sediment – air temperature difference for the summers of 2018 (blue) and 2019 (orange).*

There were greater sediment – water temperature differences ($\Delta T_{Sed-water}$) and sediment – air temperature differences ($\Delta T_{Sed-air}$) in 2018 than in 2019 (Fig 4.3). The anomaly between the two years was especially large from the end of June through July. In both summers, the peak $\Delta T_{Sed-water}$ occurred in late July or early August and was simultaneous with the peak in mean water temperature (Fig 4.1d, Fig 4.3a). Although peak $\Delta T_{Sed-water}$ occurred at the same time in the two years, the magnitude of the peaks varied significantly at 8.1 and 5.2°C in 2018 and 2019, respectively. From June 23 through October 31, the average $\Delta T_{Sed-water}$ was 3.0°C in 2018 and 0.9°C in 2019. Apart from a large spike in the $\Delta T_{Sed-air}$ in mid-June of 2019, maximum

$\Delta T_{Sed-air}$ values occurred during mid-July in 2018 and early August of 2019. Similarly to $\Delta T_{Sed-water}$, the average $\Delta T_{Sed-air}$ was much higher in 2018 (1.5℃) than in 2019 (-1.4℃). Overall, both $\Delta T_{Sed-water}$ and $\Delta T_{Sed-air}$ increased through July and then declined for the remainder of the timeseries (Fig 4.3). Trends in these temperature differences exhibited multiweek patterns within the longer term trends, where magnitudes increased over week to multi-weeklong periods and then decreased over the same timescale. The fact that neither air or mean water temperatures were significantly different between the two summers indicates that the annual variation observed in $\Delta T_{Sed-water}$ and $\Delta T_{Sed-air}$ are primarily due to the annual variation in the sediment temperature (Fig 4.1c, 4.1d; Fig 4.3).

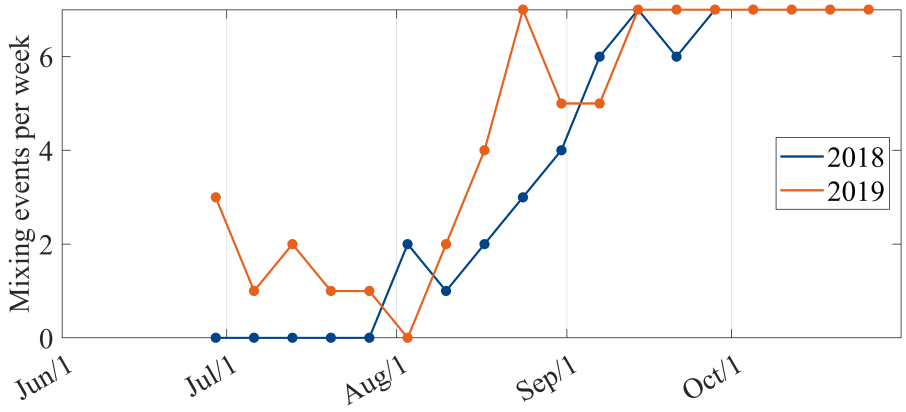

Figure 4.4. *Number of mixing events each week from June 23 to October 26 for 2018 and 2019. Dots represent the last day of the week over which mixing events were summed.*

The number of weekly mixing events differed between the two years, especially in the early summer (Fig 4.4). In 2018, there were no mixing events from late June through the end of July which shows that part of the lake's water column remained stratified for this time (Fig 4.4). In contrast, the lake experienced full mixing at least once each week in July 2019 (Fig 4.4). Although the presence of weekly mixing was largely consistent in 2019, the number of mixing events exhibited a decreasing trend from the end of June through early August in 2019 suggesting that the strength of stratification increased during this time. The upward trend in the

sediment-mean water temperature difference during the period in 2019 is consistent with this observation and suggests that patterns in $\Delta T_{Sed-water}$ could explain this increasing stratification (Fig 4.2a). By early August of both 2018 and 2019, Lake Killarney began to experience full mixing each week, generally multiple times a week (Fig 4.4). The trend in the number of mixing events per week exhibited a relatively consistent increase from the beginning of August through early September in both years. The lake began to experience daily mixing (7 mixing events per week) in early September of both summers, with the aberration of one week in late September of 2018 when the lake only mixed fully 6 out of 7 days of the week. Overall, lake mixing occurred more frequently in 2019 than in 2018, indicating that there were larger or more steady forces that generated lake mixing in the latter year. Significantly, sensitivity analysis confirms that this result remained consistent regardless of the temperature threshold, or top-bottom DT, used to define complete mixing (Fig. A3.1).

4.4.3. Arsenic and dissolved oxygen

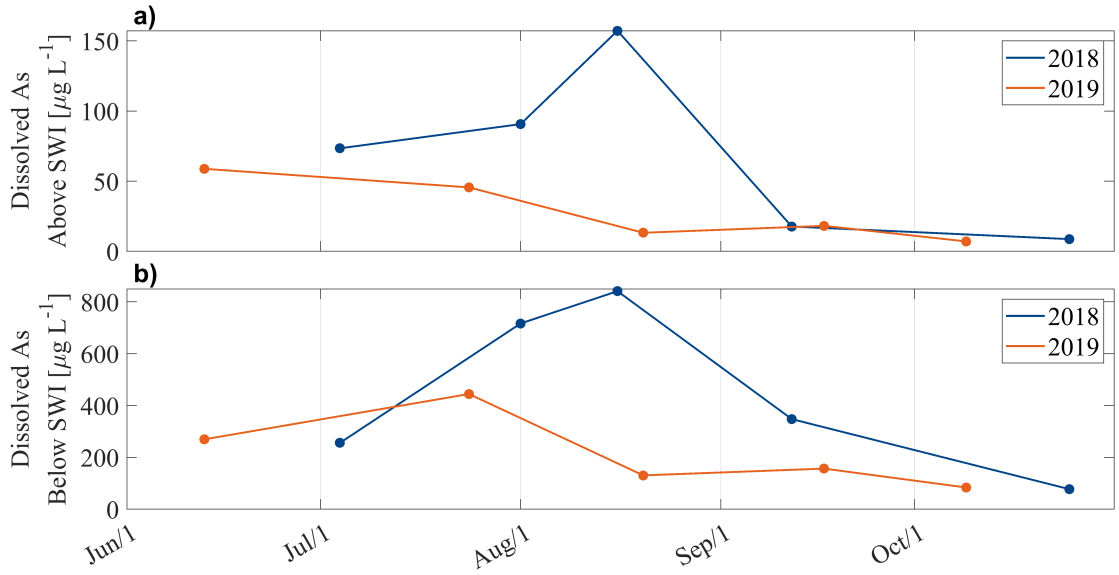

Figure 4.5. *Dissolved arsenic (As) concentrations from passive diffuser samplers: (a) bottom water, averaged from 5 to 20 cm above the sediment water interface (SWI) and (b) porewater, averaged from 5 to 20 cm below the SWI. Dots are plotted on the days that represent the middle of each passive diffuser deployment. Blue represents 2018 data and orange represents 2019 data in both panels.*

Porewater and bottom water dissolved As were elevated to greater concentrations and for a larger spatial and temporal extent in 2018 compared with 2019 (Fig 4.5a, 6b; Fig. 2.5). Porewater concentrations in 2018 ranged from 77 mg L^{-1} to 841 mg L^{-1} and had a mean and median of 448 mg L^{-1} and 348 mg L^{-1}, respectively (Fig 4.5b, Fig. A3.2). In 2019, the range, mean and median in porewater As were all smaller, with min, max, mean and median being 130 mg L^{-1}, 444 mg L^{-1}, 250 mg L^{-1} and 213 mg L^{-1}, respectively (Fig 4.5b). Similar annual differences were seen in dissolved As above the SWI (Fig 4.5a), where average concentrations were 70 mg L^{-1} and 34 mg L^{-1} in 2018 and 2019, respectively. Although the years were not statistically ($P < 0.05$) different for either porewater or bottom water arsenic concentration, it is still likely the differences in concentrations are significant, given the low sample sizes ($n = 4$ for 2018, $n = 5$ for 2019). The high porewater concentrations in 2018 likely influenced the flux from the porewaters to the bottom waters (Fig. 2.5), which also reached a higher magnitude and stayed elevated for longer in 2018 than in 2019.

The trends in As concentrations above and below the SWI were similar within each year, which fits intuition since the source of As in the bottom water is As diffusing upward from the porewaters. However, the trends vary year-to-year. In 2018, both porewater and bottom water As increased from early July to a peak in mid-August and then decreased through late October. In 2019, however, concentrations of both pools of As largely exhibited a declining trend throughout the summer and there was no obvious peak during the study period.

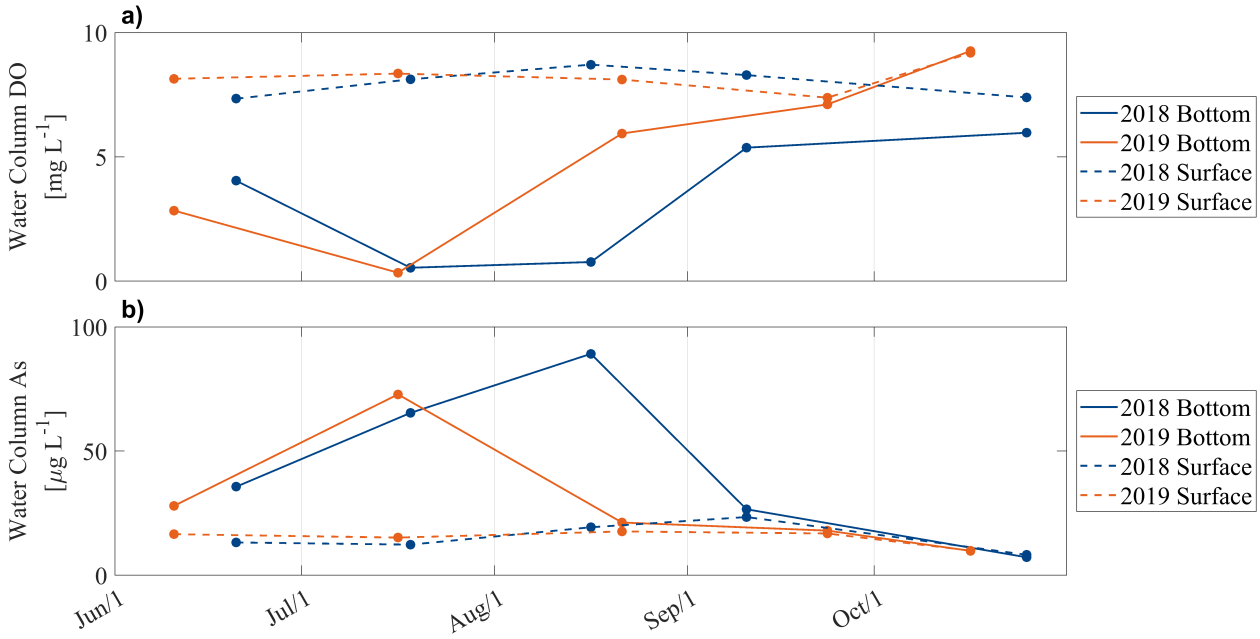

Figure 4.6. *(a) Dissolved oxygen (DO) and (b) dissolved arsenic (As) from monthly water column sampling. Solid lines are bottom water samples and dashed lines are surface water samples. Blue represents 2018 data and orange represents 2019 data in both panels.*

Trends and magnitudes of bottom water and surface water DO and As concentrations from monthly water column sampling are shown in Fig 4.6. The main variation in the bottom water DO and As trends occurred mid-summer. From July to August in 2019, the bottom water became more oxygenated (Fig 4.6a). In contrast, hypoxic conditions persisted during this time in 2018 (Fig 4.6a). In tandem, bottom water As decreased significantly in 2019 during this period, but concentrations in 2018 continued increasing through at least the middle of August to a peak of 89.1 mg L^{-1} Fig 4.6b). Overall, there was lower bottom water DO and higher bottom water As in 2018 than in 2019. Mean bottom water DO was 3.3 and 5.1 mg L^{-1} in 2018 and 2019, respectively, and mean bottom water As was 44.8 and 39.0 mg L^{-1} in 2018 and 2019, respectively. In contrast to bottom water conditions, near-surface DO and As were comparable between the two summers and relatively consistent throughout each summer. Mean summer near-surface arsenic concentration was exactly 15.8 mg L^{-1} in both 2018 and 2019, despite porewater and bottom water concentrations being much higher in 2018. The range of near-

surface arsenic concentrations in 2019 (12.7 mg L^{-1} – 17.6 mg L^{-1}) was smaller than the range in 2018 (10.7 mg L^{-1} – 23.4 mg L^{-1}). Surface DO was also similar between years, with a mean of 8.0 and 8.2 mg L^{-1} in 2018 and 2019, respectively. Starting in September of 2018 and August of 2019, concentrations in bottom and surface water As equalized, which suggests that mixing processes had homogenized the As concentrations throughout the water column at these points in the respective summers.

4.5. Discussion

4.5.1. Main findings

We observed interannual differences in the summertime arsenic concentrations in a shallow, polymictic lake. The greatest variation in concentrations occurred in the lake porewaters and the waters above the SWI, where average summertime concentrations were approximately two times greater in 2018 than in 2019 (Fig 4.5). The frequency of mixing differed between the two years, especially from late June through August. However, meteorology did not vary greatly between the summers. Differences in lake mixing behaviors between the two summers can likely be attributed to colder sediment temperatures and greater $\Delta T_{Sed-water}$ and $\Delta T_{Sed-air}$ values in 2018 compared to 2019. Although sediment temperature was colder in 2018, there were higher rates of arsenic flux from the porewaters to lake bottom waters. Consequently, our annual comparison demonstrates that sediment temperature did not seem to have a dominant effect on arsenic concentrations, despite temperature being a known control on arsenic mobilization rates in natural environments (Barrett et al., 2019; Weber et al., 2010). Ultimately, we find that physical factors, particularly the lake mixing frequency, play the largest role in controlling the flux of arsenic into lake waters, both directly, and indirectly through regulating bottom water dissolved oxygen.

4.5.2. Annual variability in meteorology

In general, meteorology did not show large year-to-year variability (Fig 4.1). However, the differences that were present, although small, were consistent with our observations of greater stratification strength in 2018 than 2019. Namely, maximum and average SW radiation were both slightly higher in 2018 than 2019, indicating that amplified solar forcing could have led to more surface water heating and the development of larger water column temperature gradients in 2018. The peak in air temperature was almost 1℃ greater in 2018 than 2019 and this peak coincided with the period when interannual difference in mixing were greatest (Fig 4.1, Fig 4.3). As reported by previous studies, air temperature can affect lake thermal regime through air-water heat exchange at the lake surface (Ahmed et al., 2023, He et al., 2015). Ahmed et al. (2022; 2023) also conducted a study in 2018 and 2019 on two shallow ponds located in Calgary, CA, and reported higher air temperatures and greater stratification in the summer of 2018, as compared to 2019. Although the study sites in Ahmed et al. (2022; 2023) are ~700 km northeast from Lake Killarney, it is possible that larger scale climate systems led to common patterns in air temperatures and water column stratification strength in all of these shallow systems. Although average wind speeds were comparable in both summers, our wind measurement is from a weather station 11 km away from the lake and may not provide an accurate measure of the wind forcing at the lake, especially considering that the lake is sheltered by surrounding houses and tress and the possibility for spatial variability of wind patterns.

4.5.3. Annual variability in stratification and mixing

We observed interannual variation in water column stratification and mixing, especially from late June through mid-August (Fig 4.2, Fig 4.4). The lake experienced large thermal gradients, both in the water column and between the sediment and the water, during this time in 2018,

which contrasts the smaller thermal gradients that were present in 2019 (Fig 4.2, Fig 4.3). Specifically, maximum $\Delta T_{Sed-water}$ was 3℃ greater in 2018 than in 2019. Other studies on shallow lakes, have reported that stratification is primarily caused by fluctuating air temperatures (Ahmed et al., 2023; He et al., 2015). However, because peak surface water temperature was only 1℃ warmer in 2018 than 2019, we can conclude that this difference in the surface water temperature cannot fully explain the large annual difference in the overall thermal gradient. Instead, the significant interannual variation in sediment temperature can likely account for much of the variance in thermal structure and water column stability between the two study years. Sediment temperature and air temperature contribute to heat flux, and thus patterns in thermal stratification, at opposite ends of the water column. Sediment heat flux more directly influences the temperature gradient of the hypolimnion, whereas air temperature more directly influences the temperature gradient of the near-surface waters. He et al. (2015) also reported that air temperature has diminishing effects on the temperature gradient at deeper depths, even in very shallow lakes. In Lake Killarney, we find that surface water stratification was more transient and was broken down regularly by convective mixing, even in the early summer of 2018 when full mixing was rare (Fig 4.2). In contrast, the bottom thermal gradient, which is set by sediment temperature, was maintained for the first 5 weeks of the study. The maintenance of stratification in the hypolimnion is what allowed DO concentrations to remain low and mobile As to exist in elevated concentrations in the porewater and bottom water (Fig 4.2, Fig 4.5, Fig 4.6). Significantly, these results suggest that, through regulation of hypolimnetic stability, the sediment temperature had a larger effect on arsenic dynamics than air temperature during our study.

Interestingly, there was large interannual sediment temperature variability present at the start of the summer sampling, which indicates that the baseline sediment temperature was set earlier in the season. MacIntyre et al. (2009) reported that the overall thermal structure of a shallow lake may be set my meteorological conditions during initial lakes warming. Following these results, we examined wind and air temperatures in March and April, the months of initial seasonal lake warming (Barrett et al., 2018; Fung et al., 2022). The average March air temperature was 8.7℃ in 2019, almost 1℃ warmer than the average air temperature in March 2018 (Table A3.1). Further, we found that there were 15 hours of high wind (> 3 m/s) during March of 2019, compared to only 3 hours of high wind in March 2018 (Fig. A3.3). These results indicate that elevated wind speeds and air temperatures in March of 2019 may have led to heat being mixed downward and ultimately transferred to the sediment during this initial spring warming period. Data from Chapter 2 also demonstrates that air temperature became colder than both sediment and average water temperatures for much of April in 2019 (Fig. 2.2d). The lake experienced a period of relatively low SW radiation, low air temperature, and high wind in early and mid-April 2019. During this time, daily maximum SW and daily average air temperature were generally much lower than during the periods before or after, whereas winds were higher than during the periods before and after (Fig. 2.2C). These forcing patterns led to a well-mixed water column during most of April, 2019 (Fig. 2.3b). It is probable that the early season transport of heat resulted in the higher sediment temperature and lower temperature gradients at the beginning of the 2019 summer, compared to the lower sediment temperature and higher temperature gradient observed at the beginning of the 2018 sampling period (Fig 4.2).

4.5.4. Annual variability in DO and arsenic

Hypoxic conditions were maintained for a longer period of time in 2018 than 2019 (Fig 4.6). The degree of this annual variation may have been understated by our temporally coarse sampling regime. Although we measured low bottom water DO in July of 2019, this sampling day occurred at the end of a ~weeklong period of stratification, which was uncharacteristic of the rest of the month's well mixed conditions (Fig 4.2. Fig 4.4). Thus, this measurement of low DO in July of 2019 may not be indicative of the overall bottom water DO conditions during this time. Future studies would benefit from more frequent DO data, which would allow for increased accuracy in the investigation and interpretation of temporal patterns in bottom water redox conditions.

Bottom water DO concentration reflects the balance of DO supply and consumption in the nearbed region and can affect the characteristics of the redox front, namely the location of the front and the spatial scale over which the transition from oxic to suboxic conditions occurs. The location of the redox front in relation to the SWI has been shown to migrate on diel and seasonal timescales (Smith et al., 2011). The location of the redox front is likely important in controlling rates of As transport from porewaters into the bottom waters. For example, if the top millimeters of the surface sediment are oxic (i.e. Müller et al., 2002; Fig 4.3, winter profiles), a large proportion of dissolved arsenic in the porewaters may be sequestered before making it past the diffusive boundary layer, which ends ~ 1 mm above the SWI (Wüest and Lorke, 2003). On the other hand, if hypoxic conditions extend above the SWI, mobile As would be exposed to turbulent mixing processes before oxidation and incorporation with solid minerals could occur. Considering the annual variation in bottom water DO, it is plausible that corresponding variations occurred in the position of the redox front, which likely played a role in the

differences observed in bottom water As between 2018 and 2019 in Lake Killarney. Profiles of DO in the region adjacent to the SWI would be instructive for examining the effect of redox front location on As flux rates and should be measured in future studies.

Annual variation in bottom water DO persisted through the end of summer, with concentrations of 6.0 and 9.1 mg L^{-1} in 2018 and 2019, respectively. Although these late season differences may be partially due to colder temperatures, and thus higher DO saturation, at the start of fall in 2019 (Fig 4.2, Fig 4.6), changes in saturation cannot fully explain the difference. As discussed above, the lake generally mixed daily during October in both years. However, our results suggest that the degree of mixing may have been different, even during this late summer period. Specifically, the sediment became noticeably warmer than the water column in late September of 2019, leading to a consistently negative $\Delta T_{Sed-water}$ during the last month of the study (Fig 4.2, Fig 4.3). In contrast, the sediment and water temperatures remained close during this same period in 2018, with surface water often becoming warmer than the sediment. These observations likely led to more stable conditions, less continuous mixing, and lower DO in the beginning of autumn of 2018 compared with 2019. Our findings are in line with previous research which shows that heat flux out of sediments drives the onset of enhanced mixing frequency during early fall in shallow lakes (Ahmed et al., 2023; Fung et al., 2022) and we show that $\Delta T_{Sed-water}$ during this time may continue to impact the degree of water column mixing and concentrations of DO.

There were large interannual differences in porewater and bottom water As concentrations from the end of July into August (Fig 4.5, Fig 4.6). The annual variation was most pronounced in the region adjacent to the SWI (Fig 4.5). One limitation of these findings is that the peeper deployments did not occur on the same dates during each summer, making it

challenging to establish a direct comparison between the data. Although elevated temperatures are known to expediate the formation of reducing conditions and increase rates of arsenic mobilization (Aurilio et al., 1994; Barrett et al., 2019; Weber et al., 2010), we significantly observed lower rates of arsenic flux during the summer with higher sediment temperatures (Fig 4.2, Fig. 2.5). Although there still may have been similar rates of mobilization from sediment minerals into the porewaters during the summers, our results show that mixing frequency, and the resulting redox conditions sequestration rates, were the largest control on how much As was released into lake bottom waters. Palmer et al. (2021) also showed that hydrologic control on DO, specifically the creation of anoxic conditions following ice over of a lake, was the largest control over the As concentrations of their study lake.

Surprisingly, average near-surface arsenic concentration was the same in both summers. However, the ranges of arsenic concentrations in the porewaters, bottom waters, and surface waters were larger in 2018 than in 2019, indicating that the lake experienced more variable conditions in 2018 and more consistent conditions in 2019. Because there was less frequent mixing in 2018, higher concentrations of As built up in the hypolimnion and then were transported in pulses to the surface water. In the extended time between the mixing events, As was likely sequestered out of the upper water column, resulting in a lower minimum surface water As concentration in 2018 than 2019. Mixing occurred more often in 2019, leading to more regular pulses of lower concentration water and the smaller ranges in As concentrations observed in the porewater, bottom water, and surface water.

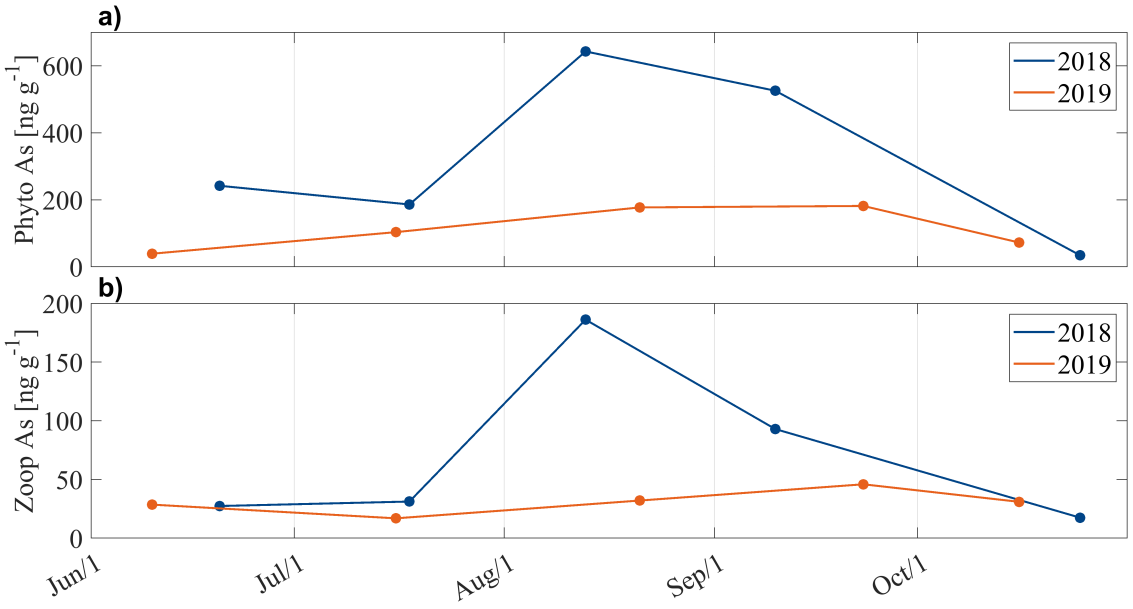

Figure 4.7. *Dry weight arsenic (As) concentrations in (a) phytoplankton and (b) zooplankton collected ~monthly.*

The annual variation in bottom water As was reflected in the uptake of the contaminant in phytoplankton and zooplankton (Fig 4.7). Maximum dry weight concentrations were 3.5 and 4 times higher in 2018 than 2019, for phytoplankton and zooplankton, respectively. These maximum concentrations occurred in August, which is consistent with the timing of previously observed patterns in plankton As in lake Killarney (Barrett et al., 2019). These differences indicate that phytoplankton took up As in the hypolimnion, since surface water As was similar in each year and could not have resulted in the large interannual variation in plankton As concentrations. Primary producers readily take up arsenic from the surrounding waters by mistaking arsenate, or As(V), the oxidized form of inorganic arsenic, for phosphate (Sanders et al. 1989, Wang et al. 2013). Although it is often thought that arsenite, or As(III), the reduced form of As, is the dominant form of inorganic As in the hypoxic porewater or bottom waters of lakes (Aggett and O'Brien, 1985; Keimowitz et al., 2005), there is an increasing amount of literature pointing to the prevalence of arsenate in these regions (Martin and Pedersen, 2002;

Spliethoff et al., 1995, Andrade et al., 2010). From the annual variation in plankton uptake, we can infer that arsenate likely persisted in the bottom waters of Lake Killarney in 2018, despite the hypoxic conditions.

Routine monitoring data from local government shows that Chlorophyll A was much higher in 2019 than 2018 (King County), which indicates that a greater number of phytoplankton were present in the latter year. The frequent mixing in July 2019 may have led to more regular nutrient fluxes and redistribution of nonmotile phytoplankton, allowing for a larger and more stable plankton population compared to the smaller numbers in 2018, when mixing and nutrient transport were less frequent. It is possible that the low As concentrations in plankton in 2019 was partially due to this higher population size and resulting dilution of As throughout the community.

4.5.5. Conclusions

We observed interannual variation in As and DO concentrations along with stratification and mixing dynamics between the summers of 2018 and 2019 in a shallow temperate lake. In 2018, there was stronger stratification, less frequent mixing, lower DO, and higher concentrations of As in lake waters. Summer 2019 was characterized by weaker stratification, more frequent mixing, higher DO, and lower concentrations of arsenic in lake waters. Air temperatures regulated surface stratification, which was broken down regularly and had minimal implications for arsenic flux in the lake. Sediment temperature had a larger impact on the bottom water thermal structure and, as a result, on bottom water DO and As concentrations. As noted, sediment temperature seem to be set by early season conditions including winter and spring air temperatures and wind patterns. These findings align with those of MacIntyre et al. (2009) who observed that characteristics of summer stratification in shallow lakes may be set by

meteorological forcing during initial lake warming. Our study demonstrates the implications and significance of these early season conditions by showing that the thermal regime established during this time influences the behavior of arsenic throughout the summer and, ultimately, the amount of As taken up into the food web. Because plankton are the base of the food web, the annual differences in uptake (Fig 4.7) may be translated to upper trophic levels, including fin fish, which are often caught and consumed from urban lakes (Chen and Folt, 2000; Shah et al., 2009).

Understanding interannual variations in contaminant levels is important for short-term and long-term management of lakes. For example, current health advisories for the consumption of biota in As-contaminated lakes should be based on the highest potential concentrations given the range of annual behaviors. Future climate change should also be taken into account when considering the fate of legacy As in contaminated systems. Warming air temperatures may alter the factors that govern arsenic mobilization and transport, including sediment temperature and mixing regime. Higher temperatures will likely increase biological activity at the SWI, which would expediate the production of reducing conditions and elevate rates of arsenic mobilization.

Results of this study indicate that the effects of climate warming on sediment temperature and mixing regime will depend on the timing on increased temperatures, as well as on other meteorological forces, including wind. In Lake Killarney, we observed that warmer air temperature combined with elevated wind speeds during initial spring warming in 2019 led to warm sediment temperatures, more frequent lake mixing, and lower arsenic concentrations throughout the entire summer. However, we expect that warm air temperatures and the absence of strong wind during initial spring warming would lead to a more stable thermal regime and less frequent summertime mixing. As observed in 2018 in this study, warmer air temperatures during

the middle of the summer (June – August) will likely cause stronger stratification, especially in the surface layer, and less overall mixing in shallow, temperate lakes.

Climate change may also affect the strength and frequency of convective mixing in shallow lakes by changing day-night temperature dynamics. Recent work has shown that air temperatures are expected to increase more at nighttime compared to daytime (Davy et al., 2017). Warmer nights would lead to decreased convective cooling, less frequent mixing, and more intense and prolonged hypoxia in shallow lake bottom waters. As a result, warmer nighttime temperatures may cause an increase in arsenic concentrations during the summertime in shallow, temperature lakes.

This study supports the growing body of literature showing that physical processes in lakes play a dominant in regulating biogeochemical characteristics and highlights the importance of investigating both physical and biogeochemical factors to gain a comprehensive and accurate understanding of contaminant behavior in shallow lakes.

4.6. References

Aggett, J., & O'Brien, G. A. (1985). Detailed Model for the Mobility of Arsenic in Lacustrine Sediments Based on Measurements in Lake Ohakuri. *Environmental Science and Technology*, *19*(3), 231–238. https://doi.org/10.1021/es00133a002

Ahmed, S. S., Loewen, M. R., Zhang, W., Ghobrial, T. R., Zhu, D. Z., Mahmood, K., & van Duin, B. (2022). Field observations of stratification in stormwater wet ponds. *Journal of Environmental Management*, *322*. https://doi.org/10.1016/j.jenvman.2022.115988

Ahmed, S. S., Zhang, W., Loewen, M. R., Zhu, D. Z., Ghobrial, T. R., Mahmood, K., & van Duin, B. (2023). Stratification and its consequences in two constructed urban stormwater wetlands. *Science of the Total Environment*, *872*. https://doi.org/10.1016/j.scitotenv.2023.162179

Andrade, C. F., Jamieson, H. E., Kyser, T. K., Praharaj, T., & Fortin, D. (2010). Biogeochemical redox cycling of arsenic in mine-impacted lake sediments and co-existing pore waters near Giant Mine, Yellowknife Bay, Canada. *Applied Geochemistry*, *25*(2), 199–211. https://doi.org/10.1016/j.apgeochem.2009.11.005

Aurilio, A. C., Mason, R. P., & Hemond, H. F. (1994). Speciation and Fate of Arsenic in Three Lakes of the Aberjona Watershed. In *Environ. Sci. Technol* (Vol. 28). https://pubs.acs.org/sharingguidelines

Barrett, P. M., Hull, E. A., King, C. E., Burkart, K., Ott, K. A., Ryan, J. N., Gawel, J. E., & Neumann, R. B. (2018). Increased exposure of plankton to arsenic in contaminated weakly-stratified lakes. *Science of the Total Environment*, *625*, 1606–1614. https://doi.org/10.1016/j.scitotenv.2017.12.336

Barrett, P. M., Hull, E. A., Burkart, K., Hargrave, O., McLean, J., Taylor, V. F., Jackson, B. P., Gawel, J. E., & Neumann, R. B. (2019). Contrasting arsenic cycling in strongly and weakly stratified contaminated lakes: Evidence for temperature control on sediment–water arsenic fluxes. *Limnology and Oceanography*, *64*(3), 1333–1346. https://doi.org/10.1002/lno.11119

Chen, C. Y., & Folt, C. L. (2000). Bioaccumulation and diminution of arsenic and lead in a freshwater food web. *Environmental Science and Technology*, *34*(18), 3878–3884. https://doi.org/10.1021/es991070c

Chen, G., Shi, H., Tao, J., Chen, L., Liu, Y., Lei, G., Liu, X., & Smol, J. P. (2015). Industrial arsenic contamination causes catastrophic changes in freshwater ecosystems. *Scientific Reports*, *5*, 1–7. https://doi.org/10.1038/srep17419

Couture, R. M., Gobeil, C., & Tessier, A. (2010). Arsenic, iron and sulfur co-diagenesis in lake sediments. *Geochimica et Cosmochimica Acta*, *74*(4), 1238–1255. https://doi.org/10.1016/j.gca.2009.11.028

Davy, R., Esau, I., Chernokulsky, A., Outten, S., & Zilitinkevich, S. (2017). Diurnal asymmetry to the observed global warming. *International Journal of Climatology*, *37*(1), 79–93. https://doi.org/10.1002/joc.4688

Fang, X., & Stefan, H. G. (1996). Dynamics of heat exchange between sediment and water in a lake. *Water Resources Research*, *32*(6), 1719–1727. https://doi.org/10.1029/96WR00274

Fung, S. R., Hull, E. A., Burkart, K., Gawel, J. E., Horner-Devine, A. R., & Neumann, R. B. (2022). Seasonal Patterns of Mixing and Arsenic Distribution in a Shallow Urban Lake. *Water Resources Research*, *58*(10). https://doi.org/10.1029/2022wr032564

Gawel, J. E., Asplund, J. A., Burdick, S., Miller, M., Peterson, S. M., Tollefson, A., & Ziegler, K. (2014). Arsenic and lead distribution and mobility in lake sediments in the south-central Puget Sound watershed: The long-term impact of a metal smelter in Ruston, Washington, USA. *Science of the Total Environment*, *472*, 530–537. https://doi.org/10.1016/j.scitotenv.2013.11.004

Giles, C. D., Isles, P. D. F., Manley, T., Xu, Y., Druschel, G. K., & Schroth, A. W. (2016). The mobility of phosphorus, iron, and manganese through the sediment–water continuum of a shallow eutrophic freshwater lake under stratified and mixed water-column conditions. *Biogeochemistry*, *127*(1), 15–34. https://doi.org/10.1007/s10533-015-0144-x

Golosov, S. D., & Ignatieva, N. v. (1999). *Hydrothermodynamic features of mass exchange across the sediment-water interface in shallow lakes*.

Golosov, S., Terzhevik, A., Zverev, I., Kirillin, G., & Engelhardt, C. (2012). Climate change impact on thermal and oxygen regime of shallow lakes. *Tellus, Series A: Dynamic Meteorology and Oceanography*, *64*(1). https://doi.org/10.3402/tellusa.v64i0.17264

He, J., Valeo, C., & Chu, A. (2015). Variation in Water Quality of a Stormwater Pond from Diurnal Thermal Stratification. In *Journal of Water Resource and Hydraulic* (Vol. 4, Issue 2).

Hoyos, C. de, & Comín, F. A. (1999). *The importance of inter-annual variability for management*. https://doi.org/10.1023/A:1017030526231

Jia, Y., Wang, L., Li, S., Cao, J., & Yang, Z. (2018). Species-specific bioaccumulation and correlated health risk of arsenic compounds in freshwater fish from a typical mine-

impacted river. *Science of the Total Environment*, *625*, 600–607. https://doi.org/10.1016/j.scitotenv.2017.12.328

Keimowitz, A. R., Zheng, Y., Chillrud, S. N., Mailloux, B., Jung, H. B., Stute, M., & Simpson, H. J. (2005). Arsenic redistribution between sediments and water near a highly contaminated source. *Environmental Science and Technology*, *39*(22), 8606–8613. https://doi.org/10.1021/es050727t

King County. (2015, December 15). *Lake Information Page - King County*. https://green2.kingcounty.gov/smalllakes/LakePage.aspx?SiteID=21#WaterQualityData

Ladwig, R., Hanson, P. C., Dugan, H. A., Carey, C. C., Zhang, Y., Shu, L., Duffy, C. J., & Cobourn, K. M. (2021). Lake thermal structure drives interannual variability in summer anoxia dynamics in a eutrophic lake over 37 years. *Hydrology and Earth System Sciences*, *25*(2), 1009–1032. https://doi.org/10.5194/hess-25-1009-2021

Likens, G. E., & Johnson, N. M. (1969). Measurement and Analysis of the Annual Heat Budget for the Sediments in Two Wisconsin Lakes. *Limnology and Oceanography*, *14*(1), 115–135. https://doi.org/10.4319/lo.1969.14.1.0115

Linge, K. L., & Oldham, C. E. (2002). Arsenic Remobilization in a Shallow Lake. *Journal of Environmental Quality*, *31*(3), 822–828. https://doi.org/10.2134/jeq2002.8220

MacIntyre, S., Fram, J. P., Kushner, P. J., Bettez, N. D., O'Brien, W. J., Hobbi, J. E., & Kling, G. W. (2009). Climate-related variations in mixing dynamics in an Alaskan arctic lake. *Limnology and Oceanography*, *54*(6 PART 2), 2401–2417. https://doi.org/10.4319/lo.2009.54.6_part_2.2401

Martin, A. J., & Pedersen, T. F. (2002). Seasonal and interannual mobility of arsenic in a lake impacted by metal mining. *Environmental Science and Technology*, *36*(7), 1516–1523. https://doi.org/10.1021/es0108537

Masunaga, E., & Komuro, S. (2020). Stratification and mixing processes associated with hypoxia in a shallow lake (Lake Kasumigaura, Japan). *Limnology*, *21*(2), 173–186. https://doi.org/10.1007/s10201-019-00600-3

Müller, B., Granina, L., Schaller, T., Ulrich, A., & Wehrli, B. (2002). P, As, Sb, Mo, and other elements in sedimentary Fe/Mn of Lake Baikal. *Environmental Science and Technology*, *36*(3), 411–420. https://doi.org/10.1021/es010940z

Müller, B., Märki, M., Dinkel, C., Stierli, R., & Wehrli, B. (2002). In Situ Measurement in Lake Sediments Using Ion-Selective Electrodes with a Profiling Lander System. *American Chemical Society*.

Nikolaidis, N. P., Dobbs, G. M., Chen, J., & Lackovic, J. A. (2004). Arsenic mobility in contaminated lake sediments. *Environmental Pollution*, *129*(3), 479–487. https://doi.org/10.1016/j.envpol.2003.11.005

Palmer, M. J., Chételat, J., Jamieson, H. E., Richardson, M., & Amyot, M. (2021). Hydrologic control on winter dissolved oxygen mediates arsenic cycling in a small subarctic lake. *Limnology and Oceanography*, *66*(S1), S30–S46. https://doi.org/10.1002/lno.11556

Powers, S. M., Robertson, D. M., & Stanley, E. H. (2014). Effects of lakes and reservoirs on annual river nitrogen, phosphorus, and sediment export in agricultural and forested landscapes. *Hydrological Processes*, *28*(24), 5919–5937. https://doi.org/10.1002/hyp.10083

Sanders, J. G., Osman, R. W., & Riedel, G. F. (1989). Pathways of arsenic uptake and incorporation in estuarine phytoplankton and the filter-feeding invertebrates Eurytemora affinis, Balanus improvisus and Crassostrea virginica. *Marine Biology*, *103*(3), 319–325. https://doi.org/10.1007/BF00397265

Shah, A. Q., Kazi, T. G., Arain, M. B., Jamali, M. K., Afridi, H. I., Jalbani, N., Baig, J. A., & Kandhro, G. A. (2009). Accumulation of arsenic in different fresh water fish species - potential contribution to high arsenic intakes. *Food Chemistry*, *112*(2), 520–524. https://doi.org/10.1016/j.foodchem.2008.05.095

Smedley, P. L., & Kinniburgh, D. G. (2002). A review of the source, behaviour and distribution of arsenic in natural waters. *Applied Geochemistry*, *17*(5), 517–568. https://doi.org/10.1016/S0883-2927(02)00018-5

Smith, L., Watzin, M. C., & Druschel, G. (2011). Relating sediment phosphorus mobility to seasonal and diel redox fluctuations at the sediment-water interface in a eutrophic freshwater lake. *Limnology and Oceanography*, *56*(6), 2251–2264. https://doi.org/10.4319/lo.2011.56.6.2251

Spliethoff, H. M., Mason, R. P., & Hemond, H. F. (1995). Interannual Variability in the Speciation and Mobility of Arsenic in a Dimictic Lake. In *Environ. Sci. Techno* (Vol. 29).

Tsay, T.-K., Member, A., Ruggaber, G. J., Effler, S. W., & Driscoll, C. T. (1992). *Thermal stratification modeling of lakes with sediment heat flux*.

Wang, Z., Luo, Z., & Yan, C. (2013). Accumulation, transformation, and release of inorganic arsenic by the freshwater cyanobacterium Microcystis aeruginosa. *Environmental Science and Pollution Research*, *20*(10), 7286–7295. https://doi.org/10.1007/s11356-013-1741-7

Wang, S., Jin, X., Bu, Q., Jiao, L., & Wu, F. (2008). Effects of dissolved oxygen supply level on phosphorus release from lake sediments. *Colloids and Surfaces A: Physicochemical and Engineering Aspects*, *316*(1–3), 245–252. https://doi.org/10.1016/j.colsurfa.2007.09.007

Weber, F. A., Hofacker, A. F., Voegelin, A., & Kretzschmar, R. (2010). Temperature dependence and coupling of iron and arsenic reduction and release during flooding of a contaminated soil. *Environmental Science and Technology*, *44*(1), 116–122. https://doi.org/10.1021/es902100h

Wilhelm, S., & Adrian, R. (2008). Impact of summer warming on the thermal characteristics of a polymictic lake and consequences for oxygen, nutrients and phytoplankton. *Freshwater Biology*, *53*(2), 226–237. https://doi.org/10.1111/j.1365-2427.2007.01887.x

5. Chapter 5: Conclusions

5.1. Main findings

5.1.1. Summary

In this work, I have examined the fate of arsenic in a shallow, temperate lake at multiple timescales. While prior work has shown that legacy arsenic in shallow lake sediments causes greater ecological and human health risks than similar levels of contamination in the sediments of deeper lake, a comprehensive understanding of the underlying mechanisms behind this phenomenon remained previously undeveloped (Barrett et al., 2018; 2019). The analysis presented in Chapters 2 – 4 of this dissertation contributes significantly to the understanding of the mechanisms that create and maintain elevated arsenic concentrations in the water columns of shallow, temperate lakes with legacy arsenic contamination. Further, our examination and analysis of vertical mixing processes in Lake Killarney at multiple temporal scales is an important addition to the scientific knowledge of the ranges in mixing behavior within temperate, polymictic lakes.

5.1.2. The importance of physical processes in biogeochemical processes

The importance of physical forces in controlling biogeochemical processes remains a prevalent theme throughout this comprehensive body of research. In all three research chapters, the interplay between stratification and mixing was shown to have significant implications for the concentrations and distribution of dissolved oxygen and arsenic throughout Lake Killarney's water column.

In Chapter 2, we found that mixing patterns varied seasonally and controlled whether arsenic was sequestered in the bottom waters or transported to lake surface waters. The overall thermal structure of the water column was most stable in springtime (Fig. 2.3). From spring to

mid-summer, periods of stable stratification with intermittent mixing led to low bottom water dissolved oxygen (DO) and a sharp gradient of arsenic in the water column, with higher concentrations in the hypolimnion and lower concentrations near the surface (Fig. 2.3, Fig. 2.5). More frequent mixing in the late summer led to higher concentrations of bottom water DO and a more homogenous distribution of arsenic throughout the water column. Through analysis of both thermistor profiles and acoustic Doppler current profiler (ADCP) data, we demonstrated that thermal convection was the key physical mixing mechanism in Lake Killarney during the summer, when arsenic was being released from the sediment (Fig. 2.4). ADCP data allowed us to visualize elevated levels of vertical turbulent intensity penetrating the water column from the late evening through early morning (Fig. 2.8).

Chapter 3 documented the control of stratification and mixing process on arsenic at weekly and daily timescales. We observed the build-up of bottom water arsenic for the first two days of the study, when there was strong bottom water stratification and elevated turbulence was confined to lake surface waters (Fig. 3.4, Fig. 3.3). In subsequent days, we documented six diel cycles in bottom water arsenic concentrations and, through timescale analysis, showed that turbulent mixing from daily convection was necessary to explain these observations.

Finally, Chapter 4 shows how interannual variation in stratification and mixing can result in vast differences in the concentrations of porewater and bottom water arsenic and the uptake of arsenic into the food web (Fig. 4.5, Fig. 4.7). Through the comparison of the 2018 and 2019 summers, we found that less frequent mixing during the early summer in 2018 supported higher concentrations of porewater arsenic and larger fluxes of arsenic into lake bottom waters compared to 2019 when full lake mixing occurred more regularly (Fig. 4.4, Fig. 4.5, Fig. A3.1). A large thermal gradient between the lake sediment and the bottom water in 2018 was crucial in

maintaining stable stratification and reducing conditions in the hypolimnion. Sediment temperature was the main control on this sediment – bottom water thermal gradient and cold sediment temperatures in 2018 were identified as a key control on mixing processes, and, thus, on the fate of arsenic.

In summary, we have demonstrated that physical processes regulate arsenic within a polymictic, contaminated lake on seasonal, interannual, and diel timescales, both directly via turbulent transport of dissolved arsenic and indirectly through moderation of bottom water redox conditions. Analysis in Chapter 3 reminds us that the movement of arsenic within the lake would be insignificant without turbulent mixing. Although this finding is intuitive when applied to the bulk lake water column, our results are significant in documenting the control that stratification and mixing processes have on near-bed arsenic behavior. This dissertation highlights the significance of spatial proximity of lake-wide functions in Lake Killarney and other shallow lakes, by showing that physical and biogeochemical processes at the lake surface and near the lakebed are interconnected and work together to control the fate of arsenic. The dynamic nature of polymictic lakes, characterized by swift transitions between stable stratification and full mixing, has important implications for other key processes, including productivity, nutrient transport, and the fate of both well-known and emerging contaminants. This work offers valuable insights for the study and management of other shallow lentic systems.

5.2. Implications

This research details the mechanisms through which legacy arsenic contamination continues to affect shallow lakes. Below, I lay out the implications of my findings for the management of shallow, temperate, arsenic contaminated systems. Additionally, I delve into the significance of

the observations and analyses in these studies and discuss how they highlight the necessity of safeguarding the water quality of shallow lakes.

5.2.1. Suggestions for current and future lake managers

This work provides a mechanistic understanding of why shallow, contaminated lakes represent an elevated health risk to the ecosystem and surrounding community. Our results are in line with previous research that concludes that management efforts should focus on shallow lakes first, especially if time or resources prevent the evaluation of all contaminated systems (Barrett et al., 2018; Hull et al., 2021).

In particular, the findings in Chapters 2 and 4 illustrate the importance of timing in the monitoring; we advise that sampling and monitoring efforts of shallow, temperate lakes with legacy arsenic contamination should be focused from mid to early summer, when there is semi-stable stratification that allows arsenic to build up in the bottom waters. Because this recommendation is based off of results from a 4 m deep lake, the best timing for monitoring may be different in deeper, polymictic lakes that exhibit slightly different seasonal mixing patterns. Additionally, results from Chapters 3 and 4 provide evidence that primary producers inhabit lake bottom waters. Chapter 3 demonstrates that primary producers control daily dissolved oxygen cycles 0.4 m above the lakebed. Chapter 4 documented large interannual differences in phytoplankton and bottom water arsenic concentrations, but not in surface water arsenic concentrations, implying that arsenic uptake by phytoplankton occurred in the bottom waters. Thus, near-bottom arsenic concentrations should be monitored carefully as they may provide a suitable metric for predicting uptake rates of arsenic into the aquatic food web.

These suggestions are supported by Hull et al. (2021), who conclude that biota testing for consumption advisories should primarily focus on shallow systems. Hull et al. (2021) also

reported that shallow lakes have higher arsenic concentrations in littoral sediments than deeper lakes; these elevated littoral arsenic concentrations have implications for the safety of shallow water play, especially for children and pets who may accidentally consume water or sediment. Our analysis of the physical mechanisms in Lake Killarney suggest that arsenic is transported to littoral sediments via a combination of frequent vertical mixing and mean horizontal flows (Fig. 3.3).

Interactions with lake users during our field work revealed a gap in the information provided to recreators. Many community members showed great interest in our research as well as concern upon finding out that there are elevated levels of arsenic in the sediment, water, and biota of Lake Killarney. I propose the implementation of informative signage at boat ramps and public beaches, offering information regarding potential health risks and educating lake users about which activities are safe. Local governments should actively engage in outreach efforts aimed at communities of greatest risk. These communities may include subsistence fishing populations who rely heavily on harvesting and consuming biota from these lakes as a significant part of their dietary intake (Hull et al., 2021).

Finally, our analysis of the overarching physical controls on lake biogeochemistry detailed in section *5.1.2* yields insights that may be applicable for the research and management of other pollutants and contaminants. Because arsenic is a redox-sensitive element, this research is most applicable to other elements and compounds at least partially influenced by redox conditions. Of note, elevated levels of phosphorus in the sediments of lakes are known to cause more extreme eutrophication in shallow lakes compared to deep lakes (Welch and Cook, 2005). Our furthered understanding of the timescales of stratification and mixing in Lake Killarney can help lake managers understand the outcomes of these physical processes in terms of internal loading and

transport of phosphorus in polymictic systems. However, the dynamic nature of polymictic lakes and the interconnectedness of physical and biogeochemical processes may increase negative impacts of emerging contaminants in shallow lakes, regardless of whether or not these emerging contaminants are influenced by redox conditions. With this in mind, the chemistry of emerging contaminants should be considered in tandem with our findings of shallow lake physical mechanisms in order to gain perspective on the potential short term and long term fate of these new sources of contamination. Finally, climate change is expected to alter the temperature regime and mixing behavior of lakes (Golosov et al., 2012). Expected increases in water column stability should be taken into account when predicting the behavior of arsenic and other contaminants in shallow lakes moving forward.

5.2.2. The necessity of protecting lakes in developing countries

Although it is necessary to continue bettering the management of local arsenic contaminated lakes, this research also highlights the need to prevent further arsenic contamination of shallow lakes in areas where industrialization is currently happening. Brönmark and Hanssen (2002) propose that the mechanisms controlling heavy metals in lakes and ponds are relatively well understood. As such, they suggest that this topic is now in the research implementation, or management, stage, and that heavy metals will have decreasing effects on lakes in developed countries in the future. In contrast, lakes and ponds in developing nations are expected to experience increasing levels of contamination, including from heavy metals such as arsenic (Brönmark and Hanssen, 2002). In hopes of reducing instances of future contamination, it will be necessary to focus efforts on research translation and collaboration with currently developing countries. Specifically, placing emphasis on the protection of urban, shallow lakes could play a

crucial role in preserving the aquatic health of these ecosystems and ensuring their status as safe sources of food and water for local populations.

5.3. References

Barrett, P. M., Hull, E. A., King, C. E., Burkart, K., Ott, K. A., Ryan, J. N., Gawel, J. E., & Neumann, R. B. (2018). Increased exposure of plankton to arsenic in contaminated weakly-stratified lakes. *Science of the Total Environment*, *625*, 1606–1614. https://doi.org/10.1016/j.scitotenv.2017.12.336

Barrett, P. M., Hull, E. A., Burkart, K., Hargrave, O., McLean, J., Taylor, V. F., Jackson, B. P., Gawel, J. E., & Neumann, R. B. (2019). Contrasting arsenic cycling in strongly and weakly stratified contaminated lakes: Evidence for temperature control on sediment–water arsenic fluxes. *Limnology and Oceanography*, *64*(3), 1333–1346. https://doi.org/10.1002/lno.11119

Brönmark, C., & Hansson, L. A. (2002). Environmental issues in lakes and ponds: Current state and perspectives. In *Environmental Conservation* (Vol. 29, Issue 3, pp. 290–307). https://doi.org/10.1017/S0376892902000218

Golosov, S., Terzhevik, A., Zverev, I., Kirillin, G., & Engelhardt, C. (2012). Climate change impact on thermal and oxygen regime of shallow lakes. *Tellus, Series A: Dynamic Meteorology and Oceanography*, *64*(1). https://doi.org/10.3402/tellusa.v64i0.17264

Hull, E. A., Barajas, M., Burkart, K. A., Fung, S. R., Jackson, B. P., Barrett, P. M., Neumann, R. B., Olden, J. D., & Gawel, J. E. (2021). Human health risk from consumption of aquatic species in arsenic-contaminated shallow urban lakes. *Science of the Total Environment*, *770*, 145318. https://doi.org/10.1016/j.scitotenv.2021.145318

Welch, E. B., & Cooke, G. D. (2005). Internal phosphorus loading in shallow lakes: Importance and control. *Lake and Reservoir Management*, *21*(2), 209–217. https://doi.org/10.1080/07438140509354430

A1. Appendix 1: Chapter 2 Supplement

Equation A1.1.

$$SeaTac_{Corrected} = SeaTac_{Raw} * 1.09 - 1.069$$

Equation A1.2.

$$Wind_{new} = Wind_{ref} * \left(\frac{height_{new}}{height_{ref}}\right)^{p}$$

$$height_{new} = 10\,m,\ height_{ref} = 2.4\,m, and\ p = wind\ profile\ exponent = 0.3$$

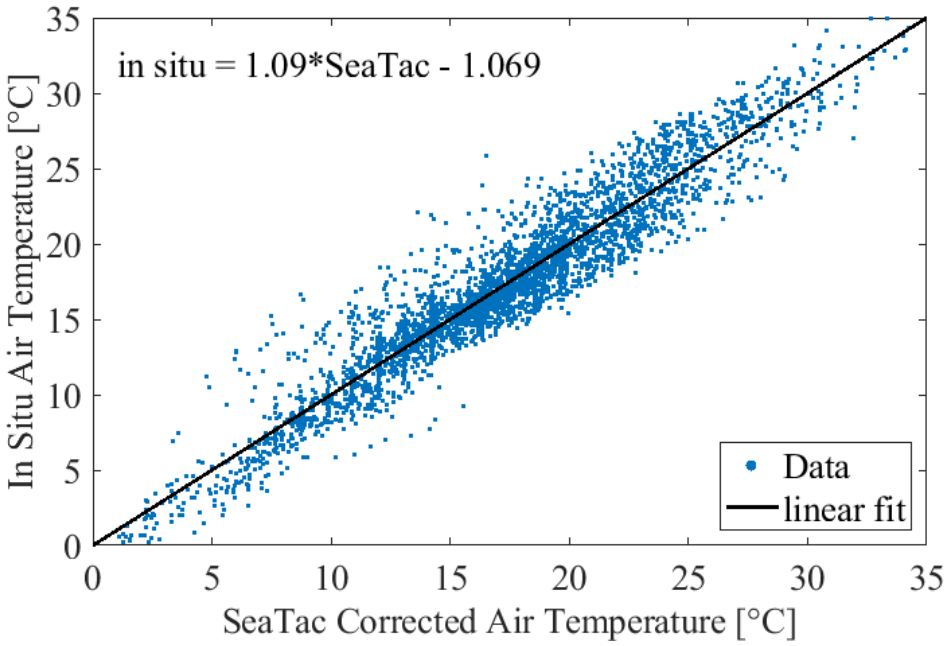

Figure A1.1. *Correlation of SeaTac and in situ air temperature data with linear fit (R^2 = 0.92, P < 0.01) and equation shown; linear fit of data was used to make a correction to the raw SeaTac air temperature data (Equation. A1.1).*

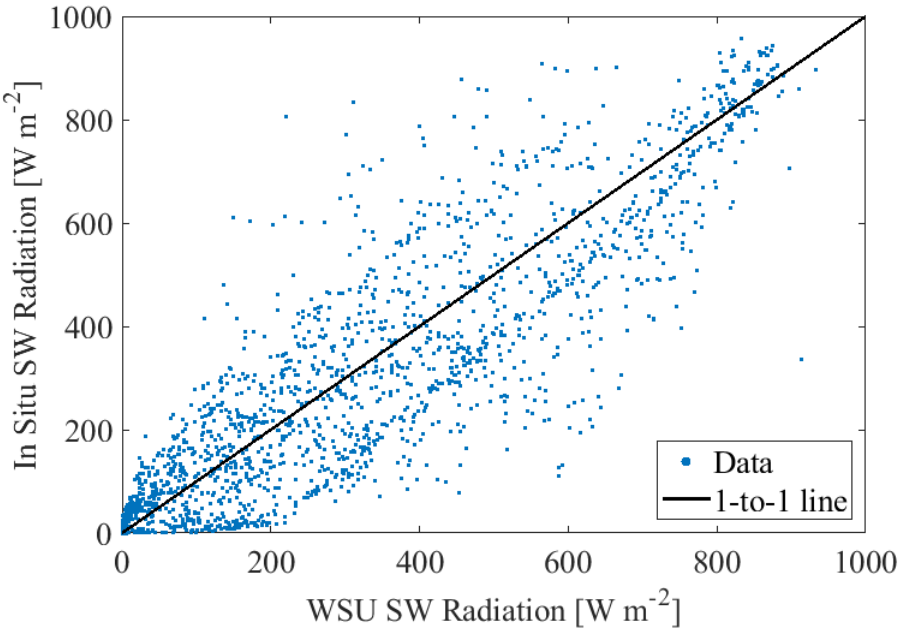

Figure A1.2. *Correlation of Washington State University (WSU) shortwave (SW) radiation measured at the Puyallup weather station and in situ SW radiation data (R^2 = 0.95, $P < 0.01$), showing that the data have a 1-1 relationship and no correction was needed.*

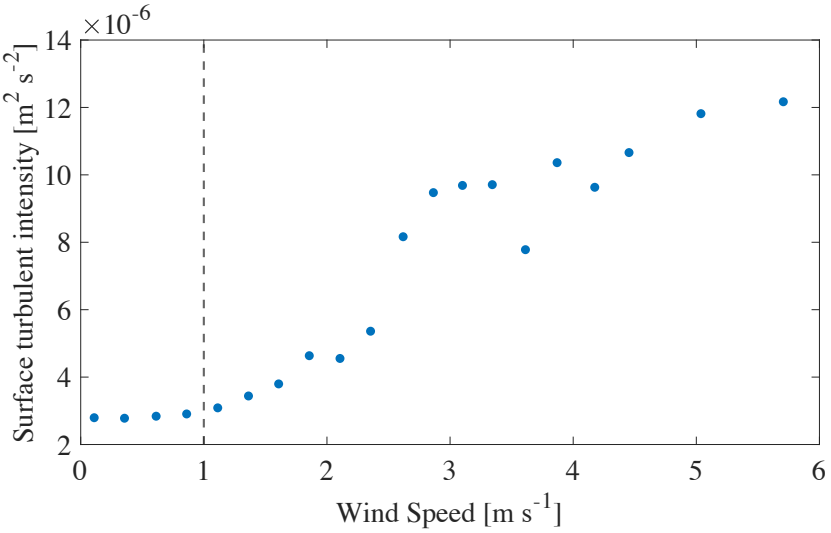

Figure A1.3. *Wind speed vs. surface vertical turbulent intensity, $\overline{(w')^2}$, where surface turbulent intensity measurements were averaged into 0.25 m s^{-1} wind speed bins. The dashed line at 1 m s^{-1} represents the threshold used to separate 'high' and 'low' wind values.*

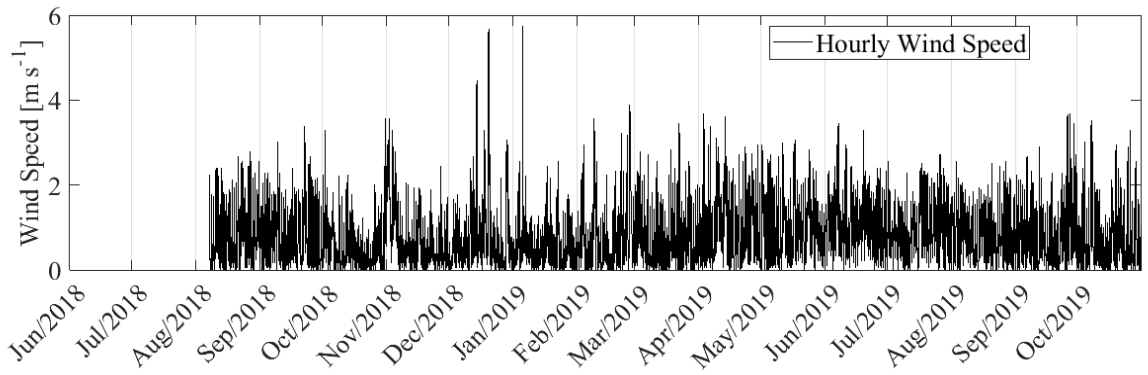

Figure A1.4. *Hourly in situ wind speed data.*

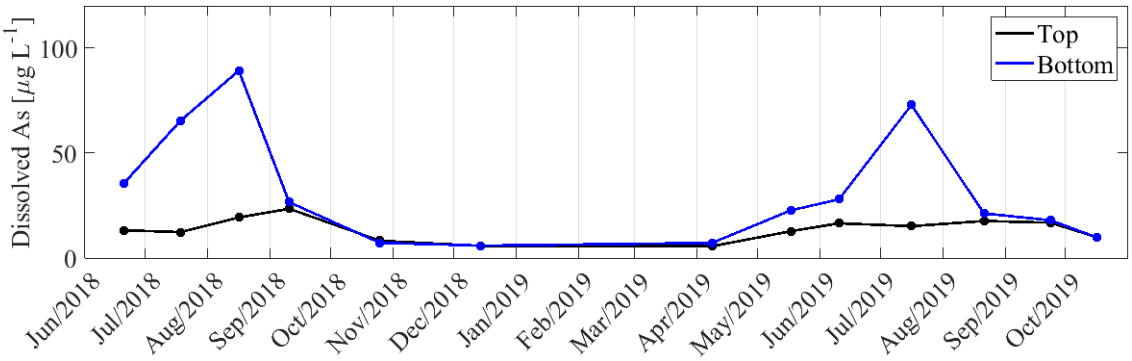

Figure A1.5. *Top and bottom water column total arsenic concentrations.*

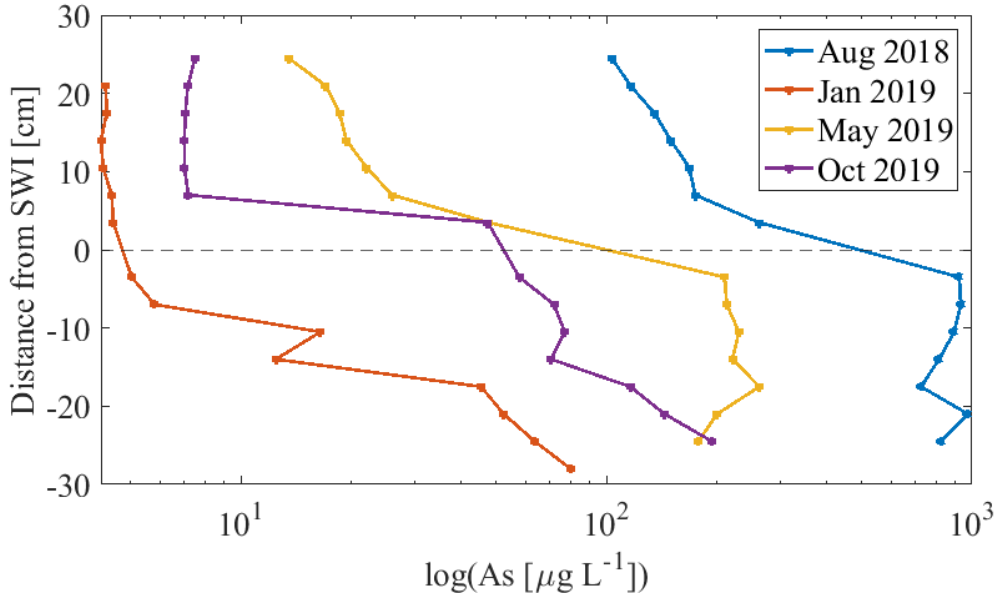

Figure A1.6. *Porewater peeper profiles representing seasonal differences in arsenic mobilization from the sediment and diffusion into bottom waters.*

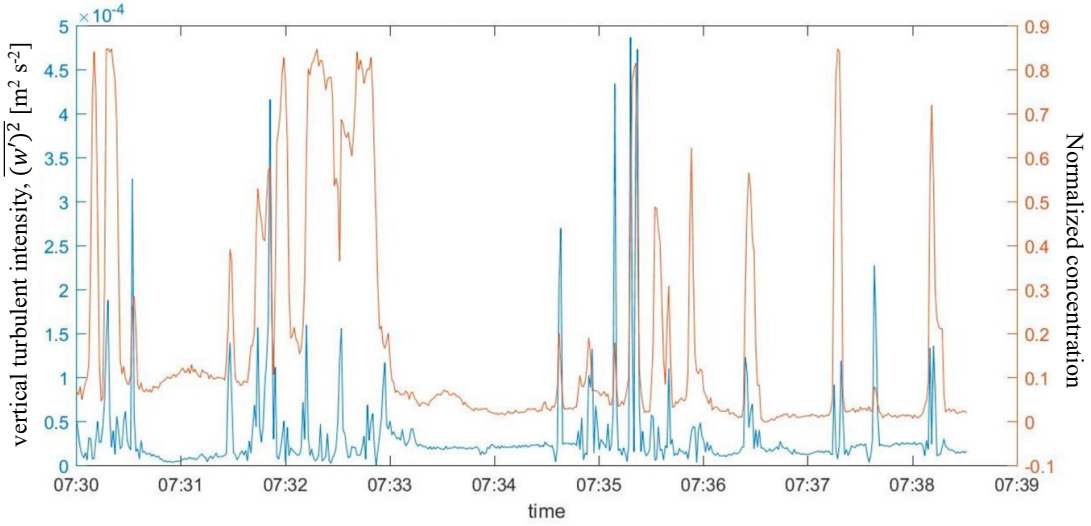

Figure A1.7. *Nine-minute timeseries of vertical turbulent intensity, $\overline{(w')^2}$, with concurrent normalized sediment concentrations both from acoustic Doppler current profiler data. Data were taken at 2.88 m depth on October 25, 2018, during a convective overturning event. *Note that normalized concentration is unitless.*

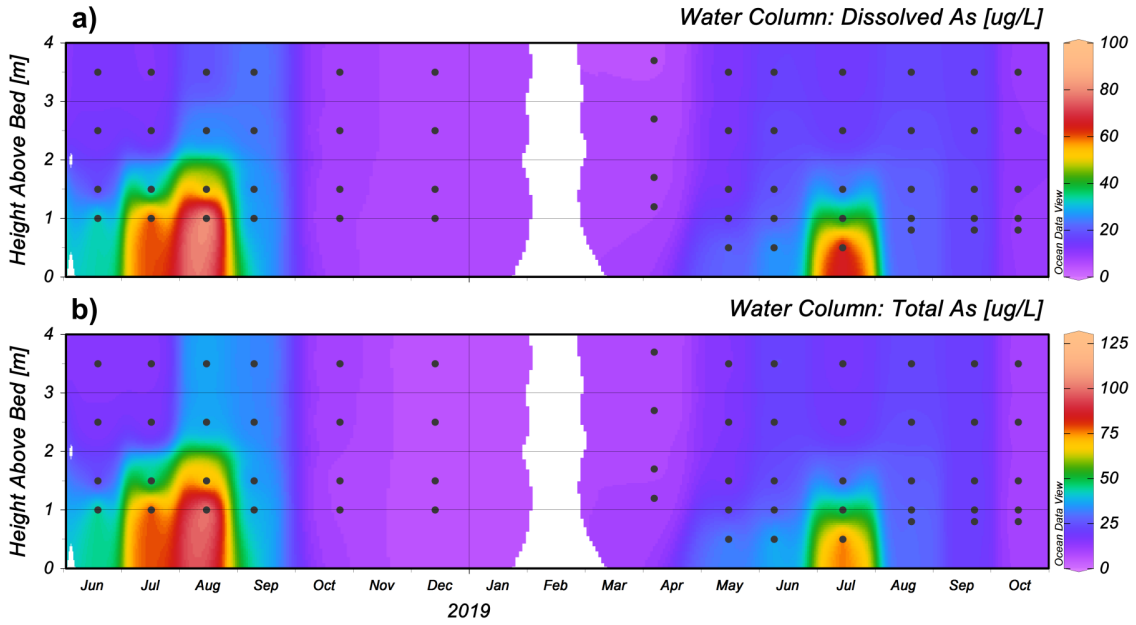

Figure A1.8. *a) Dissolved and b) total arsenic concentrations profiles from ~monthly water sampling; black dots indicate sampling date and location within the water column.*

Table A1.1. *Arsenic speciation for water samples collected on five dates, where arsenite (As(III)) and arsenate (As(V)) are inorganic forms of arsenic and monomethylarsonic acid (MMA) and dimethylarsinic acid (DMA) are organic forms of arsenic.*

Lake	Collection Date	Depth [m]	As(III) [ppb]	DMA [ppb]	MMA [ppb]	As(V) [ppb]	% Organic	% Inorganic	% As(V) total	% As(V) Inorganic	% As(III) Inorganic
Killarney	10/3/16	0.5	3.72	0.53	0.12	7.96	5.3	94.7	64.6	68.2	31.8
		1.5	5.02	0	0.14	6.82	1.2	98.8	56.9	57.6	42.4
		2.5	5.44	0	0.11	5.93	1.0	99.0	51.7	52.2	47.8
		2.5	9.41	0	0.11	2.46	0.9	99.1	20.5	20.7	79.3
		3	2.16	0	0.11	9.94	0.9	99.1	81.4	82.1	17.9
Killarney	2/1/17	0.5	0.83	0.13	0.05	4.76	3.1	96.9	82.5	85.2	14.8
		1.5	0.83	0.08	0.05	4.86	2.2	97.8	83.5	85.4	14.6
		2.5	0.84	0.14	0.05	4.32	3.6	96.4	80.7	83.7	16.3
		2.5	1.29	0.18	0.04	4.43	3.7	96.3	74.6	77.4	22.6
		3	0.86	0.13	0.03	4.69	2.8	97.2	82.1	84.5	15.5
Killarney	4/3/17	0.5	1.01	0.17	0.04	3.11	4.8	95.2	71.8	75.5	24.5
		1.5	0.96	0.17	0.04	3.25	4.8	95.2	73.5	77.2	22.8
		2.5	0.88	0.15	0.04	4.15	3.6	96.4	79.5	82.5	17.5
		2.5	1.01	0.17	0.05	3.52	4.6	95.4	74.1	77.7	22.3
		3	0.48	0.12	0.02	5.35	2.3	97.7	89.6	91.8	8.2
Killarney	7/12/17	0.5	2.99	0.67	0.17	12.66	5.1	94.9	76.8	80.9	19.1
		1.5	5.04	0.84	0.17	8.35	7.0	93.0	58.0	62.4	37.6
		2.5	6.07	0.95	0.15	18.17	4.3	95.7	71.7	75.0	25.0
		2.5	4.48	0.99	0.16	18.75	4.7	95.3	76.9	80.7	19.3
		3	3.9	0	0.07	27.84	0.2	99.8	87.5	87.7	12.3
Killarney	8/9/16	0.5	1.52	0.33	0.17	5.34	6.8	93.2	72.6	77.8	22.2
		1.5	1.73	0.41	0.18	6.19	6.9	93.1	72.7	78.2	21.8
		2.5	2.42	0.46	0.16	11.51	4.3	95.7	79.1	82.6	17.4
		2.5	2.58	0.46	0.14	10.99	4.2	95.8	77.6	81.0	19.0
		3	3.61	0	0.12	14.94	0.6	99.4	80.0	80.5	19.5

Table A1.2. *Slope and statistics for relationships plotted in Fig. 2.7c (bottom water DO vs. both bottom water and porewater As) and Fig. 2.7d (sediment temperature vs. both bottom water and porewater As).*

	Slope	**R^2**	**P-value**
Fig. 7c: Bottom water DO vs. bottom water dissolved As	-5.6	0.49	0.023
Fig. 7c: Bottom water DO vs. porewater dissolved As	-65.6	0.34	0.08
Fig. 7d: Sediment temperature vs. bottom water dissolved As	2.8	0.1	0.16
Fig. 7d: Sediment temperature vs. porewater dissolved As	19.1	0.1	0.14

A2. Appendix 2: Chapter 3 Supplement

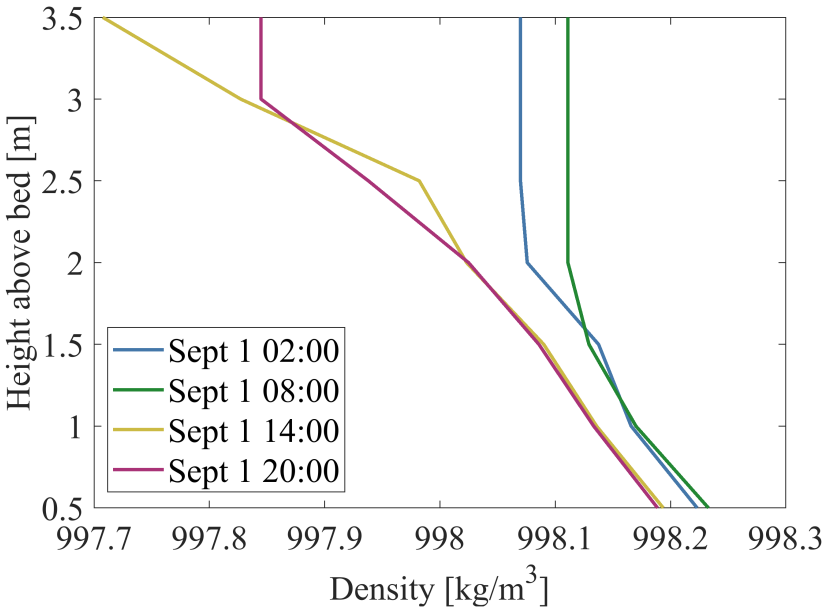

Figure A2.1. *Lake water density profiles on September 1 every 6 hours.*

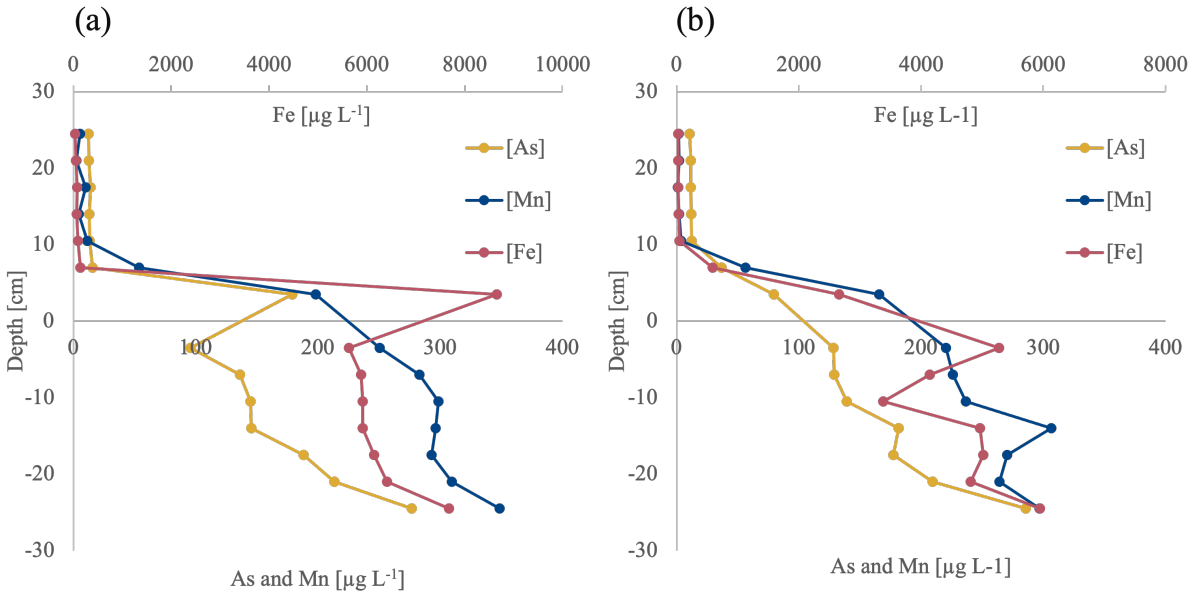

Figure A2.2. *Dissolved arsenic (As), manganese (Mn), and iron (Fe) profiles*

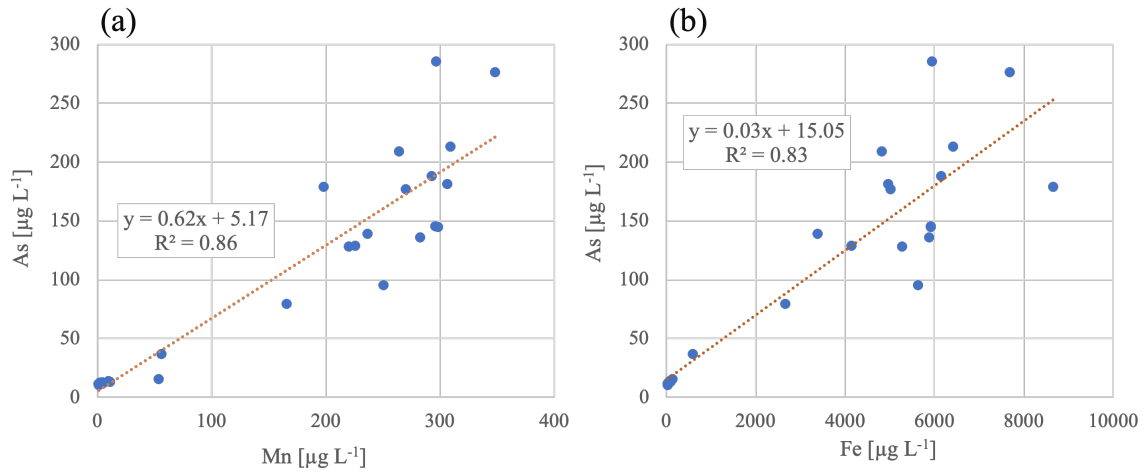

Figure A2.3. *Scatterplots of (a) dissolved manganese (Mn) and dissolved arsenic (As) and (b) dissolved iron (Fe) and dissolved arsenic (As).*

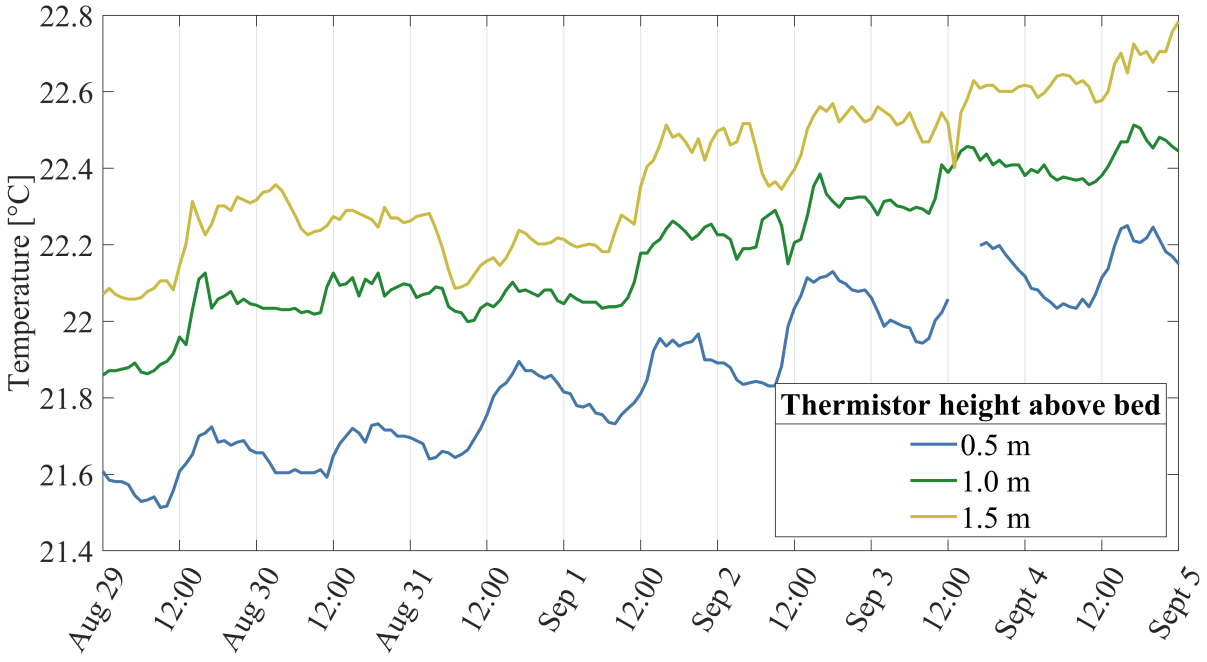

Figure A2.4. *Water temperature timeseries from thermistors at 0.5, 1.0, and 1.5 m above the lakebed.*

A3. Appendix 3: Chapter 4 Supplement

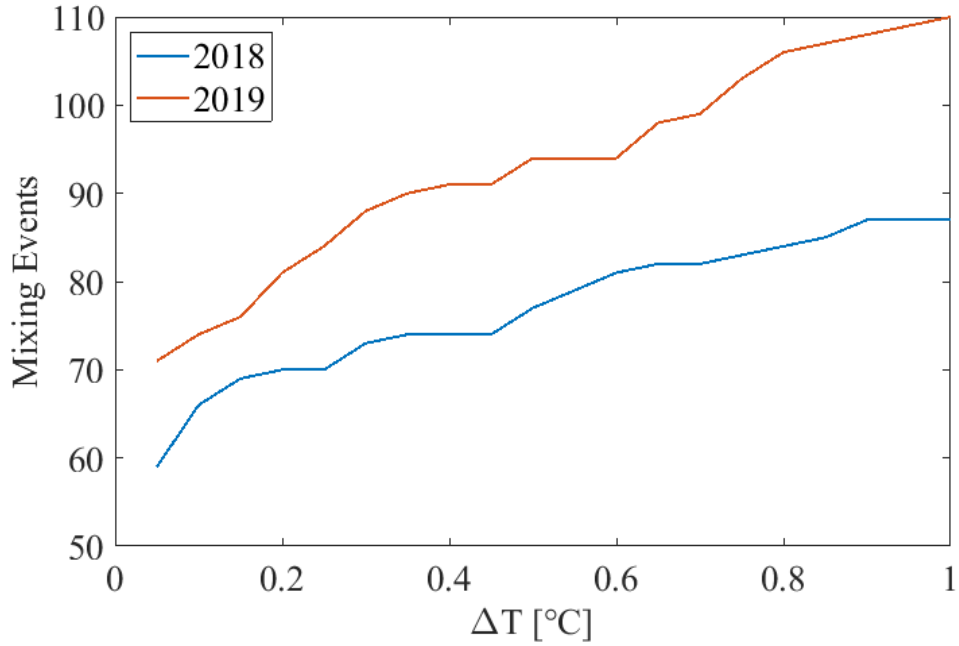

Figure A3.1. *Difference in temperature between top and bottom thermistors (ΔT) used to define whether the lake water column was fully mixed vs. number of mixing events calculated from June 23 through October 31, the period of time when there is thermistor data in both summers, for 2018 and 2019.*

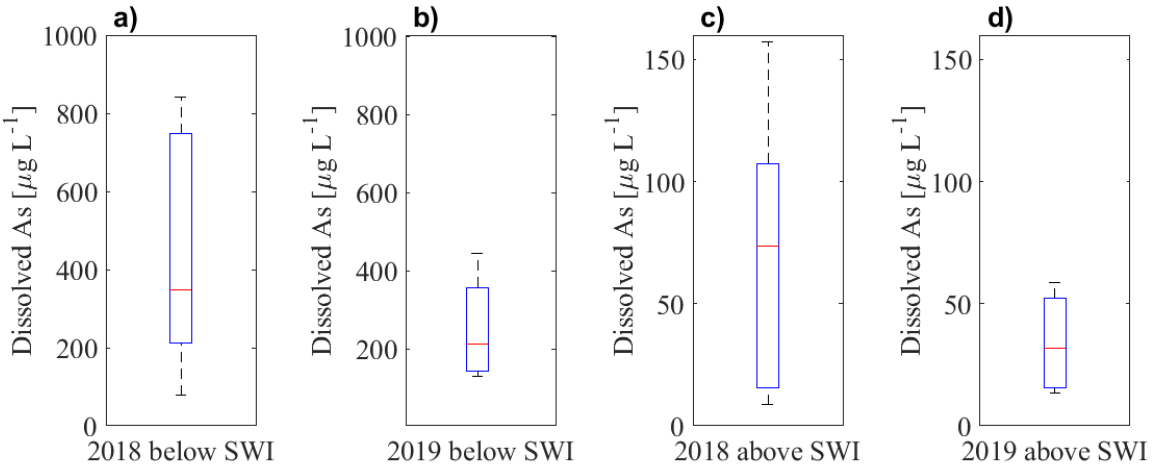

Figure A3.2. *Boxplots of (a, b) porewater and (c, d) bottom water dissolved arsenic concentrations from June 1 – October 31 in 2018 and 2019 from passive diffuser samples (n = 5 deployments in each summer). Middle lines on box plots represents median of data in plot. Note different scales for porewater and bottom water plots.*

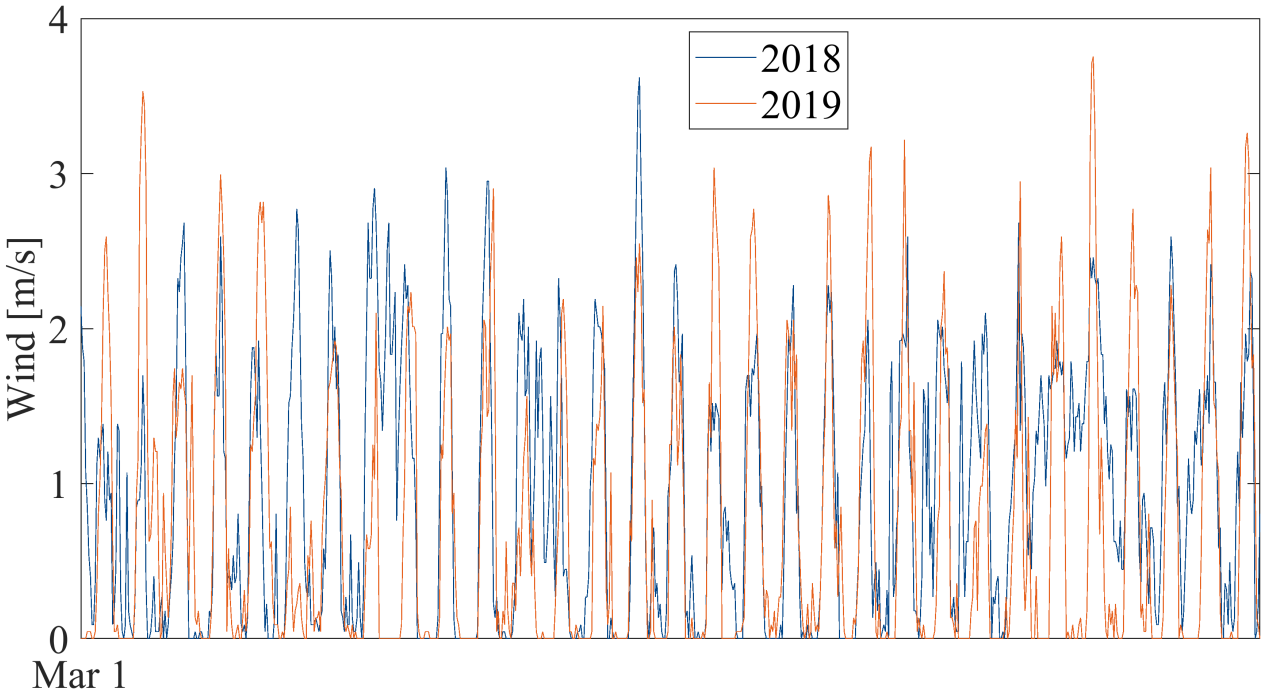

Figure A3.3. *Hourly wind measurements for the month of March in 2018 and 2019.*

Table A3.1. *Monthly average air temperatures in 2018 and 2019 from January through May.*

Month	**Avg air temp 2018 [°C]**	**Avg air temp 2019 [°C]**
Jan	7.1	7.1
Feb	5.0	2.6
March	7.8	8.7
April	10.6	11.1
May	15.5	15.4